The Role of the B1 Vacuolar H^+-ATPase Subunit in Excretion of Acid and Bicarbonate along the Collecting Duct

Dissertation

zur

Erlangung der naturwissenschaftlichen Doktorwürde

(Dr.sc.nat.)

vorgelegt der Mathematisch-naturwissenschaftlichen Fakultät

der Universität Zürich

von

Jana Kovacikova

aus der Slowakischen Republik

Promotionskomitee:

Prof. Dr. Carsten A. Wagner

Prof. Dr. Heini Murer

Prof. Dr. Jürg Biber

Zürich, 2006

Die vorliegende Arbeit wurde von der Mathematisch-naturwissenschaftlichen Fakultät der Universität Zürich im Wintersemester 2006/2007 als Dissertation angenommen.

Promotionskomitee:
Prof. Dr. Carsten A. Wagner
Prof. Dr. Heini Murer
Prof. Dr. Jürg Biber

The following work was accepted as a dissertation by the University of Zurich's faculty of Science in the winter semester 2006/2007.

Doctorate Committee:
Prof. Dr. Carsten A. Wagner
Prof. Dr. Heini Murer
Prof. Dr. Jürg Biber

CONTENTS

SUMMARY

Terminal portions of the nephron, namely the connecting tubule and the collecting duct, are responsible for fine-tuning of acid-base excretion. This is enabled by at least two types of intercalated cells (IC), type A and B. Acid secretory type A IC expressing vacuolar H^+-ATPases on the apical membrane eliminate protons from the body. On the contrary, base secretory type B IC possessing vacuolar H^+-ATPases on the basolateral membrane reabsorb protons during metabolic alkalosis. Vacuolar H^+-ATPases are composed of several subunits. Among them, the B1 subunit has been shown to be important for normal final urinary acidification in man.

The generation of B1 subunit deficient mouse model has enabled the examination of the role of this subunit for normal IC function as well as the interaction of proton transport with other transport processes.

In the first series of experiments, we focused on functional interaction between sodium reabsorption and proton secretion in the connecting tubule (CNT) and collecting duct (CD). It has been hypothesised that electrogenic sodium reabsorption via epithelial sodium channels (ENaCs) in the apical membrane of principal cells may promote H^+-ATPase-mediated proton secretion by neighbouring ICs by creating a more lumen-negative voltage. Furosemide-induced increases in sodium delivery to the CNT and CCD enhanced urinary acidification and net acid excretion in wild type mice. The effect of furosemide was abolished with amiloride or benzamil, blocking ENaC action. In mice deficient in the kidney-specific vacuolar H^+-ATPase B1

subunit, furosemide led to minimal urinary acidification. In contrast, furosemide treatment alone and in combination with hydrochlorothiazide in mice with a kidney-specific inactivation of the α subunit of ENaC in the CCD and MCD, but not in the CNT, led to normal urinary acidification. These results suggest that the B1 subunit of the vacuolar H^+-ATPase is necessary for furosemide-induced acute urinary acidification. Loss of ENaC channels in the CCD and MCD did not affect this acidification. Thus, functional expression of ENaC channels in the CNT is sufficient for furosemide-stimulated urinary acidification and identifies the CNT as a major segment in electrogenic urinary acidification.

In a second series, we investigated the contribution of the B1 subunit to normal type B IC function. The relative abundance of these cells is increased during metabolic alkalosis since they are specialized in bicarbonate secretion via the apical Cl^-/HCO_3^- exchanger, pendrin, and proton reabsorption via basolateral vacuolar H^+-ATPases. Induction of metabolic alkalosis with deoxycorticosterone acetate (DOCA) and $NaHCO_3$ resulted in a more pronounced alkalosis in B1 deficient mice. The observed alkalosis was associated with increased serum bicarbonate, hypokalemia, and hypochloremia. Furthermore, B1 deficient mice showed decreased total pendrin expression whereas the relative abundance of pendrin expressing cells was increased. H^+-ATPase activity in intercalated cells of isolated CCD was strongly reduced, demonstrating that B1 containing H^+-ATPases are essential for normal type B intercalated cell function. Furthermore, B1 deficient mice excreted larger quantities of urine which was associated with lower AQP-2 water channel abundance and a higher relative frequency of principal cells in

the connecting tubule. Thus, the B1 subunit of the H^+-ATPase is required for normal B-type IC function and its absence may also affect principal cell function. The role of the B1 subunit in bicarbonate secretion and water reabsorption have been hitherto not fully recognized and may also affect renal function in patients with ATP6V1B1 mutations.

DEUTSCHE ZUSAMMENFASSUNG DER DOKTORARBEIT

Die terminalen Nephronsegmente, d.h. das Verbindungsstück und das Sammelrohr, sind verantwortlich für die Feineinstellung der Säure-Basen-Ausscheidung. Mindestens zwei Typen von Schaltzellen existieren, Typ A und B, die diese Ausscheidung ermöglichen. Säureausscheidende A-Schaltzellen besitzen eine apikale H^+-ATPase, durch die die Protonen eliminiert werden. Im Gegensatz zu den A-Schaltzellen besitzen die B-Schaltzellen eine basolaterale H^+-ATPase, durch die die Protonen während einer metabolischen Alkalose reabsorbiert werden. Vakuoläre H^+-ATPasen bestehen aus mindestens 13 Untereinheiten. Eine von ihnen ist die B1-Untereinheit, die eine entscheidende Rolle für die finale Urinansäuerung im Menschen spielt.

Der genetische Knock-out der B1-Untereinheit in Mäusen ermöglichte es, die Rolle dieser Untereinheit für die normale Schaltzellenfunktion und die Interaktion zwischen dem Protonentransport und anderen Transportprozessen zu untersuchen.

Die ersten Experimente konzentrierten sich auf die funktionelle Interaktion zwischen der Natriumreabsorption und der Protonenausscheidung im Verbindungsstück und im Sammelrohr. In diesen Nephronsegmenten wird Natrium durch den epithelialen Na+-Kanal (ENaC) in der apikalen Membran der Hauptzellen resorbiert. Da diese Natriumreabsorption elektrogen ist, entsteht ein lumennegatives transzelluläres Potenzial, welches die Protonensekretion durch die H^+-ATPase von den benachbarten Schaltzellen

antreibt. Die durch das Diuretikum Furosemid erhöhte Natriumabgabe in das Verbindungsstück und in das Sammelrohr fördert die Urinansäuerung und die Netto- Säureausscheidung in normalen Wildtypmäusen. Blockade des ENaC Natriumkanals mit Amilorid und Benzamil hebt diese Wirkung von Furosemid auf. In den Mäusen ohne die B1-Untereinheit der vakuolären H^+-ATPase, verursachte Furosemid nur eine minimale Urinansäuerung. In Mäusen mit der nierenspezifisch inaktivierten α-Untereinheit des ENaC im kortikalen und medullären Sammelrohr – jedoch nicht im Verbindungsstück – wurde jedoch nach einer Behandlung mit entweder Furosemid alleine, oder zusammen mit Hydrochlorothiazid, eine normale Urinansäuerung beobachtet. Diese Resultate deuten darauf hin, dass die B1-Untereinheit der vakuolären H^+-ATPase für die akute, durch Furosemid induzierte Urinansäuerung notwendig ist. Der Verlust von ENaC-Kanälen im kortikalen und medullären Sammelrohr beeinflusst die Ansäuerung nicht. Die Expression von ENaC-Kanälen im Verbindungsstück ist für die Furosemid-stimulierte Urinansäuerung ausreichend. Das Verbindungsstück wird damit als das Hauptsegment der elektrogenen Urinansäuerung identifiziert.

Im zweiten Teil dieser Arbeit wurde der Einfluss der B1-Untereinheit auf die die normale B-Schaltzellenfunktion untersucht. Da dieser Typ von Schaltzellen auf die Bikarbonatsekretion durch den apikalen Cl^-/HCO_3^--Austauscher, Pendrin, und die Protonenreabsorption durch die basolaterale H^+-ATPase spezialisiert sind, wird ihre relative Häufigkeit während einer metabolischen Alkalose erhöht. Durch Induzierung einer metabolischen Alkalose mit Deoxykortikosteronazetat (DOCA) und $NaHCO_3$,

wurde in den B1-defizienten Mäusen eine ausgeprägte Alkalose verursacht, die durch einen erhöhten Serumbikarbonatwert, einer Hypokaliämie und einer Hypochlorämie charakterisiert war. Ausserdem zeigten B1-defiziente Mäuse eine gesamthafte Verminderung der Pendrin-Expression, während die relative Häufigkeit von pendrinexprimierenden Zellen anstieg. Die Aktivität der H^+-ATPase in B-Schaltzellen war stark reduziert, was darauf hinweist, dass die H+-ATPasen, die B1-Untereinheit beinhalten, für eine normale Funktion der B-Schaltzellen essentiell sind. B1-defiziente Mäuse schieden zudem grössere Mengen Urin aus, was mit einer niedrigeren Anzahl an AQP2-Kanälen und mit einer höheren relativen Häufigkeit von Hauptzellen im Verbindungsrohr assoziiert war. Demnach ist die B1-Untereinheit der H^+-ATPase notwendig für eine normale B-Schaltzellenfunktion, und ihr Fehlen kann auch die Funktion der Hauptzellen beeinträchtigen. Die Rolle der B1-Untereinheit in der Bikarbonatsekretion und in der Wasserreabsorption ist bis jetzt nicht vollständig verstanden und und die Ergebnisse dieser Arbeit können auch zum Verständnis der Pathophysiologie bei Patienten mit einer Mutation in ATP6V1B1 beitragen.

1. INTRODUCTION

Systemic pH must be maintained at the physiological level of 7.4 to assure normal function of the body. This is achieved by interactions between the body's buffering systems; the lungs and the kidneys. Apart from CO_2 levels in the blood, a potential acid which is removed by exhalation, metabolism and food intake generate also non-volatile acids and bases. A person weighing 70 kg and ingesting typical western protein-rich diet produces approximately 70 mmole of H^+ daily, which must be excreted by the kidney. The kidneys handle this acid-load by ''dividing'' 70 mmole/day of H_2CO_3 excreting approximately 70 mmole/day H^+ into the urine and simultaneously transporting 70 mmole/day of new HCO_3^- into the blood. Apart from that, the kidneys are also reclaiming virtually all HCO_3^- filtered by the glomeruli from the tubule fluid. The largest fraction of HCO_3^- is reabsorbed in the proximal tubule (~ 80%) and the thick ascending limb of the loop of Henle (~ 20 %). The connecting tubule (CNT) and the collecting duct (CD), the terminal portions of the nephron (Fig. 1A), are ultimately responsible for the fine-tuning of urine pH by reabsorbing approximately 2% of filtered bicarbonate and simultaneously secreting protons.

The epithelium of CNT and CD possess IC which specialize in acid-base transport. At least two types of intercalated cells have been described: type A and B (Fig. 1B). Acid secretory type A cells express vacuolar H^+-ATPases on the apical membrane and the Cl^-/HCO_3^- exchanger AE1 on the basolateral membrane. Type B IC secrete bicarbonate via the

apical Cl^-/HCO_3^- exchanger pendrin and reabsorb protons via vacuolar H^+-ATPases expressed on the basolateral membrane, and therefore play a crucial role during metabolic alkalosis (79).

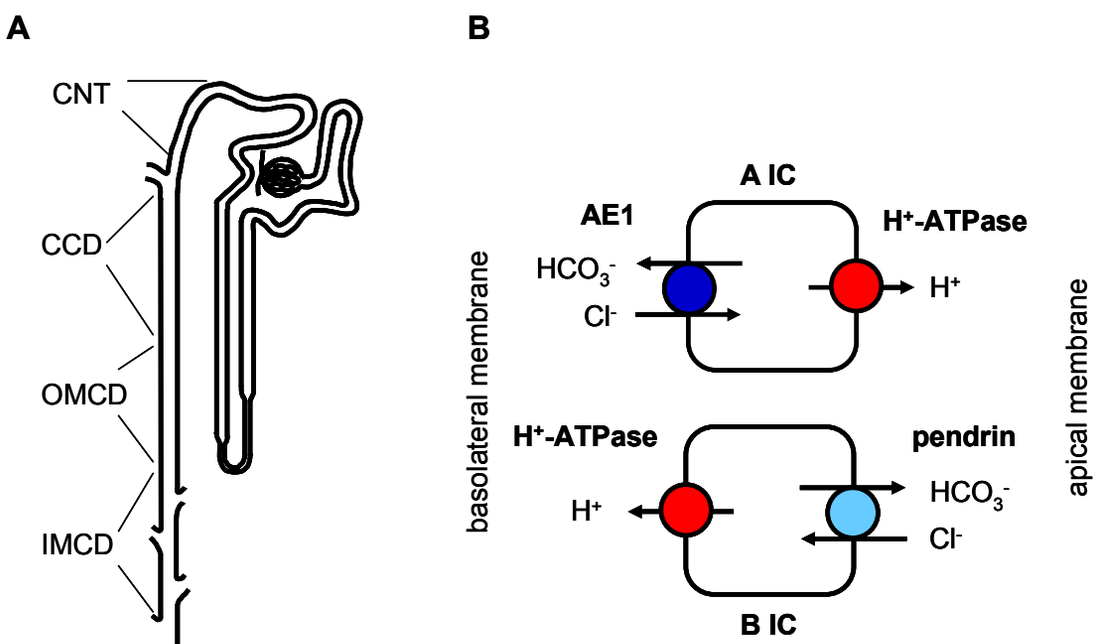

Fig. 1. Model of nephron (A) and IC (B).

CNT – connecting tubule; CCD – cortical collecting duct; OMCD – outer medullary collecting duct; IMCD – inner medullary collecting duct; IC – intercalated cells.

The vacuolar H^+-ATPase is composed of 13 distinct subunits forming V_0 and V_1 domains. The cytosolic V_1 domain hydrolyses ATP which

provides energy for proton extrusion through the transmembrane, V_0 domain. One of the V_1 domain subunits is also the B subunit existing in the B1 and B2 isoforms. Whereas the B2 subunit is ubiquitously expressed, the B1 subunit has been found only in a limited numbers of tissues such as the kidneys, testis and inner ear (77). In man, mutations in the gene encoding for the B1 subunit result in distal renal tubular acidosis (43), a disease when distal nephron fails to excrete acid leading to the development of metabolic acidosis in the setting of otherwise normal renal function (23).

The generation of a B1 subunit-deficient mouse (32) has made it possible to study the contribution of this subunit to normal H^+-ATPase function in type A and B IC and additionally to investigate the interaction of proton secretion with other transport processes.

2. ACID-BASE TRANSPORT IN THE COLLECTING DUCT

The collecting duct, located in the terminal portion of the nephron, is a heterogeneous epithelium involved in the control of acid-base status, sodium-potassium balance and water homeostasis. It comprises several segments such as the connecting tubule (CNT), cortical collecting duct (CCD), outer medullary collecting duct (OMCD) and inner medullary collecting duct (IMCD) all of which consist of two types of cells; principal cells (PC) (also called segment specific cells) and intercalated cells (IC).

Principal cells specialize in water reabsorption mediated by apical AQP2 and also maintain sodium and potassium homeostasis. This is enabled by sodium reabsorption through the epithelial sodium channel ENaC residing on the apical membrane and potassium secretion through the ROMK channel (Renal Outer Medullary K channel). In the CNT and CCD, sodium reabsorption generates a lumen-negative voltage of -5 to -40 mV favouring potassium and proton secretion (19, 83). In the OMCD and IMCD negligible sodium reabsorption occurs so that the subsequent H^+-secretion is Na^+-independent, and as a result, the lumen potential becomes positive (84, 85).

Intercalated cells, accounting for approximately 40% of cells in the collecting duct, are involved in acid-base homeostasis. Based on their morphological and functional features at least two types of intercalated cells have been distinguished: type A and type B IC. Type A IC express anion exchanger AE1 on the basolateral membrane and vacuolar H^+-ATPases on the apical membrane, thus allowing for proton secretion and bicarbonate

reabsorption. In the cytosol of these cells, carbonic anhydrase II (CAII) catalyzes the hydration of CO_2, generating H^+ and HCO_3^-. Bicarbonate is extruded through the basolateral membrane via the Cl^-/HCO_3^- -exchanger AE1 while protons are secreted through vacuolar H^+-ATPases (and a negligible portion through H^+/K^+-ATPases) located on the apical membrane. In the lumen, protons bind to HCO_3^- ions generating H_2CO_3, which in turn are converted to CO_2 and H_2O. CO_2 may diffuse back into the cell to replenish the substrate for CAII, allowing the cycle to continue. Urinary HCO_3^- losses are thus minimized by this titration. Protons secreted into the lumen are also titrated by other buffers such as ammonia and phosphate leading to the further enhancement of proton secretion. Type A IC can be found in CNT, CCD, OMCD and in initial part of IMCD (46, 73) and are virtually absent in the terminal two-thirds of the IMCD (14). Type B IC reverse the polarity of A IC, and thus mediate bicarbonate secretion and proton reabsorption. In these cells bicarbonate secretion is enabled via pendrin, which is also used as a specific marker of type B IC localized on the apical membrane (64). Proton reabsorption is achieved by the action of vacuolar H^+-ATPases expressed on the basolateral membrane. Thus, type B IC, found in CNT and CCD play an essential role particularly during metabolic alkalosis (66) by conserving protons and excreting bicarbonate.

It has been shown that the induction of acidosis or alkalosis produces changes in relative abundance of different IC subtypes (6, 13, 66, 78). In addition, the existence of the third type of IC, so-called non-A, non-B cells have been reported. These cells express pendrin on the apical

membrane, similar to type B IC, and also express H^+-ATPases on the apical membrane like that of type A IC (46, 73, 80). They are found in the CNT and CCD and are therefore considered a possible intermediate state between the type A and B IC. This quality is termed ‘’intercalated cell plasticity’’ (reviewed in (2). In cell culture, some investigators (27) observed the conversion of type B IC to type A IC as well as to PC and suggest the B IC as a ‘’stem’’ cell (27). Other studies have reported that the B cells, following an intracellular acid-load, reversed their apical Cl^-/HCO_3^- activity to the basolateral Cl^-/HCO_3^- activity (53); (26). However, there is lack of evidence that interconversion between the different cell types occurs *in vivo*.

3. RENAL VACUOLAR H^+-ATPase

Vacuolar H^+-ATPases are multisubunit proteins which utilize the energy stemming from ATP hydrolysis to transport protons across membranes. They belong to the superfamily of ATPases that are divided into three subclasses: *1*) P-type ATPases such as Na^+-K^+-ATPases, Ca^{2+}-ATPases, and H^+-K^+-ATPases; *2*) mitochondrial F_1F_0-ATPases; and *3*) V-type (vacuolar) H^+-ATPases (56).

Vacuolar H^+-ATPases are expressed in virtually all cells. They are found in the membranes of intracellular organelles such as lysosomes, the Golgi apparatus, secretory vesicles, and endosomes. Their role is to acidify the intracellular compartment, creating an optimal pH environment for enzyme function (71). In some tissues they are expressed also in the plasma membrane and mediate proton extrusion from the cell, thus contributing to the specialized function of the tissue. In osteoclasts, protons transported by vacuolar H^+-ATPase serve to dissolve bone matrix (74). In the inner ear they secrete protons into endolymph (21, 29, 69) and in the epididymis they acidify luminal fluid which is necessary for sperm maturation (11). In the kidney vacuolar H^+-ATPases are involved in acid-base transport, thus contributing to overall body homeostasis.

3.1. Structure of the vacuolar H^+-ATPase

Vacuolar H^+-ATPases consist of two domains, a cytosolic catalytic V_1 domain (640 kDa) and a transmembrane V_0 domain (240 kDa), together forming a protein complex of ~900 kDa (36, 58) (Fig. 2). The V_0 domain is composed of 5 subunits termed a, c, c', c'' and d (61) which form a proton-translocating pore. The a subunit, existing in 4 isoforms, is suggested to be important for assembly and function of the H^+-ATPase (45, 48). Mutations in the kidney specific a4 isoform cause distal renal tubular acidosis (42).

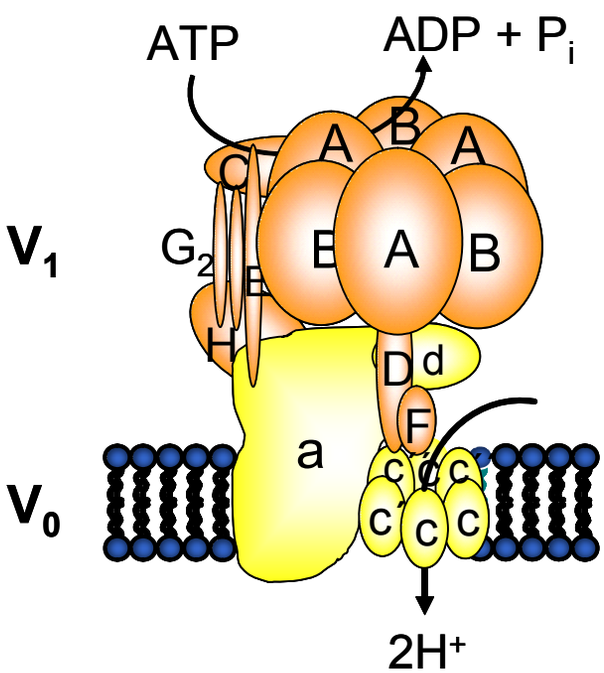

Fig. 2. Structural model of the vacuolar H^+-ATPase

The cytosolic V_1 domain hydrolyzes ATP, providing energy for active proton transport. It is composed of 8 subunits categorized as A-H present in the stoichiometry of A_3:B_3:C:D:E_2:F:G_2:H (58). Previous work with yeast revealed that the B subunit is crucial for vacuolar H^+-ATPase function. Mutants with the disrupted gene encoding the B subunit result in a lethal phenotype unless grown in media with a narrow acidity range around pH 5.5 (57, 89). The B subunit exists in two isoforms, namely B1 and B2, differing in their carboxy termini raising the possibility that they are fulfilling different functions (59, 62). The carboxy terminus of the B1 subunit, but not the B2 subunit, possesses a PDZ domain which can interact with other PDZ proteins.(12). Thus, the PDZ domain may enable the interactions of the B1 subunit with other proteins which could mediate trafficking or regulation of the B1 subunit containing H^+-ATPases (12). Furthermore, mutations in the B1 subunit have been shown to cause inherited distal renal tubular acidosis (43).

3.2. Vacuolar H^+-ATPase in the kidney

The vacuolar H^+-ATPase was shown by immunohistochemistry to be localized in the microvilli of the proximal tubule brush border, in the apical and basolateral membranes of the initial segment of the thin descending limb, and in the apical plasma membranes of thick ascending limb, in distal

tubule, connecting tubule and collecting duct (14) with the highest levels in the proximal tubule and intercalated cells of the collecting duct.

In the proximal tubule protons are excreted mainly by the action of Na^+/H^+ exchangers, especially by the NHE-3 isoform (20); (81). Up to 40% of proximal tubule proton secretion appears to be mediated by the vacuolar H^+-ATPase expressed in the brush border membrane (18, 81).

In the collecting duct, the vacuolar H^+-ATPase is the main transporter mediating proton secretion. Intercalated cells of the collecting duct showed apical, basolateral, diffuse or even bipolar patterns of H^+-ATPase distribution (8, 13). Vacuolar H^+-ATPase residing on the apical membrane of A IC is involved in the proton extrusion into the lumen, which is coupled to the bicarbonate reabsorption via the anion exchanger AE1 on the basolateral membrane. B IC expressing H^+-ATPases on the basolateral membrane and the anion exchanger pendrin on the apical membrane reverse this process and are activated during metabolic alkalosis (33, 51). In the CCD, all subtypes of IC are detectable. In the outer stripe of the outer medulla, A-cells predominate, but a few residual B-cells can be found. In the inner stripe of the outer medulla, only A-IC are present. In the inner medulla, the epithelium initially contains between 5 and 10% A-IC, and these cells disappear from the epithelium in the middle and terminal portions of the inner medullary collecting duct (14).

In addition to vacuolar H^+-ATPases, a H^+-K^+-ATPase has been found in the outer medullary collecting duct (28, 86, 87). It has, however, emerged that its contribution to overall proton secretion in this segment is

minor and that H^+-K^+-ATPases may rather play an important role as a potassium scavenging pathway during systemic potassium depletion (25, 35).

3.2.1. Role of the B1 vacuolar H^+-ATPase subunit in the kidney

The B subunit is a part of the cytosolic V_1 domain and exists in two isoforms: B1 and B2 (75); (31). Whereas the B2 subunit is considered to be ubiquitous and mediates the acidification of intracellular organelles, the B1 subunit has been identified only in a limited number of tissues. The B1 subunit has been detected in epidydimis (11, 15, 70), the vas deferens (11), the ciliar body of the eye (82), in the inner ear (43, 69), the lung (54) and in intercalated cells of the kidney (59).

Recently one study (60) demonstrated the expression of the ubiquitous B2 subunit along the nephron, including A and B IC. Under baseline conditions the B2 subunit was predominantly seen in the cytosol. However, under conditions that require insertion of the H^+-ATPase into the membrane, such as chronic carbonic anhydrase inhibition, the B2 subunit was also detected in the apical membrane of of A IC. In contrast, basolateral expression of B2 subunit in B-IC was weak or not observed. Thus, basolateral targeting of the B2 subunit in B-IC may be less efficient (60).

This distinct pattern of B isoforms distribution might be explained by a different structure of their carboxy termini. The B1 subunit, but not the B2 subunit, possesses a PDZ domain what is known to interact with other PDZ

proteins. These PDZ protein-protein interactions could be involved in the targeting or trafficking of the H^+-ATPase (12). It was demonstrated that the PDZ protein NHE-RF1 colocalizes with the B1 subunit in the membrane of B IC. However NHE-RF1 was not detected in A IC. This indicates that NHE-RF1 is required for basolateral targeting (12) and therefore the PDZ domain lacking B2 subunit may not be able to reach the basolateral membrane of B IC (60).

4. REGULATION OF RENAL VACUOLAR H^+-ATPase

4.1. Adaptive regulation

In the kidney, proton secretion by intercalated cells is regulated to a great extent by modulating the amount of vacuolar H^+-ATPase at the cell surface. Vacuolar H^+-ATPase proteins are shuttled to and from the apical membrane via specialized intracellular acidic vesicles (2, 8). It has been shown that in systemic acidosis the number of cortical intercalated cells with apical membrane vacuolar H^+-ATPase expression increases and the number of cells with basolateral vacuolar H^+-ATPase expression decreases (8, 70). Conversely, in systemic alkalosis, the number of cells with basolateral vacuolar H^+-ATPase expression increases, whereas apical vacuolar H^+-ATPase expression decreases (8, 70).

4.2. Hormonal regulation

Vacuolar H+-ATPases are strongly regulated by the renin-angiotensin-aldosterone system. This system is especially known for its effect on sodium homeostasis and blood pressure regulation but has also influence on the renal handling of acid and bases..

Angiotensin II is formed in two steps from angiotensinogen. In the first step angiotensinogen is activated by the protease renin to

angiotensin I, which is then converted to angiotensin II by the angiotensin converting enzyme (ACE) in the second step. Angiotensin II binds to two receptor subtypes, AT_1 being activated by picomolar angiotensin II concentrations and AT_2 activated by (high) nanomolar concentrations (5). AT_1 was found in vessels and along the entire nephron (4). Activation of the AT_1 receptor triggers the events that lead to the increase in blood pressure, such as vasoconstriction and increase in Na^+, HCO_3^-, and fluid reabsorption (4). Sodium and bicarbonate reabsorption as well as proton secretion are achieved by AT_1 receptor activation and subsequent stimulation of Na^+/HCO_3^- cotransporter, NHE-3 and the vacuolar H^+-ATPase (34); (63). The AT_2 receptor is also expressed in the kidney and seems to antagonize the effects of the AT_1.

Aldosterone is synthesized and released from adrenal glands in response to several stimuli such as angiotensin II, hypokalemia, or metabolic acidosis. It serves primarily to enhance Na^+ reabsorption in kidney and colon, thereby regulating extracellular volume and blood pressure (76). The action of aldosterone is classically mediated by altering transcription of target genes after binding to the mineralocorticoid receptor. In the kidney, mineralocorticoid receptors are expressed along the entire length of the connecting segment and collecting duct (49). Activation of these receptors results in changes of transcription/translation of target proteins. These changes can occur either early (within 30 min) or up to several hours (early genes), or alternatively start only after several hours (late genes). Apart from this genomic effect aldosterone also has nongenomic effects (76); (50).

In the collecting duct aldosterone is enhancing proton secretion via vacuolar H^+-ATPase by at least three distinct mechanisms: 1) Stimulation of electrogenic Na^+ reabsorption through the luminal epithelial Na^+ channel (76)) resulting in lumen-negative potential, which increases the electrical driving force for H^+ secretion in the cortical collecting duct (37). 2) A direct action on H^+ secretion via transcriptional/translational pathways that has been shown in turtle bladder and in rat medullary collecting duct (3, 24). 3) Trafficking of H^+-ATPase to the membrane (88), a rapid nongenomic effect that cannot be prevented by the mineralocorticoid receptor blocker spironolactone. On the contrary, this effect can be inhibited by the colchicine induced disruption of microtubules. In addition, inhibition of protein kinase C-dependent processes with chelerythrine abolished the stimulatory effect of aldosterone, pointing to a role of protein kinase C in this signaling cascade (88).

Other hormones involved in regulation of acid-base transport are thyroid hormones (55), endothelin, kallikrein, calcitonin and vasopressin (77).

5. DISTAL RENAL TUBULAR ACIDOSIS

Primary distal renal tubular acidosis (dRTA) arises when the collecting duct fails to remove excess acid into the urine. It is characterized by the failure of the kidney to produce acid urine appropriately in the presence of systemic metabolic acidosis in the setting of otherwise normal renal function (23). If the metabolic acidosis is compensated such that arterial pH is within normal limits, dRTA can be diagnosed by demonstrating the failure of urinary acidification after oral ammonium chloride administration. However, investigators also use furosemide (9), causing increased distal sodium delivery that also results in urine acidification (and kaliuresis) under normal circumstances.

Failure to appropriately excrete the normal nonvolatile acid products of the diet in dRTA results in hypokaliemic hyperchloremic metabolic acidosis of varying severity. Primary dRTA is almost always accompanied by variably severe nephrocalcinosis and/or nephrolithiasis associated with hypercalciuria. Urinary citrate is low because citrate reabsorption is upregulated in the proximal tubule to provide new bicarbonate (1 citrate = 2 bicarbonate). Abnormal calcium deposition in dRTA is attributed largely both to this hypocitraturia and to urine alkalinity. The chronic acidosis and low bicarbonate result in the leaching of bone, leading to rickets or osteomalacia in severe or untreated cases (42).

dRTA can be inherited in an autosomal dominant or an autosomal recessive manner. Patients with dominant (type 1a) dRTA suffer

from growth impairment, rickets and erythrocytosis (1) while patients with recessive dRTA develop progressive and irreversible bilateral sensorineural hearing loss (dRTA type 1b) (16).

Type 1b dRTA is caused by mutations in the ATP6V1B1 (B1) and ATP6V0A4 (a4) subunits of the vacuolar H^+-ATPase or in the AE1 Cl^-/HCO_3^- exchanger (Karet 2002). Furthermore, hypoaldosteronism or inhibition of mineralocorticoid receptor results in renal tubular acidosis associated with hyperkaliemia (type IV RTA) (38, 67) with the clinical picture similar to the dRTA.

5.1. Mutations in the B1 H^+-ATPase subunit (type 1b dRTA)

ATP6V1B1, the gene encoding the B1-subunit of H^+-ATPase, resides on chromosome 2 and has made it an excellent candidate gene for dRTA because of its kidney specificity. Upon previous screening for mutations in patients with dRTA, fifteen different mutations have been revealed. Interestingly, almost all of the affected individuals had bilateral sensorineural hearing loss (43). Expression of *ATP6V1B1* was also demonstrated in the human and mouse cochlea at the apical surface of interdental cells and in endolymphatic sac epithelium, a major site of acid secretion into endolymph (43). This acid secretion is possibly mediated by H^+-ATPase containing the B1 subunit. *ATP6V1B1* expression has also been observed in the male genital

tract, another site with a particular acidification requirement for sperm maturation (39).

5.2. Mutations in the a4 H^+-ATPase subunit (type 1c dRTA)

ATP6V0A4, the gene encoding the a4 H^+-ATPase subunit resides on chromosome 7 (68). It was demonstrated in yeast that this 116 kDa subunit is important for assembly and the function of H^+-ATPase (44). Apart from the presence or absence of hearing loss, there do not appear to be major phenotypic differences between patients with *ATP6V1B1* and *ATP6V0A4* mutations. Interestingly, long-term follow-up of the patients with *ATP6V0A4* mutations who showed at the time of diagnosis normal hearing revealed that they develop mild to moderate hearing loss during the second to forth decade of life (72).

6. MOUSE MODELS USED IN THIS STUDY

6.1. B1 H^+-ATPase subunit deficient mice

The *Atp6v1b1-/-* mouse was generated in order to elucidate the contribution of B1 subunit to distal urinary acidification. The Atp6v1b1 gene was disrupted by homologous recombination (30, 32). In contrast to human dRTA patients harbouring the *ATP6V1B1* mutation, *Atp6v1b1* –/– mice appear healthy and grow normally. *Atp6v1b1* –/– mice fed a standard diet produce significantly more alkaline urine than that of wild-type littermates, without developing systemic acidosis. However, after oral acid challenge with NH_4Cl, *Atp6v1b1* –/– mice become acidotic, while maintaining an inappropriately alkaline urine, which makes them a useful model of recessive human dRTA. Clearance studies in anesthetized mice infused with furosemide suggest that the urinary acidification defect resulting from the loss of a functional B1 subunit may localize to the distal nephron. Increased sodium delivery from the thick ascending limb, sufficient to induce a significant urinary acidification in wild-type mice, was not associated with urinary acidification in *Atp6v1b1* –/– mice (47). Study of Atp6v1b1-/- mice of both sexes show that they are fertile (30, 32) and have preserved hearing and no abnormalities in inner ear (22).

6.2. Mice with specific inactivation of αENaC subunit in collecting duct

The epithelial sodium channel (ENaC) is composed of three subunits termed α,β and γ (17). It is expressed in the aldosterone sensitive distal nephron (ASDN) which comprises the late distal convoluted tubule (DCT), CNT and CD. The role of ENaC is to mediate electrogenic sodium reabsorption which provides the electrochemical gradient for potassium secretion by ROMK channel. Inhibition of ENaC, e.g. by amiloride, leads to

natriuresis, hyperkaliemia and metabolic acidosis.

Mice with complete innactivation of the α,β or γ subunit genes die within 2-4 days after birth as a consequence of lung fluid-clearence failure (40) and acute pseudohypoaldosteronism with severe hyperkaliemia and metabolic acidosis (7, 52). Therefore, to study sodium reabsorption along the ASDN, the Scnn1a^{loxloxCre} mouse with the specific inactivation of the αENaC subunit in the collecting duct but not in the connecting tubule was generated (41, 65). This subunit plays an essential role in trafficking of the channel to the membrane (10).

In our studies Scnn1a^{loxloxCre} mice were used to investigate the functional interaction between sodium reabsorption and vacuolar H^+-ATPase mediated distal urinary acidification.

7. AIM OF THE WORK

The CNT and CD are the final regions of the nephron involved in the control of acid-base excretion. The fulfilment of this role is enabled by the epithelium which is composed of IC specialized in acid-base transport. In addition to intercalated cells, CNT and CD contain also principal cells which are involved in potassium secretion via the ROMK channel and in sodium reabsorption via ENaC. Sodium reabsorption creates a negative transtubular membrane voltage which in turn favours proton secretion by vacuolar H^+-ATPase expressed in the neighbouring type A IC. Thus, factors such as furosemide, which increase sodium delivery to the distal part of the nephron, such as furosemide, lead to enhanced sodium reabsorption by this nephron segment and subsequently also to enhanced proton secretion.

The B1 H^+-ATPase subunit has been shown to play a crucial role in disposing of acid equivalents in humans (43). The generation of mice deficient for the B1 subunit has made it possible to investigate the contribution of this subunit to the normal H^+-ATPase function in type A and B IC. Furthermore it also provided a suitable model for studying functional interaction between sodium reabsorption and urinary acidification in the connecting tubule and collecting duct.

The aim of this study was to investigate:

1. Functional interaction between sodium reabsorption via ENaC and proton secretion via H^+-ATPAse in the collecting duct using B1 H^+-ATPase subunit and αENaC subunit deficient mice
2. The contribution of B1 H^+-ATPase subunit to the function of type B intercalated cells during alkalosis.

8. PUBLICATIONS THAT CONTRIBUTED TO THIS WORK

http://www.kidney-international.org

see commentary on page 1674

The connecting tubule is the main site of the furosemide-induced urinary acidification by the vacuolar H^+-ATPase

J Kovacikova[1], C Winter[1], D Loffing-Cueni[2], J Loffing[2,3], KE Finberg[4], RP Lifton[4], E Hummler[2], B Rossier[2] and CA Wagner[1]

[1]*Institute of Physiology and Center for Integrative Human Physiology, University of Zurich, Zurich, Switzerland;* [2]*Department of Pharmacology and Toxicology, University of Lausanne, Lausanne, Switzerland;* [3]*Department of Medicine – Anatomy, University of Fribourg, Fribourg, Switzerland and* [4]*Department of Genetics, Yale Medical School, New Haven, Connecticut, USA*

Final urinary acidification is achieved by electrogenic vacuolar H^+-ATPases expressed in acid-secretory intercalated cells (ICs) in the connecting tubule (CNT) and the cortical (CCD) and initial medullary collecting duct (MCD), respectively. Electrogenic Na^+ reabsorption via epithelial Na^+ channels (ENaCs) in the apical membrane of the segment-specific CNT and collecting duct cells may promote H^+-ATPases-mediated proton secretion by creating a more lumen-negative voltage. The exact localization where this supposed functional interaction takes place is unknown. We used several mouse models performing renal clearance experiments and assessed the furosemide-induced urinary acidification. Increasing Na^+ delivery to the CNT and CCD by blocking Na^+ reabsorption in the thick ascending limb with furosemide enhanced urinary acidification and net acid excretion. This effect of furosemide was abolished with amiloride or benzamil blocking ENaC action. In mice deficient for the IC-specific B1 subunit of the vacuolar H^+-ATPase, furosemide led to only a small urinary acidification. In contrast, in mice with a kidney-specific inactivation of the alpha subunit of ENaC in the CCD and MCD, but not in the CNT, furosemide alone and in combination with hydrochlorothiazide induced normal urinary acidification. These results suggest that the B1 vacuolar H^+-ATPase subunit is necessary for the furosemide-induced acute urinary acidification. Loss of ENaC channels in the CCD and MCD does not affect this acidification. Thus, functional expression of ENaC channels in the CNT is sufficient for furosemide-stimulated urinary acidification and identifies the CNT as a major segment in electrogenic urinary acidification.

Kidney International (2006) **70**, 1706–1716. doi:10.1038/sj.ki.5001851; published online 20 September 2006

KEYWORDS: H^+-ATPase; epithelial Na^+-channel; connecting tubule; furosemide; distal renal tubular acidosis (dRTA); mouse

Correspondence: *CA Wagner, Institute of Physiology and Center for Integrative Human Physiology, University of Zurich, Winterthurerstrasse 190, Zurich CH-8057, Switzerland. E-mail: Wagnerca@access.unizh.ch*

Received 2 January 2006; revised 28 June 2006; accepted 18 July 2006; published online 20 September 2006

The kidneys play a central role in maintaining acid–base homeostasis by reabsorbing bicarbonate and excreting acid equivalents generated by metabolism. Final urinary acidification takes place in the connecting tubule (CNT) and along the different segments of the collecting duct (CD) namely the cortical (CCD), outer medullary, and initial inner medullary collecting duct (MCD). These parts of the nephron are composed of segment-specific cells reabsorbing Na^+ and secreting K^+ and of intercalated cells (ICs) involved in acid–base transport. Many studies have described functionally and morphologically at least two types of ICs: type A and type B.[1–3] Type A ICs secrete protons via an apically expressed vacuolar H^+-ATPase.[4] This proton secretion is functionally coupled to the basolateral anion exchanger AE1 releasing bicarbonate into blood. Type B ICs reverse this process, thereby secreting bicarbonate into urine and absorbing protons.[1,5] The role of a third subtype, non-A/non-B ICs, is not fully clarified yet.

Proton secretion through vacuolar H^+-ATPases in the CNT and CCD is electrogenic and is thought to be indirectly coupled to Na^+ reabsorption.[4,6] Na^+ reabsorption through the amiloride-sensitive epithelial Na^+ channel (ENaC) expressed in neighboring segment-specific cells creates a more lumen-negative potential which has been hypothetized to enhance H^+ secretion by H^+-ATPases.[7–10] In the MCD, ENaC expression is much lower than in the CNT and CCD,[11] the lumen potential is more positive and H^+ secretion is independent from Na^+ absorption.[12]

The ENaC consists of three subunits termed α, β, γ.[13,14] Loss-of-function mutations in either the human α, β, or γ subunits of ENaC cause pseudohypoaldosteronism type 1 characterized by severe neonatal salt wasting, hyperkalemia, and metabolic acidosis.[15] The α subunit plays an essential role in the trafficking of the channel to the cell surface as well as forming part of the pore.[13] Apart from the kidney, ENaC is also expressed in distal colon and in upper and lower airways where it also mediates Na^+ reabsorption.[14] Mice with complete inactivation of αENaC develop acute postnatal respiratory distress and die within 40 h of birth from failure

to clear their lungs from liquid.[16] Recently, a novel mouse model has been generated with specific inactivation of αENaC in the entire CD but not in CNT,[17] providing a tool for studying sodium balance as well as disturbances of proton secretion secondary to defective Na^+ absorption.

The vacuolar H^+-ATPase is composed of at least 13 subunits of which several cell- and tissue-specific isoforms exist.[4,18,19] The B subunit forms part of the peripheral domain V_1 and two isoforms of this subunit, B1 and B2, have been identified. Whereas the B2 isoform (ATP6V1B2) is almost ubiquitously expressed and appears to serve in most cells a house-keeping function, the B1 isoform (ATP6V1B1) has a more limited tissue distribution: specialized cells of the epididymis,[20,21] the vas deferens,[21] the ciliary body of the eye,[22] the inner ear,[23] and all subtypes of ICs of the kidney.[20,24] Mutations in the gene encoding the B1 subunit result in distal renal tubular acidosis (dRTA) in man characterized by the inability of the distal nephron to appropriately acidify the urine.[23] A mouse model deficient for the *Atp6v1b1* gene has recently been generated with impaired urinary acidification.[25] Vacuolar H^+-ATPase activity is almost completely absent from the CCD. Interestingly, enhanced luminal appearance of the B2 subunit has been noted in B1-deficient ICs, suggesting that the B2 isoform could compensate for the loss of B1.[25] Nevertheless, *Atp6v1b1*-deficient mice develop a more severe metabolic acidosis with inappropriately alkaline urine when challenged with an oral acid-load (NH_4Cl) characteristic of dRTA.

Different subtypes of dRTA have been proposed and classified based on clinical tests.[26,27] These tests include oral NH_4Cl- or parenteral Na_2SO_4-loading and application of furosemide, which all lead to an acute urinary acidification in healthy subjects but not in patients with specific subtypes of dRTA. Furosemide inhibits the luminal $Na^+/K^+/2Cl^-$ cotransporter in the thick ascending limb, thereby increasing the delivered fraction of Na^+ to the subsequent nephron segments and stimulating Na^+ reabsorption through ENaC. Patients lacking an appropriate urinary acidification after furosemide application have been classified as suffering from the 'voltage-defective' form of dRTA.[9]

In order to test for and localize the possible functional interaction between Na^+ reabsorption and H^+ secretion in the different parts of the distal nephron, we performed clearance studies in mice treated acutely with furosemide, hydrochlorothiazide, and amiloride, and measured urinary acidification and net acid excretion (NAE).

RESULTS

Colocalization of vacuolar H^+-ATPase and ENaC in neighboring cells in the collecting system

Immunostaining of mouse kidney with antibodies against calbindin D28k, B1 subunit of the vacuolar H^+-ATPase, and the β subunit of the ENaC revealed that the B1 subunit of the H^+-ATPase is exclusively expressed in CNTs and CDs which were identified on account of their characteristic localization in the cortical labyrinth and the medullary rays, respectively, and by their strong labelling with antibodies against the beta subunit of the epithelial sodium channel (ENaC) and the calcium-binding protein calbindin D28k (Figure 1). Higher magnification showed that the B1 subunit is only expressed in a subtype of epithelial cells lining CNT and CD that do not express βENaC or calbindinD28k. This staining pattern is consistent with an exclusive localization of the B1 subunit in ICs[28,29] which are intermingled between the ENaC (and calbindin) positive CNT and CD (principal) cells.

The effect of furosemide and amiloride on urinary acidification

In a first group of control animals, the effect of acute furosemide and subsequent amiloride application on urinary

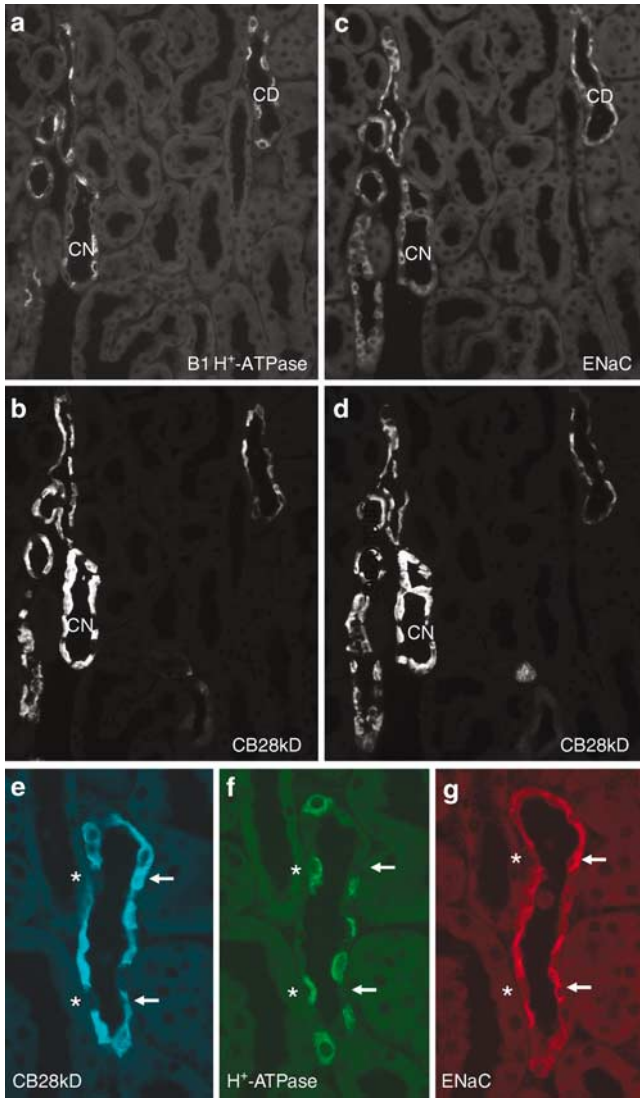

Figure 1 | Localization of vacuolar H^+-ATPases and the ENaC along the CNT and CCD in mouse kidney. (**a**–**d**) Consecutive mouse kidney sections (**a**/**b** and **c**/**d**) were stained against the B1 subunit of the vacuolar H^+-ATPase, the β subunit of the ENaC, and the calbindinD28k protein. Original magnification ×400. (**e**–**g**) Higher magnification of a CCD. ICs positive for the B1 subunit are marked with *, arrows indicate segment-specific cells stained for βENaC and calbindinD28k. Original magnification ×650.

acidification was tested. As shown in Figure 2a, the initial urinary pH was similar in all groups before the application of furosemide. A bolus of furosemide (2 μg/g of body weight (BW)) after 60 min lowered the urinary pH with being significantly more acidic after 90 min (furosemide: pH 6.16±0.08 versus control: pH 6.49±0.07), after 120 min (furosemide: pH 5.72±0.10 versus control: pH 6.39±0.08), and 150 min (furosemide: 5.63±0.084 versus control: pH 6.16±0.05). The furosemide-induced urinary acidification was completely abolished by the subsequent administration of amiloride or benzamil, inhibitors of ENaC activity: pH 6.09±0.09 in the furosemide+amiloride group versus 5.72±0.10 in furosemide-alone group after 120 min as well as after 150 min: pH 6.19±0.12 for furosemide+amiloride versus pH 5.63±0.08 for furosemide alone. The urine production and excretion remained stable in the control group during the entire experiment, whereas it increased in furosemide-treated animals from 1.9±0.3 μl/g after 60 min to 5.2±0.8 μl/g after 90 min. A similar effect was observed in mice treated subsequently with amiloride, resulting in an increase in urine output from 3.0±0.6 μl/g BW after 60 min to 6.5±0.7 μl/g BW after 90 min. (Figure 2b). The analysis of urinary electrolyte excretion revealed that the fractional excretion (FE in %) of sodium and chloride increased in mice treated with furosemide plus amiloride (Figure 2d and e) with a maximum after 120 min (FE of sodium 1.67±0.31% for furosemide+amiloride versus 0.25±0.08% in control and FE of chloride 2.29±0.38% in furosemide+amiloride versus 0.70±0.24% in control). As summarized in Table 1 and Figure 3, furosemide treatment resulted in a slightly decreased blood potassium concentration (4.8±0.3 mmol/l in furosemide versus 5.7±0.2 mmol/l in control) and augmented blood bicarbonate concentration (21.0±0.7 with furosemide versus 19.7±1.0 mmol/l under control).

Thus, treatment of mice with furosemide led to the expected increase in urinary output with an increase in fractional sodium and potassium excretion accompanied by a strong urinary acidification as described previously for rats and humans.[9] The stimulation of urinary acidification was abolished by the ENaC inhibitors amiloride and benzamil

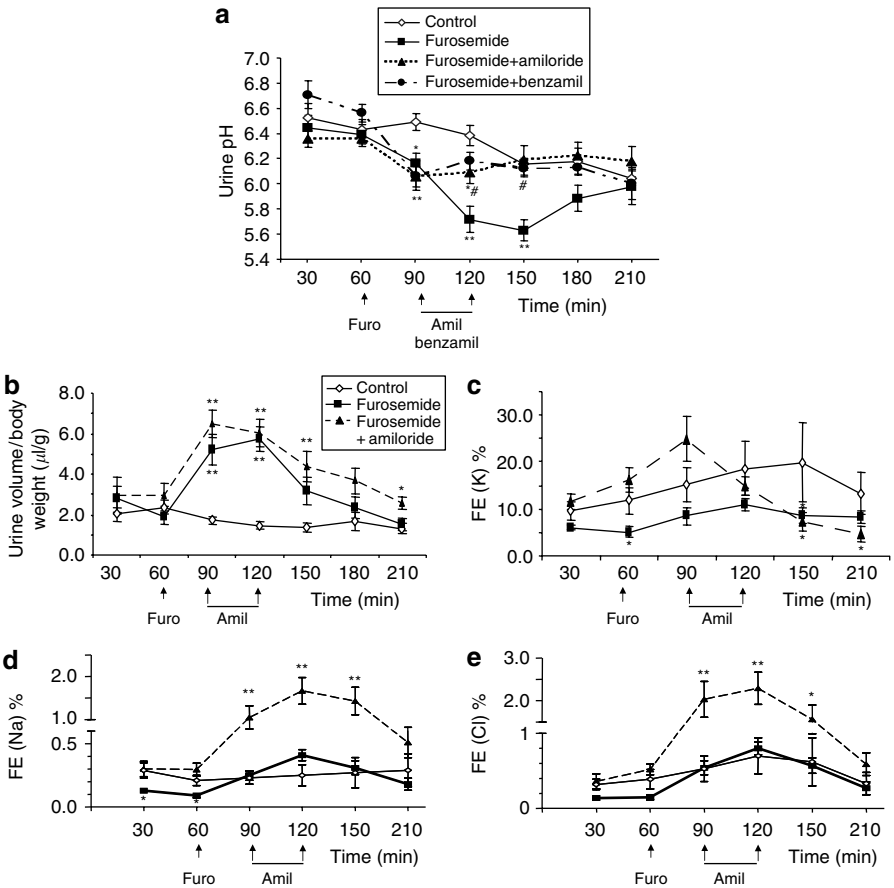

Figure 2 | Effect of furosemide and amiloride on urinary pH and electrolyte excretion. (**a**) Application of furosemide (2 μg/g BW) ($n=17$) caused acidification of urinary pH compared to untreated wild-type mice (*Atp6v1b1* +/+, $n=13$). The effect of furosemide on urine pH was reversed in mice treated subsequently with amiloride (5 μg/g BW) ($n=14$) or benzamil (2 μg/g BW) ($n=6$). (**b**) Urine production and excretion remained stable in the control group during the experiment, whereas it increased in furosemide- and amiloride-treated animals. (**c**) The FE (%) of potassium increased in furosemide-treated animals and was reversed by the addition of amiloride. (**d**, **e**) The FE % of sodium and chloride showed an increase of both electrolytes in the furosemide- and amiloride-treated animals. $^{*}P<0.05$ and $^{**}P<0.001$ versus control, $^{\#}P<0.05$ between furosemide treatment and furosemide+benzamil/furosemide+amiloride.

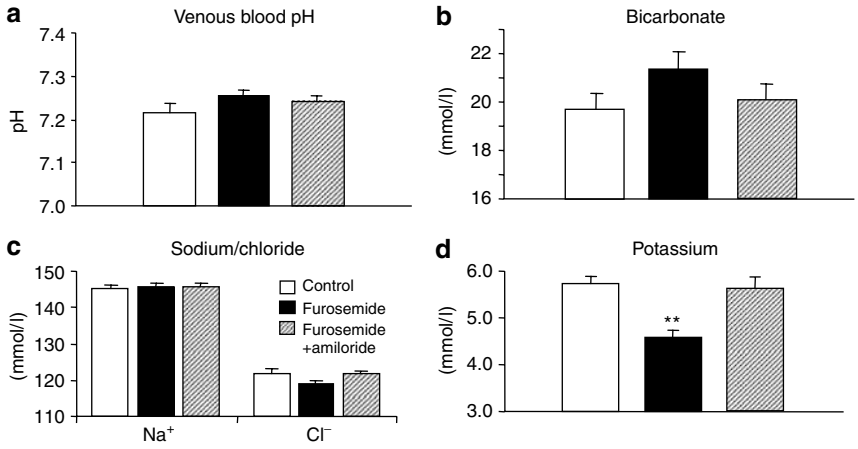

Figure 3 | Effect of furosemide and amiloride on blood pH and electrolytes. (**a–d**) Furosemide treatment resulted in decreased blood potassium concentration as expected from the increased urinary excretion. Blood bicarbonate levels showed a tendency to be higher which did not reach statistical significance. $^{**}P<0.001$ versus control.

consistent with a role of ENaC in the furosemide-induced urinary acidification. A similar effect of amiloride and the structurally unrelated ENaC blocker triamterene on the furosemide-induced urinary acidification has also been reported in rats.[30]

The furosemide-induced urinary acidification is reduced in mice deficient for the IC-specific vacuolar H^+-ATPase B1 subunit (ATP6V1B1)

To demonstrate that the furosemide-induced urinary acidification depended on the activity of vacuolar H^+-ATPases localized in ICs, we used a mouse model deficient for the IC-specific B1 subunit (*Atp6v1b1* −/−). *Atp6v1b1* −/− furosemide-treated mice exhibited a markedly higher basal urine pH than the *Atp6v1b1* +/+ furosemide-treated mice (pH 7.19±0.16 versus 6.44±0.10) and only a mild urinary acidification upon furosemide administration could be observed: pH 6.86±0.15 versus 5.72±0.10 after 120 min (Figure 4a). The residual urinary acidification observed in the B1-deficient mice may be owing to a partial compensation by the B2 isoform which is more luminally localized in ICs of *Atp6v1b1* −/− mice.[25] To assess the effect of the treatments on NAE, we measured total NH_3/NH_4^+ and total phosphate excretion in urine and estimated NAE from these data as the urine samples were too small to measure titratable acidity. Both total NH_3/NH_4^+ and total phosphate excretion increased in response to furosemide as described previously in rats.[30] Application of furosemide increased NAE from 2.9±0.3 mmol/l/mg/dl creatinine in control animals to 6.2±0.6 mmol/l/mg/dl creatinine (Figure 4b). In mice given amiloride, NAE showed a tendency to be lower ($P=0.08$). In contrast, in benzamil-treated mice and in the B1-deficient mice, NAE was significantly lower (benzamil: 3.7±0.6 mmol/l/mg/dl creatinine, B1 KO: 4.4±0.4 mmol/l/mg/dl creatinine).

Atp6v1b1 −/− furosemide-treated mice also had a strikingly higher urine output than the *Atp6v1b1* +/+ furosemide-treated mice after 60 min before the furosemide administration: 3.2±0.83 μl/g BW versus 1.9±0.34 μl/g BW (Figure 4c). Furosemide administration led to a more profound diuresis in *Atp6v1b1* −/− mice: 8.9±1.0 μl/g BW versus 5.2±0.7 μl/g BW after 90 min (Figure 4c). In addition, *Atp6v1b1* −/− mice had a significantly lower basal FE of potassium than *Atp6v1b1* +/+ mice (1.89±0.24 versus 6.09±0.60%) (Figure 4d), basal FE of sodium (0.06±0.01 versus 0.13±0.01%) (Figure 4e), and basal FE of chloride (0.04±0.01 versus 0.14±0.01%) (Figure 4f) pointing to a defect in urine concentration. Furosemide administration further revealed a significant difference in the FE of potassium, whereas the FE of sodium and chloride did not differ between *Atp6v1b1* −/− and *Atp6v1b1* +/+ mice (Figure 4e and f). As summarized in Table 1 and Figure 5, analysis of blood electrolytes revealed differences in potassium and bicarbonate levels.

The CD-specific loss of αENaC expression in Scnn1a^{loxloxCre} mice does not affect the furosemide-induced urinary acidification and diuretic response

Scnn1a^{loxloxCre} mice lack the alpha subunit of the ENaC in the CCD and MCD but not in the connecting segment.[17] We used these mice to test for the furosemide-stimulated urinary acidification. Basal urine output, urine pH, and electrolyte content were not significantly different between control mice (*Scnn1a*^{loxlox}) and mice with the specific ablation of αENaC expression (*Scnn1a*^{loxloxCre}) (compare Tables 1 and 2). Furosemide administration caused urinary acidification in both genotypes to a similar extent: *Scnn1a*^{loxlox} and *Scnn1a*^{loxloxCre} mice: pH 6.00±0.10 versus 5.89±0.09 after 120 min (Figure 6a). Also, estimated NAE at the time point 150 min was similar in both groups of mice (Figure 6b; Scnn1a^{loxlox} 5.4±0.9 mmol/l/mg/dl creatinine versus Scnn1a^{loxloxCre} 4.2±0.6 mmol/l/mg/dl creatinine, $P=0.31$). No difference between *Scnn1a*^{loxlox} and *Scnn1a*^{loxloxCre} mice in urine output could be detected (7.9±1.9 μl/g BW versus 8.2±1.1 μl/g BW after 90 min.) (Figure 6c). Furosemide also failed to unmask a possible difference between *Scnn1a*^{loxlox}

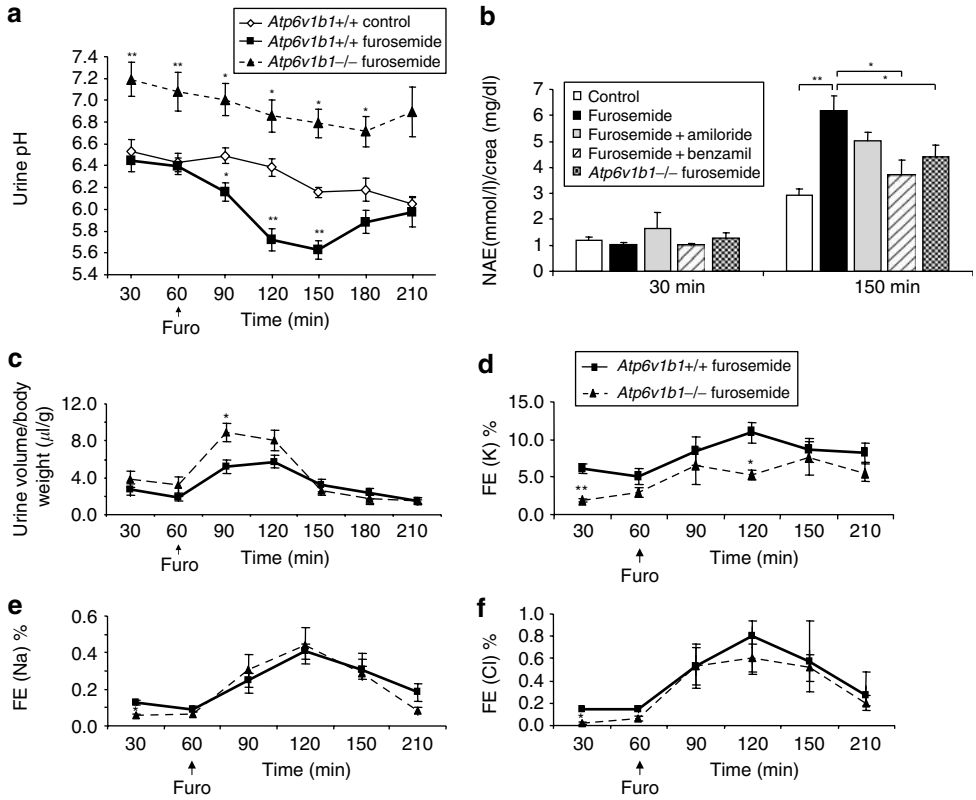

Figure 4 | Effect of furosemide on urine pH and electrolyte excretion in mice deficient for the B1 vacuolar H^+-ATPase subunit (*Atp6v1b1* −/−). (**a**) *Atp6v1b1* −/− received furosemide (2 µg/g BW) ($n = 9$) and urine pH acidified only mildly. $^{**}P < 0.001$ versus control. (**b**) Estimated NAE at the time point 30 min and 150 min. NAE increased after furosemide application and the rise in NAE was significantly reduced after application of benzamil and in the *Atp6v1b1*-deficient mice ($^{*}P < 0.05$ significant difference between furosemide-treated animals and other groups). (**c**) Furosemide administration led to a more profound diuresis in *Atp6v1b1* −/− in comparison to *Atp6v1b1* +/+ mice. (**d–f**) The FE of Na^+ and Cl^- was similar in both genotypes; however, the FE % for potassium was lower in B1-deficient mice. Values of control and furosemide-treated animals from Figure 2 are shown again for comparison. $^{*}P < 0.05$ and $^{**}P < 0.001$ versus *Atp6v1b1* +/+ treated with furosemide.

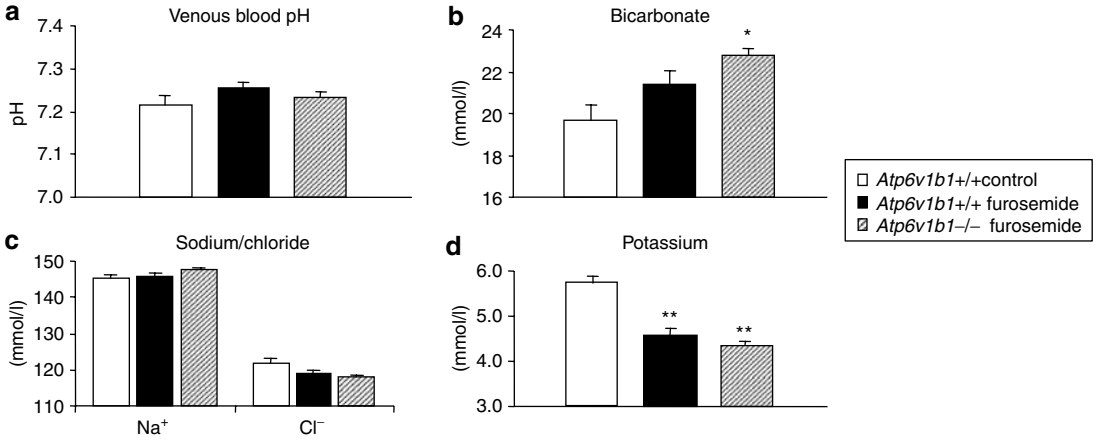

Figure 5 | Effect of furosemide on blood pH and electrolytes in *Atp6v1b1* −/− mice. (**a–d**) Blood potassium levels were also lower in B1-deficient mice after treatment with furosemide. Bicarbonate was higher than in untreated wild-type animals. Values from wild-type animals are shown again in Figure 3 for comparison. $^{*}P < 0.05$ and $^{**}P < 0.001$ versus control.

and *Scnn1a*^{loxloxCre} mice in the FE of sodium: 1.87 ± 0.42% versus 2.13 ± 0.54% after 120 min (Figure 6e and Table 2). However, blood electrolyte analysis revealed a significantly lower blood bicarbonate concentration (23.5 ± 0.7 mmol/l in *Scnn1a*^{loxlox} versus 21.3 ± 0.7 mmol/l in *Scnn1a*^{loxloxCre} (Table 2 and Figure 7b). Thus, after application of furosemide, no significant difference was found in the diuretic response, urinary acidification, and electrolyte excretion suggesting

Table 1 | Summary of blood pH, gas, and electrolytes of wild-type mice left untreated (control) and wild-type and Atp6V1b1-deficient mice treated with furosemide and amiloride at the end of the experimental period

	Atp6v1b1 +/+ control	*Atp6v1b1* +/+ furosemide	*Atp6v1b1* +/+ furosemide amiloride	*Atp6v1b1* −/− furosemide
pH	7.22 ± 0.02	7.24 ± 0.02	7.24 ± 0.02	7.25 ± 0.04
pCO_2 (mmHg)	50.6 ± 3.9	50.8 ± 2.0	47.7 ± 2.1	53.8 ± 7.4
HCO_3^- (mmol/l)	19.7 ± 1.0	21.0 ± 0.7	19.8 ± 0.4	21.8 ± 1.6*
K^+ (mmol/l)	5.7 ± 0.2	4.8 ± 0.3**	5.5 ± 0.2	4.3 ± 0.1**
Na^+ (mmol/l)	145.5 ± 0.8	147.7 ± 0.9	145.4 ± 0.5	147.6 ± 1.4
Cl^- (mmol/l)	121.8 ± 1.5	120.9 ± 0.8	121.1 ± 0.8	119.6 ± 2.4
Serum creatinine (mg/dl)	0.14 ± 0.02	0.11 ± 0.01	0.13 ± 0.02	0.12 ± 0.01
Weight (g)	27.5 ± 1.5	29.6 ± 1.1	25.4 ± 1.1	24.6 ± 1.0
CrCl/BW 30 min (μl/min/g)	18.3 ± 4.2	33.4 ± 6.1	15.6 ± 4.9	28.5 ± 6.0
CrCl/BW 90 min (μl/min/g)	18.7 ± 4.7	44.6 ± 8.5*	19.0 ± 3.4	26.6 ± 5.6
CrCl/BW 120 min (μl/min/g)	13.8 ± 3.9	33.2 ± 4.6**	22.1 ± 7.0	20.3 ± 9.2
NH_3/NH_4^+ (mM)/creatinine (mg/dl), 30 min	1.04 ± 0.05	0.94 ± 0.08	1.47 ± 0.52	1.18 ± 0.15
NH_3/NH_4^+ (mM)/creatinine (mg/dl), 150 min	1.40 ± 0.0.18	2.60 ± 0.08	2.04 ± 0.08	2.56 ± 0.26
NAE (mM/creatinine (mg/dl), 30 min	1.21 ± 1.11	1.03 ± 0.07	1.63 ± 0.64	1.29 ± 0.20
NAE (mM/creatinine (mg/dl), 150 min	2.91 ± 0.28	6.16 ± 0.59	5.02 ± 0.33	4.40 ± 0.44*

BW, body weight; CrCl, creatinine clearance; NAE, net acid excretion.
*Marks significant differences $P < 0.05$, **$P < 0.001$.

Table 2 | Summary of blood pH, gas, and electrolytes of *Scnn1a*^{loxlox} and *Scnn1a*^{loxloxCre} mice deficient for the alpha ENaC subunit treated with furosemide and hydrochlorothiazide

	Scnn1a^{loxlox} furosemide	*Scnn1a*^{loxloxCre} furosemide	*Scnn1a*^{loxlox} furosemide HCT	*Scnn1a*^{loxloxCre} furosemide HCT
pH	7.28 ± 0.02	7.28 ± 0.03	7.33 ± 0.03	7.25 ± 0.03
PCO_2 (mmHg)	51.4 ± 2.2	47.3 ± 3.1	43.9 ± 4.9	55.4 ± 2.1*
HCO_3^- (mmol/l)	23.5 ± 0.7	21.3 ± 0.7*	21.9 ± 0.9	23.3 ± 1.3
K^+ (mmol/l)	4.4 ± 0.2	4.4 ± 0.3	4.5 ± 0.2	4.9 ± 0.2
Na^+ (mmol/l)	147.8 ± 0.9	147.8 ± 0.7	147.6 ± 0.8	148.0 ± 0.5
Cl^- (mmol/l)	119.9 ± 1.8	120.2 ± 1.3	114.2 ± 1.5	114.6 ± 1.6
Serum creatinine (mg/dl)	0.15 ± 0.02	0.11 ± 0.01	0.14 ± 0.03	0.13 ± 0.02
Weight (g)	25.4 ± 1.9	24.9 ± 1.2	33.6 ± 1.7	29.9 ± 1.9
CrCl/BW 30 min (μl/min/g)	14.4 ± 3.4	21.7 ± 3.3	24.15 ± 6.3	29.0 ± 4.4
CrCl/BW 90 min (μl/min/g)	21.5 ± 3.7	20.8 ± 2.7	21.6 ± 3.0	22.4 ± 4.1
CrCl/BW 120 min (μl/min/g)	10.5 ± 2.0	13.9 ± 2.2	12.8 ± 1.7	13.4 ± 2.4
NH_3/NH_4^+ (mM)/creatinine (mg/dl), 30 min	1.25 ± 0.30	1.47 ± 0.73		
NH_3/NH_4^+ (mM)/creatinine (mg/dl), 150 min	2.24 ± 0.36	1.82 ± 0.24		
NAE (mM/creatinine (mg/dl), 30 min	1.46 ± 0.32	1.93 ± 0.70		
NAE (mM/creatinine (mg/dl), 150 min	5.41 ± 0.90	4.25 ± 0.60		

BW, body weight; CrCl, creatinine clearance; NAE, net acid excretion.
*Marks significant differences $P < 0.05$, **$P < 0.001$.

that preserved expression of αENaC in the CNT is sufficient to maintain the furosemide-induced urinary acidification.

In order to inhibit a possible compensatory increase in Na^+ absorption in the distal tubule via the thiazide-sensitive Na^+/Cl^- cotransporter, furosemide was applied together with hydrochlorothiazide. Figure 8a shows that the urinary pH of *Scnn1a*^{loxloxCre} mice did not differ significantly from the urine pH of *Scnn1a*^{loxlox} mice before furosemide and hydrochlorothiazide (furo + HCT) administration. After administration of furosemide together with hydrochlorothiazide (furo + HCT), *Scnn1a*^{loxloxCre} mice decreased their urine pH to the same extent as the *Scnn1a*^{loxlox} mice: pH 5.77 ± 0.12 versus pH 5.66 ± 0.10 after 120 min. Urine output, fractional electrolyte excretion and systemic electrolyte, and blood gas status were not distinguishable between both mouse lines (Figures 8 and 9 and Table 2).

DISCUSSION

In the present study, we investigated the functional interaction between renal Na^+ reabsorption through ENaC and H^+ secretion by vacuolar H^+-ATPases in the connecting segment and CCD. Both ENaC and vacuolar H^+-ATPases containing the B1 subunit isoform are expressed together in the same nephron segments, namely CNT and CCD in neighboring cells. H^+ secretion by vacuolar H^+-ATPases is electrogenic and thought to be indirectly coupled to Na^+ reabsorption.[31] According to this hypothesis, Na^+ reabsorption through ENaC creates a more lumen-negative transtubular voltage which in turn would enhance H^+ secretion by vacuolar H^+-ATPases. Thus, the furosemide-induced increase in Na^+ delivery to the CNT and CCD and the subsequent reabsorption of this delivered fraction through ENaC may result in urinary acidification mediated by vacuolar H^+-ATPases.

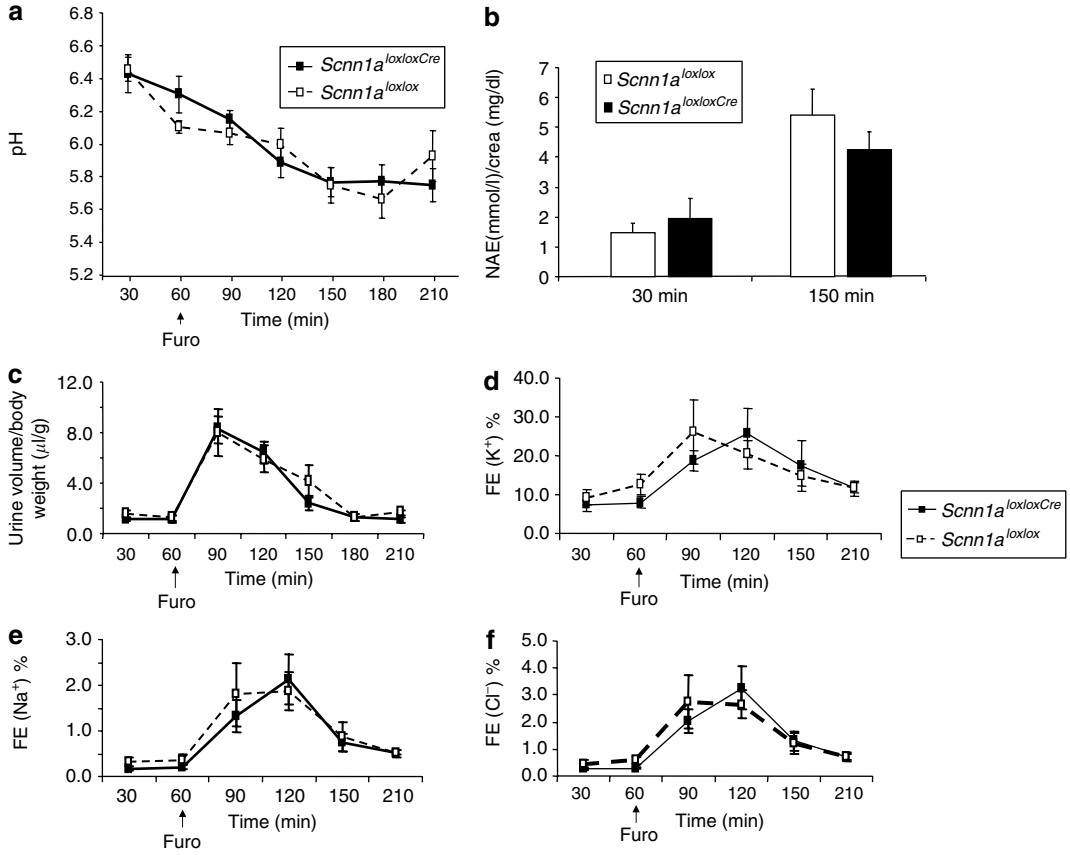

Figure 6 | Effect of furosemide on urine pH and electrolyte excretion in *Scnn1a*^{loxlox} and *Scnn1a*^{loxloxCre} mice. (**a**) The effect of furosemide on urinary acidification in *Scnn1a*^{loxlox} ($n=10$) and *Scnn1a*^{loxloxCre} ($n=12$) mice. Furosemide administration did not show any difference in urine pH between *Scnn1a*^{loxlox} and *Scnn1a*^{loxloxCre} mice. (**b**) No difference in the furosemide-induced increase in the estimated rate of NAE was observed between *Scnn1a*^{loxlox} and *Scnn1a*^{loxloxCre} treated with furosemide. (**c**) Urine volume/BW in *Scnn1a*^{loxlox} ($n=11$) and *Scnn1a*^{loxloxCre} ($n=10$) mice. No difference between *Scnn1a*^{loxlox} and *Scnn1a*^{loxloxCre} mice in urine output was reported. (**d**–**f**) FE of potassium, sodium, and chloride in *Scnn1a*^{loxlox} ($n=6$) and *Scnn1a*^{loxloxCre} ($n=7$) mice. Furosemide-induced increase of FE of potassium, sodium, and chloride did not differ between *Scnn1a*^{loxlox} and *Scnn1a*^{loxloxCre} mice.

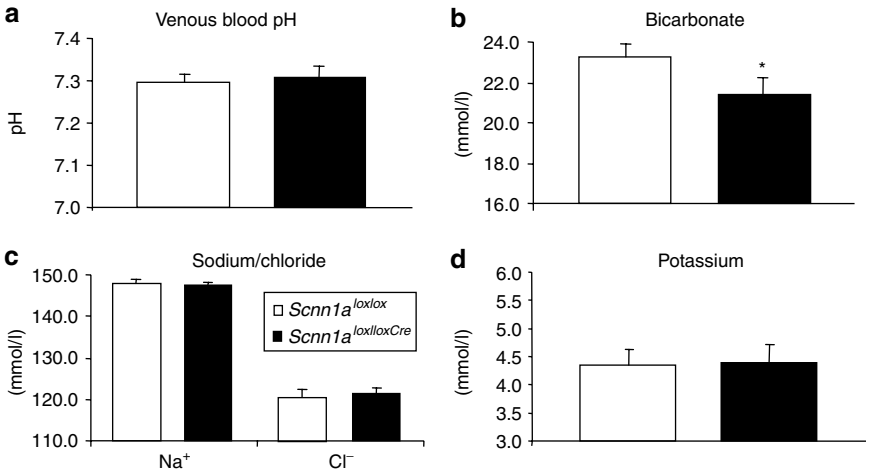

Figure 7 | Effect of furosemide on blood pH and electrolytes in *Scnn1a*^{loxlox} and *Scnn1a*^{loxloxCre} mice. *Scnn1a*^{loxloxCre} mice had a significantly lower bicarbonate concentration. Other parameters were not different. *$P<0.05$ versus *Scnn1a*^{loxlox}.

Several types of defects in distal renal tubular acidification have been classified based on provocative tests using infusions containing sulfate, bicarbonate, or phosphate, oral NH_4Cl loading or furosemide application and the respective response in urinary pH, net acid, and electrolyte excretion as well as the ability to sustain a blood–urine PCO_2 gradient.[32] At least three types of dRTA have been distinguished, a 'secretory type' with a defect supposed in the proton-secretory proton pumps, a

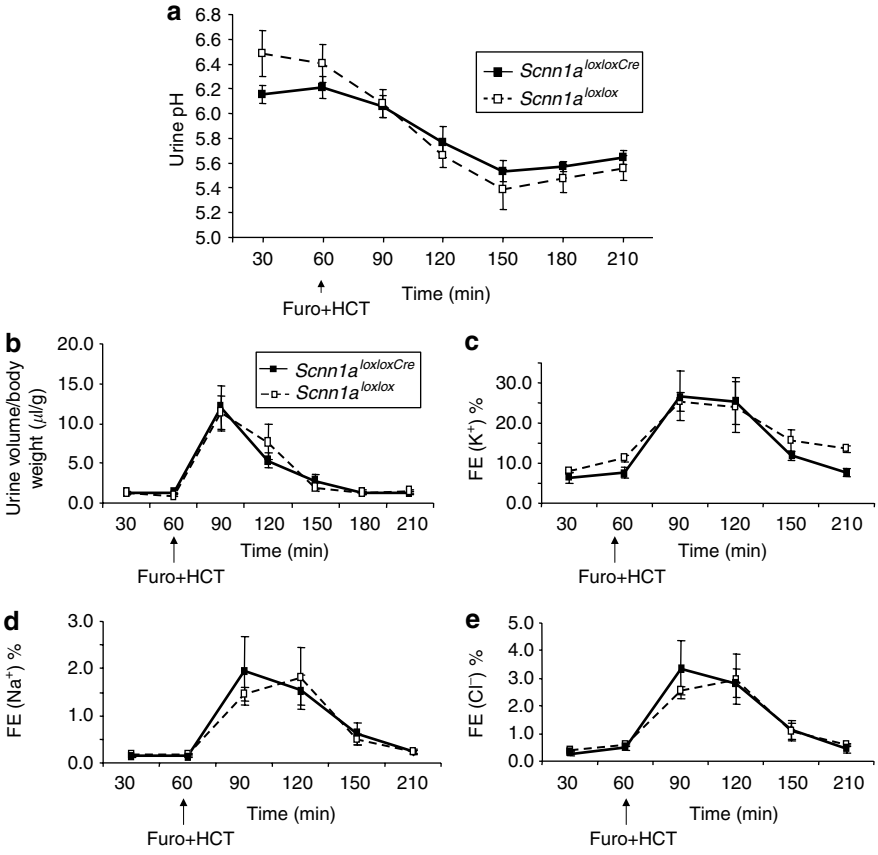

Figure 8 | (a) Effect of furosemide (2 µg/g BW) and hydrochlorothiazide (HCT, 0.05 µg/g BW) on urinary acidification in *Scnn1a*^{loxlox} ($n = 6$) and *Scnn1a*^{loxloxCre} ($n = 6$) mice. Urine pH of *Scnn1a*^{loxloxCre} mice did not differ significantly from the urine pH of *Scnn1a*^{loxlox} mice neither before nor after furosemide + HCT administration. (**b**–**e**) Urine output and FE of potassium, sodium, and chloride in furosemide- and hydrochlorothiazide-treated *Scnn1a*^{loxlox} ($n = 5$) and *Scnn1a*^{loxloxCre} ($n = 7$) mice. No difference between *Scnn1a*^{loxlox} and *Scnn1a*^{loxloxCre} mice in urine output, FE of potassium, sodium, and chloride was reported.

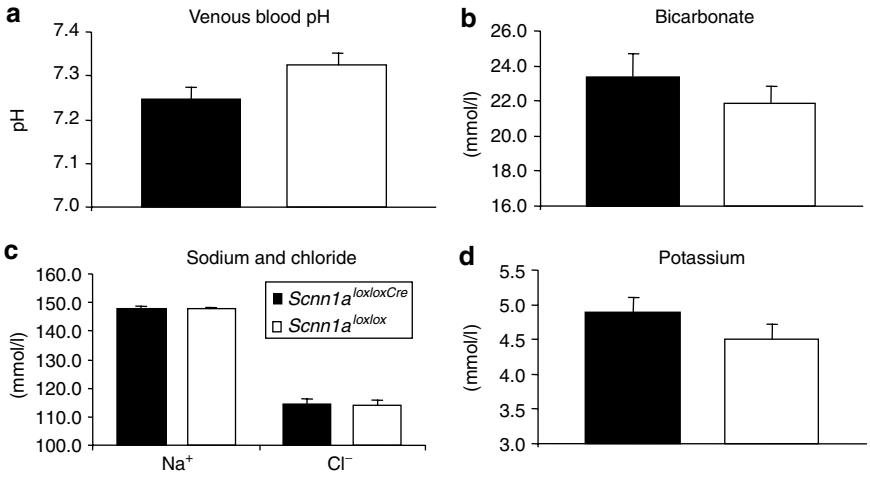

Figure 9 | Blood pH and electrolytes in furosemide- and hydrochlorothiazide-treated *Scnn1a*^{loxlox} ($n = 5$) and *Scnn1a*^{loxloxCre} ($n = 7$) mice. No significant difference between *Scnn1a*^{loxlox} *and Scnn1a*^{loxloxCre} mice in blood pH and electrolytes could be observed.

'back-leak type' where H^+ or HCO_3^- may leak back, and a 'voltage-defective type' where the inability to produce an acid urine may result from the failure to produce a favorable lumen-negative potential facilitating proton secretion.[9,26,33] Consistent with these functional classifications, application of amiloride to patients and experimental animals reduces urinary proton secretion.[9,32,34] LiCl has been used as another tool to induce the voltage-dependent defect; however, several

studies have indicated that the defects induced by LiCl and amiloride are different.[35] The defect induced by administration of LiCl can be restored by Na_2SO_4 infusion[32] and is associated with altered expression levels of H^+/K^+-ATPases and H^+-ATPases.[36]

In our experiments, furosemide induced a strong urinary acidification. This acidification apparently depends on the activity of vacuolar H^+-ATPases containing the B1 isoform as no or only a mild acidification could be observed in *Atp6v1b1* deficient mice. Thus, vacuolar H^+-ATPases are the main mediator of the furosemide-induced urinary acidification. The result also suggests that H^+/K^+-ATPases, the other potential acid-secretory pumps, do not play an important role as an acid-secretory mechanism under these experimental conditions. However, we observed a lower urinary potassium excretion in the B1-deficient mice. The mechanism is presently unknown. A stimulation of H^+/K^+-ATPases, potentially induced by a higher urinary flow rate, could contribute to this effect.

The effect of furosemide was blunted by amiloride inhibiting ENaC-dependent Na^+ absorption as evident from the increased fractional Na^+ excretion and decreased fractional K^+-excretion. In a separate group of animals, the consequence of the genetic ablation of ENaC channel function was tested in *Scnn1a*^{loxloxCre} mice. These animals lack the alpha subunit of ENaC which is essential for ENaC function and results in no detectable ENaC channel function and loss of luminal localization of beta and gamma subunits in the CCD and outer medullary CD.[17] In the CNT, however, ENaC function and localization has remained normal.[17] In the control and αENaC-deficient mice, furosemide induced normal urinary acidification with a similar increase in fractional Na^+, Cl^-, and K^+ excretion. In order to rule out a compensatory increase in Na^+ absorption by the thiazide-sensitive Na^+/Cl^- cotransporter, we also tested for the combined effect of furosemide and hydrochlorothiazide which caused a stronger urinary acidification and diuretic response to the same extent in both groups of animals. Thus, the furosemide-induced urinary acidification involves the activity of an amiloride- and benzamil-sensitive mechanism, most likely ENaC. In view of the normal capacity of *Scnn1a*^{loxloxCr} mice to reabsorb Na^+ and to respond to furosemide and hydrochlorothiazide, it appears that the residual ENaC function in the CNT may be sufficient for the furosemide-induced urinary acidification. However, it cannot be completely ruled out that amiloride acts also on a mechanism distinct from ENaC and that this mechanism is still operative in the *Scnn1a*^{loxloxCre} mice. Based on mathematical modelling of transport processes involved in acid secretion and electrolyte transport along the CD, it has been recently proposed that the generation of a more lumen-negative potential by the action of ENaC could hardly account for changes in vacuolar H^+-ATPase activity.[7] Weinstein[7] argued that the change in transtubular voltage is minor compared to the ability of the pump to be active even against a larger voltage gradient, and proposed that amiloride interacts also with other mechanisms. These calculations were made for the CCD and may not fully apply for the CNT which was identified here as the main target of furosemide. However, our results do not completely rule out that some of the urinary acidification induced by furosemide took place in the CCD and that amiloride acted on a mechanism distinct from ENaC. This mechanism, however, remains to be identified and local opposing pH gradients must also be taken into consideration. In addition, Hropot *et al.*[30] reported that the structurally unrelated triamterene has a similar inhibitory effect on the furosemide-induced urinary acidification strongly suggesting that ENaC is the common target.

This identifies the CNT as the major segment mediating furosemide-induced urinary acidification. Similar conclusions have been reached with respect to the Na^+-absorbing capacity of the CNT versus CCD.[17] Further experiments establishing a complete genetic ablation of αENaC expression along the entire CNT and CD will be helpful to prove this hypothesis.

In summary, the furosemide-induced urinary acidification requires vacuolar H^+-ATPases containing the B1 subunit, is inhibited by amiloride, and is not altered in a mouse model with preserved ENaC function in the CNT but loss of ENaC function in the CCD and outer medullary collecting duct. The results point to a hitherto unrecognized major role of the CNT in electrogenic H^+-secretion and the urinary acidification induced by furosemide.

MATERIALS AND METHODS

Animals

Experiments were performed on *Atp6v1b1* +/+ and *Atp6v1b1* −/− mice[25]) and *Scnn1a*^{loxloxCre} and *Scnn1a*^{loxlox} mice.[17] They were maintained on a standard diet and had a free access to drinking water. All experiments were performed according to Swiss Animal Welfare laws and approved by the Local Veterinary Authority.

The generation, breeding, and genotyping of *Atp6v1b1*−/−, *Scnn1a*^{loxlox}, and *Scnn1a*^{loxloxCre} has been described previously.[17,25]

Blood and urinary parameters

Mice were anesthetized intraperitoneally (ketamine 1 μl/g BW and xylazine 1 μl/g BW), placed on a heated table maintained at 37°C and a catheter was placed into the urinary bladder. Urine was collected every 30 min during the whole period of 3.5 h for the measurement of urine volume, pH, sodium, chloride, potassium, and creatinine concentrations. To prevent dehydration, mice were constantly supplemented with 125 mM NaCl and 25 mM $NaHCO_3$ (pH 7.4) according to their urinary output. At the end of the experiment, heparinized mixed venous blood was collected for the measurement of pH, blood gases, sodium, potassium, chloride, and creatinine concentrations. After an initial recovery phase and collection of a baseline value at 30 min, at 60 min *Atp6v1b1* +/+, *Atp6v1b1* −/−, *Scnn1a*^{loxlox}, and *Scnn1a*^{loxloxCre} mice were administered furosemide 2 μg/g BW subcutaneously; some of the *Scnn1a*^{loxlox} and *Scnn1a*^{loxloxCre} mice were also given hydrochlorothiazide 0.05 μg/g BW together with furosemide. Two subgroups of *Atp6v1b1* +/+ mice received additionally amiloride 5 μg/g BW subcutaneously or benzamil 2 μg/g BW subcutaneously after 90 and 120 min of the experiment. All drugs were finally dissolved in

125 mM NaCl + 25 mM $NaHCO_3$. Control mice received only 125 mM NaCl + 25 mM $NaHCO_3$.

Urinary pH was immediately measured; urine and blood electrolytes and other blood parameters (pCO_2, pO_2) were determined using a blood gas analyzer (ABL 505, Radiometer, Copenhagen, Denmark). Urinary creatinine was measured by the Jaffe method. Serum creatinine was determined by an enzymatic reaction (F DAOS method, Wako Creatinine F L-Type kit, Wako Chemicals GmbH, Germany). Total urinary NH_3/NH_4^+ was measured using the Berthelot protocol,[37] total urinary phosphate using a commercial kit (Sigma, Buchs, Switzerland). NAE was estimated from the concentration of total NH_3/NH_4^+, total phosphate as the major titratable acid, and urine pH using the Henderson–Hasselbalch equation and assuming blood pH 7.4.

Immunohistochemistry

Fixation of mouse kidneys and tissue processing for immunohistochemistry was performed as described previously.[28] Consecutive cryosections (4–5 μm thick) of the fixed kidneys were placed on chrom-alum gelatine-coated slides, preincubated with 10% normal goat serum in phosphate-buffered saline, and afterwards incubated overnight at 4°C with mouse-anti-chicken calbindin D28k antibodies (Swant Bellinzona, Switzerland, dilution 1/20 000 in phosphate-buffered saline-1% bovine serum albumin) that was applied together with either rabbit-anti-rat βENaC antisera[17] (dilution 1/1000 in phosphate-buffered saline-1% bovine serum albumin) or rabbit-anti-rabbit B1 subunit of H^+-ATPase[20] (dilution 1/1000 in phosphate-buffered saline-1% bovine serum albumin). Binding sites of the primary antibodies were revealed with fluorescein isothiocynate-coupled goat-anti-mouse immunoglobulin G and Cy3-coupled goat-anti-rabbit immunoglobulin G (both from Jackson Immuno Research Laboratories, West Grove, PA, USA).

Statistical analysis

All data were tested for statistical analysis using paired and unpaired Student's *t*-tests and analysis of variance, and only data with $P < 0.05$ were considered statistically significant. A minimum of 6–8 animals was used for each measurement and treatment.

ACKNOWLEDGMENTS

The study has been supported by grants from the Swiss National Research foundation to CA Wagner (31-068318) and J Loffing (3200B0-105769/1) and the University Research Priority Program 'Integrative Human Physiology' of the University of Zurich. We acknowledge the technical assistance of Nicole Fowler-Jaeger.

REFERENCES

1. Schuster VL. Function and regulation of collecting duct intercalated cells. *Annu Rev Physiol* 1993; **55**: 267–288.
2. Kim J, Kim YH, Cha JH *et al.* Intercalated cell subtypes in connecting tubule and cortical collecting duct of rat and mouse. *J Am Soc Nephrol* 1999; **10**: 1–12.
3. Alper SL, Natale J, Gluck S *et al.* Subtypes of intercalated cells in rat kidney collecting duct defined by antibodies against erythroid band 3 and renal vacuolar H^+-ATPase. *Proc Natl Acad Sci USA* 1989; **86**: 5429–5433.
4. Wagner CA, Finberg KE, Breton S *et al.* Renal vacuolar H^+-ATPase. *Physiol Rev* 2004; **84**: 1263–1314.
5. Wagner CA, Geibel JP. Acid-base transport in the collecting duct. *J Nephrol* 2002; **5**(suppl): S112–S127.
6. Koeppen BM, Helman SI. Acidification of luminal fluid by the rabbit cortical collecting tubule perfused *in vitro*. *Am J Physiol* 1982; **242**: F521–F531.
7. Weinstein AM. A mathematical model of rat collecting duct III. Paradigms for distal acidification defects. *Am J Physiol Renal Physiol* 2002; **283**: F1267–F1280.
8. Weinstein AM. A mathematical model of rat collecting duct I. Flow effects on transport and urinary acidification. *Am J Physiol Renal Physiol* 2002; **283**: F1237–F1251.
9. Batlle DC. Segmental characterization of defects in collecting tubule acidification. *Kidney Int* 1986; **30**: 546–554.
10. Chang H, Fujita T. A numerical model of acid–base transport in rat distal tubule. *Am J Physiol Renal Physiol* 2001; **281**: F222–F243.
11. Loffing J, Kaissling B. Sodium and calcium transport pathways along the mammalian distal nephron: from rabbit to human. *Am J Physiol Renal Physiol* 2003; **284**: F628–F643.
12. Jacobsen HJ, Furuya H, Breyer MD. Mechanism and regulation of proton transport in the outer medullary collecting duct. *Kidney Int* 1991; **40**: S51–S56.
13. Kellenberger S, Schild L. Epithelial sodium channel/degenerin family of ion channels: a variety of functions for a shared structure. *Physiol Rev* 2002; **82**: 735–767.
14. Rossier BC, Pradervand S, Schild L *et al.* Epithelial sodium channel and the control of sodium balance: interaction between genetic and environmental factors. *Annu Rev Physiol* 2002; **64**: 877–897.
15. Lifton RP, Gharavi AG, Geller DS. Molecular mechanisms of human hypertension. *Cell* 2001; **104**: 545–556.
16. Hummler E, Barker P, Gatzy J *et al.* Early death due to defective neonatal lung liquid clearance in alpha-ENaC-deficient mice. *Nat Genet* 1996; **12**: 325–328.
17. Rubera I, Loffing J, Palmer LG *et al.* Collecting duct-specific gene inactivation of alphaENaC in the mouse kidney does not impair sodium and potassium balance. *J Clin Invest* 2003; **112**: 554–565.
18. Nelson N, Harvey WR. Vacuolar and plasma membrane proton-adenosinetriphosphatases. *Physiol Rev* 1999; **79**: 361–385.
19. Nishi T, Forgac M. The vacuolar (H+)-ATPases – nature's most versatile proton pumps. *Nat Rev Mol Cell Biol* 2002; **3**: 94–103.
20. Finberg KE, Wagner CA, Stehberger PA *et al.* Molecular cloning and characterization of *Atp6v1b1*, the murine vacuolar H^+-ATPase B1-subunit. *Gene* 2003; **318**: 25–34.
21. Breton S, Smith PJ, Lui B, Brown D. Acidification of the male reproductive tract by a proton pumping (H^+)-ATPase. *Nat Med* 1996; **2**: 470–472.
22. Wax MB, Saito I, Tenkova T *et al.* Vacuolar H^+-ATPase in ocular ciliary epithelium. *Proc Natl Acad Sci USA* 1997; **94**: 6752–6757.
23. Karet FE, Finberg KE, Nelson RD *et al.* Mutations in the gene encoding B1 subunit of H^+-ATPase cause renal tubular acidosis with sensorineural deafness. *Nat Genet* 1999; **21**: 84–90.
24. Nelson RD, Guo XL, Masood K *et al.* Selectively amplified expression of an isoform of the vacuolar H^+-ATPase 56-kilodalton subunit in renal intercalated cells. *Proc Natl Acad Sci USA* 1992; **89**: 3541–3545.
25. Finberg KE, Wagner CA, Bailey MA *et al.* The B1 subunit of the H^+ATPase is required for maximal urinary acidification. *Proc Nat Acad Sci USA* 2005; **102**: 13616–13621.
26. Arruda JA, Kurtzman NA. Mechanisms and classification of deranged distal urinary acidification. *Am J Physiol* 1980; **239**: F515–F523.
27. DuBose Jr TD, Alpern RJ. Renal tubular acidosis. In: Scriver CR, Beaudet AL, Sly WS, Valle D (eds). *The Metabolic and Molecular Bases of Inherited Disease*, 8th edn, McGraw-Hill: New York, 2001, pp 4983–5021.
28. Loffing J, Loffing-Cueni D, Valderrabano V *et al.* Distribution of transcellular calcium and sodium transport pathways along mouse distal nephron. *Am J Physiol Renal Physiol* 2001; **281**: F1021–F1027.
29. Biner HL, Arpin-Bott MP, Loffing J *et al.* Human cortical distal nephron: distribution of electrolyte and water transport pathways. *J Am Soc Nephrol* 2002; **13**: 836–847.
30. Hropot M, Fowler N, Karlmark B *et al.* Tubular action of diuretics: distal effects on electrolyte transport and acidification. *Kidney Int* 1985; **28**: 477–489.
31. Hamm LL, Alpern RJ. Cellular mechanisms of renal tubular acidification. In: Seldin DW, Giebisch G (eds). *The Kidney: Physiology and Pathophysiology*, 3rd edn, Lippincott Williams & Wilkins: Philadelphia, 2000, pp 1935–1979.
32. DuBose Jr TD, Caflisch CR. Validation of the difference in urine and blood carbon dioxide tension during bicarbonate loading as an index of distal nephron acidification in experimental models of distal renal tubular acidosis. *J Clin Invest* 1985; **75**: 1116–1123.

33. Batlle D, Flores G. Underlying defects in distal renal tubular acidosis: new understandings. *Am J Kidney Dis* 1996; **6**: 896–915.
34. Kornandakieti C, Tannen RL. H^+ transport by the aldosterone-deficient rat distal nephron. *Kidney Int* 1984; **25**: 629–635.
35. Mehta PK, Sodhi B, Arruda JA, Kurtzman NA. Interaction of amiloride and lithium on distal urinary acidification. *J Lab Clin Med* 1979; **93**: 983–994.
36. Eiam-Ong S, Dafnis E, Spohn M *et al.* H-K-ATPase in distal renal tubular acidosis: urinary tract obstruction, lithium, and amiloride. *Am J Physiol* 1993; **265**: F875–F880.
37. Quentin F, Chambrey R, Trinh-Trang-Tan MM *et al.* The Cl^-/HCO_3^- exchanger pendrin in the rat kidney is regulated in response to chronic alterations in chloride balance. *Am J Physiol Renal Physiol* 2004; **287**: F1179–F1188.

The B1 H^+-ATPase (Atp6v1b1) subunit is required for type B intercalated cell function during alkalosis

Jana Kovacikova[1], Karin Finberg[2], Carsten A. Wagner[1]

[1]Institute of Physiology and Zurich Center for Human Integrative Physiology (ZIHP), University of Zurich, Zurich, Switzerland; [2]Department of Pathology, Massachusetts General Hospital, Harvard Medical School, Boston, MA, USA

Corresponding author:
Carsten A. Wagner
Institute of Physiology
University of Zurich
Winterthurerstrasse 190
CH-8057 Zurich
Switzerland
Phone: +41-44-63 50659
Fax: +41-44-63 56814
E-mail: Wagnerca@access.unizh.ch

ABSTRACT

Non-type A intercalated cells (IC) in the connecting tubule (CNT) and cortical collecting duct (CCD) express the luminal Cl^-/HCO_3^- exchanger pendrin and apical and/or basolateral vacuolar H^+-ATPases containing the B1 subunit isoform. The main function of non-type A-ICs is the excretion of bicarbonate during metabolic alkalosis. Non-type A-IC may also participate in chloride reabsorption. Mutations in the B1 subunit (ATP6V1B1) in man cause distal renal tubular acidosis due to its importance in acid secretion by type A-ICs. However, the function of the B1 isoform in non-type A-ICs has remained elusive. Induction of metabolic alkalosis resulted in a more pronounced alkalosis in B1 deficient mice associated with increased blood bicarbonate, hypokalemia, and hypochloremia. Furthermore, total pendrin expression was reduced in B1 deficient mice whereas the relative abundance of pendrin expressing cells was increased. H^+-ATPase activity in ICs was strongly reduced. Moreover, the a4 and A H^+-ATPase subunits did not associate with the basolateral domain of B1 deficient non-A-ICs. Thus, the B1 subunit is required for the formation of complete and functional basolateral H^+-ATPases complexes. B1 deficient mice excreted also larger quantities of urine which was associated with lower AQP-2 water channel abundance and a higher relative frequency of principal cells in the connecting tubule. Thus, the B1 H^+-ATPase subunit is critical for normal non-type A IC function and its loss may also affect the function of principal cells.

INTRODUCTION

The final urinary secretion of acid or base equivalents is fine tuned by intercalated cells (IC) along the connecting tubule (CNT) and collecting duct (CD) and involves the action of vacuolar H^+-ATPases and several Cl^-/HCO_3^- -exchangers. Many studies have described functionally and morphologically at least two types of IC: type A and type B (1, 15, 25). The existence of a third type (non-A-non-B IC) has been proposed (12, 27). However, the functional significance of this subtype has not been clarified. A type IC secrete protons via an apically expressed vacuolar H^+-ATPase (32). This proton secretion is functionally coupled to the basolateral anion exchanger AE1 releasing bicarbonate into blood. Non-type A-ICs (i.e. type B-IC and non-A-non-B-IC) express the anion exchanger pendrin apically and vacuolar H^+-ATPases on the apical and/or basolateral membrane and functionally reverse these processes, thus, secreting bicarbonate (25, 34). Thus, non-A-IC mediate the excretion of an alkali-load during metabolic alkalosis (15, 25). Furthermore, recently a role of non-A-ICs in transcellular chloride reabsorption via the apical Cl^-/HCO_3^- -exchanger pendrin has been proposed (22, 28, 37, 39).

The vacuolar H^+-ATPase is composed of at least 13 subunits. Several studies (18, 42) demonstrated that the B subunit plays an essential role in vacuolar H^+-ATPase function. This subunit is a part of the peripheral catalytic V_1 domain and exists in two highly homologous isoforms: B1 and B2 (29). The B2 subunit is considered to be ubiquitous and seems mainly to mediate the acidification of intracellular organelles. The B1 subunit, on the contrary, has been identified in a limited number of tissues, often in cells where plasma membrane H^+-ATPase mediates proton extrusion. The B1 subunit has been detected in specialized cells of the epididymis (3, 4, 7), the vas deferens, the ciliar body of the eye (41), in the inner ear (11) and in all subtypes of intercalated cells of the kidney (7, 19).

Mutations in the gene encoding the B1 subunit (ATP6V1B1) result in distal renal tubular acidosis (dRTA) in man characterized by the inability of the distal nephron to appropriately acidify the urine (11). A mouse model deficient for the *Atp6v1b1* gene showed impaired H^+-secretion in the collecting duct (6, 14). These findings demonstrate the importance of the B1 subunit as a part of the apical H^+-ATPase complex for normal type A-

IC function. However, the function of H^+-ATPases containing the B1 subunit in non-type A-ICs has remained elusive to date.

Basolateral H^+-ATPases in type B IC are thought to be important for H^+ absorption during metabolic alkalosis. Metabolic alkalosis causes hypertrophy of type B-IC with amplification of the basolateral plasma membrane and the insertion of proton pumps into this membrane (25). Thus, IC respond to metabolic alkalosis by increasing bicarbonate secretion presumably via the apical Cl^-/HCO_3^- -exchanger pendrin, and enhancement of proton absorption across the basolateral membrane of type B IC.

In non-type A-IC H^+-ATPases function in series with pendrin (PDS). In the kidney, pendrin is expressed exclusively in the distal convoluted tubule (DCT), CNT, and CCD in the apical membrane of non-type A-ICs (38). However, pendrin deficient mice are not spontaneously alkalotic. Under conditions that increase pendrin function such as administration of aldosterone analogues together with $NaHCO_3$ application or dietary NaCl restriction, differences between *Pds* -/- and *Pds*+/+ mice in arterial blood pH and blood pressure become apparent (30, 39).

Here we tested for a role of H^+-ATPases containing the B1 isoform in the function of non-type A intercalated cells and used a mouse model lacking the B1 subunit (Atp6v1b1-/-). During metabolic alkolosis, B1 deficient mice displayed a distinct defect of non-type A-ICs.

METHODS

Animals

Experiments were performed on *Atp6v1b1 +/-* and *Atp6v1b1 -/-* mice (6) All experiments were performed according to Swiss Animal Welfare laws and approved by the local veterinary authority (Kantonales Veterinäramt Zürich). The generation and breeding of *Atp6v1b1-/-* deficient mice (all in the C57BL/6J background) has been described previously (6, 14).

Metabolic cage studies

Atp6v1b1 +/- and *Atp6v1b1 -/-* mice (male, 6-10 animals per group) were kept in metabolic cages and had free access to standard mouse chow and drinking water. After 24 hours urine was collected, mice were injected with deoxycorticosterone acetate (DOCA) 2 mg/ animal s.c. and switched to alkaline diet for 4 days. The alkaline diet consisted of standard mouse chow and addition of 0.28 M $NaHCO_3$ plus 2 % sucrose to drinking water. Daily food and water intake, and body weights were measured and urine was collected under oil. At the end of experiment mixed arterial and venous blood was collected for the measurement of pH, blood gases, electrolytes, and creatinine concentrations.

Urinary pH was measured using a pH microelectrode, urine and blood electrolytes and other blood parameters (pCO_2, pO_2) were determined using a blood gas analyzer (ABL 505, Radiometer, Copenhagen, Denmark). Urinary creatinine was measured by the Jaffe method. Creatinine in serum was determined by an enzymatic reaction (F DAOS method) using a commercial kit (Wako Creatinine F L-Type kit, Wako Chemicals GmbH, Germany). Urinary ammonium was measured by the method of Berthelot, urinary phosphate and citrate were determined using a commercial kit (Sigma Diagnostics, St. Louis, Mo., USA and Citric acid kit, Boehringer Mannheim, Germany).

Immunohistochemistry

Atp6v1b1 +/- and *Atp6v1b1 -/-* mice were anesthetized with ketamine/xylazine and perfused through the left ventricle with PBS followed by paraformaldehyde-lysine-periodate (PLP) fixative (16). Kidneys were removed and fixed overnight at 4°C by immersion in PLP. Kidneys were washed three times with PBS, and 7-µm cryosections were cut after cryoprotection with 0.9 M sucrose in PBS/ 0.02% sodium azide for at least 1 h. Immunostaining was carried out as described (33). The following primary antibodies were used: rabbit anti-pendrin 1:1000, rabbit anti-a4 H^+-ATPase 1:1000 (36), rabbit anti-A H^+-ATPase, rabbit anti-B1 H^+-ATPase 1:500, rabbit anti-B2 H^+-ATPase, goat anti AQP-2 (Santa Cruz Biotechnology), 1:400 and mouse anti-calbindin D28k 1:20 000 (SWANT, Bellinzona, Switzerland). The secondary antibodies were donkey anti-rabbit 586 and donkey anti-goat 488 (Molecular Probes) at 1:1,000 and 1:300, respectively. All antibodies were tested and no staining was detected with pre-immune sera, in the presence of the immunizing peptide, or when the primary antibodies were omitted.

Western blotting

Animals were killed, and kidneys were rapidly harvested. Immunoblotting was performed on total kidney crude membrane fractions as described previously (33). The primary antibodies were rabbit anti-pendrin 1:5000, AQP2 1:10 000 (kindly provided by J. Loffing, University of Fribourg, Switzerland), and mouse monoclonal anti-actin (42 kD; Sigma, St. Louis, MO) 1:5000. The secondary antibodies (donkey anti-rabbit 1:10,000 IgG conjugated with horseradish peroxidase [Amersham Life Sciences] and sheep anti-mouse 1:5000 IgG-conjugated with alkaline phosphatase) were detected with the enhanced chemiluminescence ECL kit (Amersham Pharmacia Biotech, UK) or the CDP star kit (Roche Diagnostics, Basel, Switzerland).

For each sample, the ratio of the protein of interest to actin was determined and used to calculate the ratio between the group of *Atp6v1b1* +/- mice and *Atp6v1b1* -/- mice.

Tubule Preparation and Intracellular pH Measurements

Intracellular pH (pH_i) was monitored in single type intercalated cells in isolated CCDs that were prepared as described (36). CCDs were identified and incubated with the pH-sensitive dye BCECF (1 μM, Molecular Probes) for 10 min and washed to remove all nondeesterified dye. Each experiment was calibrated with the high K^+/nigericin technique as described (35, 36). All experiments were performed in the absence of bicarbonate. The initial solution was a HEPES-buffered Ringer solution (125 mM NaCl/3mMKCl/1 mM $CaCl_2$/1.2 mM $MgSO_4$/2mMKH_2PO_4/32.2 mM Hepes, pH 7.4). Cells were acidified by using the NH_4Cl (20 mM) prepulse technique and washed into a Na^+-free solution (Na^+ was replaced by equimolar concentrations of *N*-methyl-D-glucamine). The rate of H^+-ATPase activity was determined as the concanamycin-sensitive pH_i alkalinization rate in the absence of Na^+. Rates were calculated over the same range of pH_i (6.40–6.80) for all cells studied. All chemicals were of highest purity and were purchased from Sigma (St. Louis, Mo., USA).

Statistical analysis

All data were tested for statistical analysis using Student's t-tests and only data with $P < 0.05$ were considered statistically significant.

RESULTS

The B1 isoform is part of the basolateral H^+-ATPase complex in mouse kidney during metabolic alkalosis

Immunostaining of mouse kidney with antibodies against the B1 subunit of the vacuolar H^+-ATPase confirmed the localization at the basolateral side of intercalated cells of the cortical collecting duct (Fig. 1) as described previously in mouse and rat kidney (7, 19). Staining was absent from kidneys of *Atp6v1b1-/-* mice. Thus, the B1 subunit forms part of the basolateral H^+-ATPase complex of non-type A intercalated cells in mouse kidney.

Absence of the B1 subunit enhances susceptibility to metabolic alkalosis

To test for a role of the B1 subunit in non-type A intercalated cells, we induced metabolic alkalosis using the aldosterone analogue desoxycorticosterone (DOCA, 2 mg/mouse s.c.) and addition of $NaHCO_3$ to the drinking water as described previously (30).

Treatment with DOCA and $NaHCO_3$ resulted in a significantly stronger metabolic alkalosis in B1 deficient mice than in the control littermates. Blood pH and bicarbonate concentration were higher in *Atp6v1b1*-/- mice (Table 1, Fig. 2A). Metabolic alkalosis was associated with hypokalemia and hypochloremia in *Atp6v1b1* -/- mice (Tab. 1, Fig. 2C, D) as described previously in similar states (10). However, hypokalemia and hypochloremia were significantly more pronounced in *Atp6v1b1-/-* mice. Prior to the treatment, urine pH of *Atp6v1b1* -/- mice was significantly more alkaline as described previously (6) (Tab 2, Fig. 3A). Treatment with DOCA and $NaHCO_3$ increased urine pH to a similar extent in *Atp6v1b1-/-* mice to 8.57 ± 0.01 and in *Atp6v1b1*+/- to 8.33 ± 0.05 (Tab. 2, Fig. 3A). Consistently, urine HCO_3^- excretion increased in both groups with HCO_3^- levels significantly higher in *Atp6v1b1-/-* (Fig. 2B). Furthermore, alkaline diet-induced elevated urinary potassium and sodium losses were more apparent in *Atp6v1b1-/-* mice (Fig. 3C, D). However, a significant difference in urine chloride concentration was observed only in the first day of treatment (Fig. 3E). Water and bicarbonate intake were similar in both groups.

Thus, absence of the B1 H^+-ATPase subunit makes mice more susceptible to metabolic alkalosis suggesting an important role in the clearance from an alkali load.

H^+-ATPase localizes to apical and basolateral membranes of IC in Atp6v1b1 -/- and Atp6v1b1 +/- mice

To establish the presence and distribution of H^+-ATPase subunits in the connecting tubule and cortical collecting duct, the two segments participating in active bicarbonate secretion, we performed immunostaining against the a4 and A H^+-ATPase subunits. The a4 subunit belongs to the membrane bound V_0 sector, whereas the A subunit forms part of the cytosolic V_1 sector (32). In kidneys from alkalotic *Atp6v1b1+/-* mice antibodies against the a4 or A subunit clearly stained the basolateral membrane of a subpopulation of intercalated cells in the CCD (Fig. 4) as described previously for these and other H^+-ATPase subunits in mouse, rat or rabbit kidney during alkalosis (2, 13, 26, 31). In the CCD of *Atp6v1b1-/-* mice, staining for the membrane bound a4 subunit was preserved in the basolateral membrane of CCD intercalated cells. In contrast, the A subunit showed mostly a diffuse and cytoplasmic or a clear apical staining but was almost absent from the basolateral side (Fig. 4). In the apical membrane of type A intercalated cells, staining for the B2 isoform has been observed under conditions of acidosis or in the absence of the B1 isoform suggesting a compensatory mechanism (6, 21). However, we failed to detect staining for the B2 subunit in the basolateral membrane of alkalotic *Atp6v1b1+/-* and *Atp6v1b1-/-* mice whereas a clear staining of the apical membrane was seen in most CCD intercalated cells (Fig. 4).

H^+-ATPase activity is attenuated in IC from alkalotic Atp6v1b1-/- mice

To assess the H^+-ATPase activity in non-type A intercalated cells we used isolated CCDs from alkalotic mice. Under these conditions, the majority of intercalated cells in the mouse CCD are non-type A intercalated cells. The initial intracellular pH (pH_i) of single intercalated cells in superfused CCDs was 7.19 ± 0.02 in *Atp6v1b1+/-* and 7.27 ± 0.02 in *Atp6v1b1-/-.* Removal of Na^+ from the bath led to an intracellular acidification, which was

further enhanced after an NH_4Cl prepulse (20 mM) (Fig. 5). In the continued absence of Na^+ the IC of *Atp6v1b1+/-* mice alkalinized pH_i by 0.042 ± 0.003 pH_i units/min.. In contrast, in the IC of *Atp6v1b1-/-* mice the alkalinization rate was only 0.023 ± 0.002 pH_i units/min ($p < 0.001$) (Fig. 5). Readdition of Na^+ to the bath led to a rapid alkalinization to the initial pH_i values in both groups mediated by Na^+/H^+ exchange (36). We used concanamycin (200 nM, a specific vacuolar H^+-ATPase inhibitor, to separate H^+-ATPase activity from H^+/K^+-ATPase activity (5). Under these conditions, the alkalinization rate declined to 0.021 ± 0.001 pH_i units/min in *Atp6v1b1-/-* and to 0.023 ± 0.001 pH_i units/min in *Atp6v1b1+/-* most likely representing H^+/K^+-ATPase activity. H^+-ATPase activity was calculated by subtracting '' concanamycin'' values from ''control'' values within the respective groups. H^+-ATPase activity in IC from *Atp6v1b1-/-* mice was approximately 7-fold lower than in IC from *Atp6v1b1+/-* (0.003 ±0.001 vs. 0.019 ±0.002; $p < 0.001$) (Fig. 5).

Pendrin expression is reduced in kidneys from Atp6v1b1-/- mice

Pendrin in kidney is exclusively expressed in non-type A intercalated cells and its abundance, localization, and presence have been linked to non-type A IC functions such as bicarbonate secretion and chloride absorption (22, 23, 33, 39). Under control conditions pendrin protein expression was lower in *Atp6v1b1-/-* mice (0.56 ± 0.04 vs. 1.0 ± 0.11; $p < 0.01$) (Fig. 6A, B). Similarly, under DOCA + $NaHCO_3$ treatment pendrin abundance was reduced in B1 deficient mice (0.48 ± 0.03 vs. 1.0 ± 0.13; $p < 0.01$) (Fig. 6C, D).

To test possible differences in subcellular localization of pendrin, immunostaining against pendrin was performed on kidney samples from *Atp6v1b1-/-* and *Atp6v1b1+/-* mice. Pendrin was seen in the cortex in the CNT and CCD localized in a rim in the apical membrane of a subpopulation of intercalated cells both in *Atp6v1b1* -/- and *Atp6v1b1* +/- mouse kidneys (Fig. 7). Thus, the abundance of pendrin is reduced but the apical localization is preserved in kidneys of mice deficient for the B1 H^+-ATPase subunit.

Alkalotic Atp6v1b1 -/- mice have higher abundance of non-type A intercalated cells and principal cells

To further characterize the underlying cause for the reduced pendrin expression, we assessed the relative abundance of type A and non-type A intercalated cells and principal cells in the CNT and CCD. Kidneys were stained against pendrin and the principal cell specific proteins calbindin D28k (CNT) and AQP2 (CNT and CCD). Cells were counted as being pendrin positive (non-type A intercalated cells), AQP-2/calbindin positive (principal cells) or pendrin and AQP2/calbindin negative (type A intercalated cells).

In the CNT of *Atp6v1b1-/-* mice the percentage of type A IC declined to 3.8 ± 0.5 % from 12.0 ± 2.3 % in *Atp6v1b1+/-* ($p < 0.0017$) without changing the percentage of non-type A IC significantly (30.6 ± 1.3 % in *Atp6v1b1-/-* vs. 33.9 ± 1.5 % in *Atp6v1b1+/-*, n.s.). However, the percentage of principal cells was significantly increased (65.7 ± 1.5 in *Atp6v1b1-/-* vs. 54.1 ± 2.8 in *Atp6v1b1+/-*) (Table 3). In contrast, in the CCD of *Atp6v1b1-/-* mice a significantly larger population of non-type A IC was observed (30.8 ± 2.0 % vs. 22.3 ± 1.3 %), whereas the abundance of type A IC was significantly decreased (4.5 ± 0.7 % vs. 19.4 ± 2.2 %). The percentage of CCD principal cells in *Atp6v1b1-/-* mice was slightly increased without reaching significance (64.7 ± 1.9 % vs. 58.4 ± 2.5 %) (Table 3). Thus, absence of the B1 subunit in animals treated with DOCA/HCO_3^- causes remodelling of the connecting tubule and cortical collecting duct with an increase in the relative abundance of non-type a IC in the CCD and more principal cells in the CNT.

***Dysregulation of AQP2 in Atp6v1b1-/-* mice**

Metabolic cage studies showed a tendency to higher urinary output in *Atp6v1b1-/-* under control conditions and after treatment with DOCA/$NaHCO_3^-$ (Table 2). This tendency was associated with significantly lower urinary osmolarity under control conditions (*Atpv1b1+/-:* 2256.8 ± 188.0 mOsm versus *Atp6v1b1-/-:*1708.8 ± 84.6 mOsm.). In addition, we had recently observed that B1 deficient mice had a significantly higher urinary flow upon application of the diuretic furosemide during clearance experiments (14). Thus, absence of the B1 subunit may also alter renal water handling and urinary concentration. To investigate

this possibility we tested AQP2 abundance in control and DOCA/$NaHCO_3$ treated kidneys. Under control conditions AQP2 expression in *Atp6v1b1*-/- mice was not significantly different (glycosylated band: 1.54 ± 0.19 versus 1.0 ± 0.22 in *Atp6v1b1*+/- and non-glycosylated band: 1.31 ± 0.12 versus 1.0 ± 0.23 in *Atp6v1b1*+/-) (Fig. 8A-C). DOCA/$NaHCO_3$ treatment resulted in downregulation of AQP2 in *Atp6v1b1*-/- mice (glycosylated band: 0.36 ± 0.03 versus 1.0 ± 0.12 in *Atp6v1b1*+/-; $p< 0.01$ and non-glycosylated band: 0.35 ± 0.05 versus 1.0 ± 0.07 in *Atp6v1b1*+/-; $p< 0.001$) (Fig. 8D-F).

DISCUSSION

Vacuolar H^+-ATPases are expressed in all types of intercalated cells and to date no specific subunit isoforms have been identified that can be linked to the function of only one subtype of intercalated cells (32). The B1 subunit isoform is almost exclusively expressed in the intercalated cells with only low abundance also in the thick ascending limb (17, 19). Its importance in type A intercalated cell function has been highlighted by the fact that mutations in the *ATP6V1B1* gene in patients leads to distal renal tubular acidosis (11). Also, genetic ablation of the murine homologue, *Atp6v1b1*, impairs maximal urinary acidification (6, 14). However, the function of the B1 isoform in non-type A intercalated cells has remained elusive. Therefore, we investigated the role of the B1 H^+-ATPase subunit in non-type A IC function using a mouse model lacking the B1 subunit.

We used a treatment that has been shown to provoke metabolic alkalosis in mice (23). Our findings clearly demonstrate that the B1 subunit is critical for non-type A intercalated cell function both on the systemic level of the whole animal as well as on the cellular level. *Atp6v1b1-/-* mice developed a more pronounced alkalosis with hypochloremia and hypokalemia. This alkalosis is most likely due to the failure of non-type A intercalated cells to excrete appropriate amounts of bicarbonate into urine. Even though urinary bicarbonate/ creatinine was elevated in B1 deficient mice, this may be rather due to exceeding the threshold for bicarbonate reabsorption in the proximal tubule which is in the range of 25-28 mM (9). B1 deficient mice showed blood bicarbonate levels well above this threshold. However, the abundance of pendrin representing most likely the apical and rate-limiting bicarbonate extruding pathway in non-type A intercalated cells was strongly reduced in kidneys of B1 KO mice. Absence of pendrin has been previously shown to impair bicarbonate excretion in the cortical collecting duct from pendrin deficient mice (23). The reduction in pendrin expression reflects decreased pendrin abundance per cell as detailed cell counts demonstrated that the number of pendrin expressing cells is markedly increased which may represent a compensatory mechanism to counter-act alkalosis. Similarly, Wall and colleagues have demonstrated that in the kidney of the pendrin deficient mouse, several transport proteins of non-type A-IC are down-regulated (39). Taken together, it appears that loss of proteins critically involved either in proton or bicarbonate extrusion

affects the expression of the other components of this functional transport unit. The loss of this transport unit apparently triggers remodelling of the cellular composition of the connecting tubule and cortical collecting duct, as shown here. The underlying mechanism of this compensatory remodelling remains to be identified.

Regulation of H^+-ATPase activity may involve assembly of domains or subunits and trafficking to the membrane (20, 32). Immunohistochemistry demonstrated that absence of the B1 subunit from the basolateral side of non-type A-IC could not be compensated by the B2 subunit isoform. The B2 isoform was only found in the apical domain of intercalated cells in the B1 deficient mouse but was never seen on the basolateral side. The a4 subunit, belonging to membrane bound V_0 domain was still found in the basolateral side of non-type A-IC indicating that trafficking of the pump or at least of parts of it is not generally impaired in the absence of the B1 isoform. In control animals, the A subunit, part of the cytosolic V_1 domain and directly neighboring the B (B1 or B2) subunit, was frequently found in the basolateral domain of non-type A-IC. In contrast, in the absence of the B1 subunit, the A subunit was seen either in the apical domain or was rather diffusely distributed in the cytosol. Similarly, Yang et al. demonstrated recently that in the assembly of H^+-ATPase complexes in vitro was disturbed in the presence of mutated B1 subunits (43). Thus, the B1 subunit may be required for the normal assembly of the V_1 and V_0 domains of basolateral H^+-ATPase complexes both *in vitro* and *in vivo*. This notion is also supported by the fact that H^+-ATPase activity of intercalated cells in the CCD from B1 deficient mice is strongly reduced. As we were not able to distinguish between type A and non-type A IC and between apical and basolateral H^+-ATPase activity in our preparation, the residual activity may reflect either type A intercalated cells or apical H^+-ATPase complexes. However, it should be noted that pendrin staining and cell counts indicated that a large fraction of intercalated cells in the CCD were non-type A-IC.

Apart from the alkalosis, *Atp6v1b1v1* -/- mice showed a tendency to have increased blood osmolarity and significantly decreased urinary osmolarity pointing to a possible urinary concentrating defect. Total AQP2 expression was decreased under these conditions whereas the relative abundance of AQP2 positive cells was increased suggesting an adaptive process possibly limiting excessive water loss. The underlying mechanism of

AQP2 dysregulation is not clear at this state, however, expression of the B1 subunit in principal cells (24) and bafilomycin-sensitive AQP2 recycling have been described (8). Since the presence of other H^+-ATPase subunits was not confirmed in these recycling vesicles (24) and the vesicles fail to acidify their lumen (40) the B1 subunit may perform functions in principal cells unrelated to classic H^+-ATPase activity.

Thus, the B1 subunit is critical for normal formation and function of basolateral H^+-ATPase complexes in non-type A intercalated cells. To our knowledge, this is the first *in vivo* evidence for the importance of this subunit to H^+-ATPase assembly. In addition, the function of the B1 subunit may also extend to the regulation of AQP2 water channels either directly or indirectly.

Acknowledgements

This study was supported by grants from the Swiss National Science foundation (31-1099677/1) and the 6th EU framework project EuReGene (005085) to C. A. Wagner. We also acknowledge support from the ZIHP Core facility for rodent physiology and the University Research Priority Program 'Integrative Human Physiology' of the University of Zurich.

FIGURE LEGENDS

Table 1

Blood parameters in *Atp6v1b1+/-* and *Atp6v1b1 -/-* mice treated by DOCA/$NaHCO_3$ for 4 days. N = 6 mice/ group, values are means ± SE. **p< 0.01 and ***p < 0.001 *Atp6v1b1*+/- versus *Atp6v1b1-/-* mice.

Table 2

Urine parameters from control and DOCA/$NaHCO_3$ treated *Atp6v1b1+/-* and *Atp6v1b1-/-* mice. Animals were kept in metabolic cages and 24 hour urine collections performed before (control) and after 4 days of DOCA/$NaHCO_3$ treatment. Values are as means ± SE; V volume; BW body weight; CreaCl creatinine clearance; crea creatinine; FE fractional excretion. *p < 0.05, **p< 0.01 and ***p < 0.001 DOCA/$NaHCO_3$ *Atp6v1b1*+/- respectively *Atp6v1b1*-/- versus control *Atp6v1b1*+/- respectively *Atp6v1b1*-/- mice. $^{\#}$p < 0.05, $^{\#\#}$p < 0.01 and $^{\#\#\#}$p < 0.001 control *Atp6v1b1*-/- versus control *Atp6v1b1*+/- mice. $^{\&}$p < 0.05, $^{\&\&}$p< 0.01 and $^{\&\&\&}$p < 0.001 DOCA/$NaHCO_3$ *Atp6v1b1*-/- versus DOCA/$NaHCO_3$ *Atp6v1b1+/-* mice.

Table 3

Relative abundance of different cell types in the CNT and CCD of DOCA/$NaHCO_3$ treated *Atp6v1b1+/-* and *Atp6v1b1-/-* mice. Values are means ± SE. **p < 0.01 and ***p < 0.001 *Atp6v1b1*+/- versus *Atp6v1b1-/-* mice.

Figure 1

Staining for the B1 subunit in kidneys from *Atp6v1b1+/-* and *Atp6v1b1-/-* mice. (A,B) The B1 subunit (red) localized in kidneys of *Atp6v1b1+/-* to the apical and basolateral (marked with *) membranes of intercalated cells in the CCD. Principal cells are stained with AQP2/ calbindin D28k (green). **(C, D)** No staining for B1 was detected in kidneys from *Atp6v1b1-/-* mice. Original magnification: A: 630 x, B-D: 400 x.

Figure 2

Blood parameters after 4 days DOCA/$NaHCO_3$ treatment. (A) *Atp6v1b1*-/- mice had a more alkaline blood pH, **(B)** increased HCO_3^- level, **(C)** hyperchloremia and **(D)** hypokaliemia. **p < 0.01 and ***p < 0.001 *Atp6v1b1*+/- versus *Atp6v1b1*-/- mice.

Figure 3

Urine pH and electrolyte levels before and after 4 days DOCA/$NaHCO_3$ treatment. (A) Prior to the treatment urine pH was significantly higher in *Atp6v1b1*-/- mice and increased in both groups during the treatment. **(B-E)** Urinary electrolyte excretion. *p < 0.05, **p < 0.01 and ***p < 0.001 *Atp6v1b1*+/- versus *Atp6v1b1*-/- mice.

Figure 4

Localization of H^+-ATPase subunits in CCD non-type A intercalated cells. (A, B) The B2 subunit (red) was found mostly in the cytosol of CCD intercalated cells in kidneys of *Atp6v1b1+/-* animals (A) whereas a more pronounced apical B2 staining was observed in the CCD of B1 deficient mice (B). **(C, D)** The a4 subunit (red) was located to the apical and basolateral (arrow) membrane of CCD intercalated cells both in *Atp6v1b1+/-* and *Atp6V1b1-/-* animals. **(E, F)** The A subunit (red) was seen in the apical and basolateral (arrow) membrane of CCD intercalated cells in control animals, but could not be found in the basolateral membrane in the absence of the B1 subunit **(G,H)**. Principal cells were stained with antibodies against AQP2 and calbindin D28k (green). Original magnification 400 – 600 x.

Figure 5

H^+-ATPase activity in single CCD intercalated cells of *Atp6v1b1+/-* and *Atp6v1b1-/-* mice.

(A-D) Original tracings of intracellular pH measurements in single intercalated cells in CCDs isolated from the kidney of alkalotic *Atp6v1b1*+/- and *Atp6v1b1*-/- mice in the absence and presence of the specific H^+-ATPase inhibitor concanamycin (200 nM). **(E)** Summary of pH_i recovery rate measurements and calculation of H^+-ATPase activity (difference control – concanamycin). ***p < 0.001 *Atp6v1b1*+/- versus *Atp6v1b1*-/-.

Figure 6

Pendrin abundance in control and DOCA/$NaHCO_3$ treated mice. Pendrin expression was reduced both in control **(A,B)** and DOCA/$NaHCO_3$ treated **(C,D)** A*tp6v1b1*-/- mice. **p < 0.01 *Atp6v1b1*+/- versus *Atp6v1b1*-/-.

Figure 7

Pendrin localization is preserved in *Atp6v1b1* -/- mice. Immunostaining against pendrin (red) did not show any difference between alkalotic *Atp6v1b1*+/- and *Atp6v1b1*-/- mice. Principal cells were stained with AQP2 (green). Original magnification 400 x.

Figure 8

AQP2 abundance is reduced in alkalotic *Atp6v1b1-/-* mice. **A-C)** Under control conditions *Atp6v1b* -/- mice have slightly increased AQP2 abundance without reaching significance. **(D-F)** In *Atp6v1b1-/-* mice DOCA/$NaHCO_3$ treatment resulted in decreased AQP2 abundance. Gly glycosylated AQP2, non-gly non-glycosylated AQP2. **p < 0.01 and ***p < 0.001 *Atp6v1b1*+/- versus *Atp6v1b1*-/-.

REFERENCES

1. Alper, SL, Natale, J, Gluck, S, Lodish, HF & Brown, D: Subtypes of intercalated cells in rat kidney collecting duct defined by antibodies against erythroid band 3 and renal vacuolar H^+-ATPase. *Proc Natl Acad Sci U S A,* 86**:**5429-33, 1989.

2. Bastani, B, Purcell, H, Hemken, P, Trigg, D, Gluck, S: Expression and distribution of renal vacuolar proton-translocating adenosine triphosphatase in response to chronic acid and alkali loads in the rat. *J Clin Invest,* 88**:**126-36, 1991.

3. Breton, S, Smith, P J, Lui, B, Brown, D: Acidification of the male reproductive tract by a proton pumping (H^+)-ATPase. *Nat Med,* 2**:**470-2, 1996.

4. Brown, D, Lui, B, Gluck, S & Sabolic, I: A plasma membrane proton ATPase in specialized cells of rat epididymis. *Am J Physiol,* 263**:**C913-C916, 1992.

5. Dröse, S, Altendorf, K: Bafilomycins and concanamycins as inhibitors of V-ATPases and P-ATPases. *J Exp Biol,* 200**:**1-8, 1997.

6. Finberg, KE, Wagner, C A, Bailey, M A, Paunescu, T G, Breton, S, Brown, D, Giebisch, G, Geibel, J P, Lifton, R P: The B1 subunit of the H^+ATPase is required for maximal urinary acidification. *Proc Nat Acad Sci USA,* 102**:**13616-13621, 2005.

7. Finberg, KE, Wagner, C A, Stehberger, P A, Geibel, J P, Lifton, R P: Molecular Cloning and Characterization of *Atp6v1b1*, the Murine Vacuolar H^+-ATPase B1-Subunit. *Gene,* 318**:**25-34, 2003.

8. Gustafson, CE, Katsura, T, McKee, M, Bouley, R, Casanova, JE & Brown, D: Recycling of AQP2 occurs through a temperature- and bafilomycin-sensitive trans-Golgi-associated compartment. *Am J Physiol Renal Physiol,* 278**:**F317-26, 2000.

9. Igarashi, T, Sekine, T, Inatomi, J, Seki, G: Unraveling the molecular pathogenesis of isolated proximal renal tubular acidosis. *J Am Soc Nephrol,* 13**:**2171-2177, 2002.

10. Jacobson, HR & Seldin, DW: On the generation, maintenance, and correction of metabolic alkalosis. *Am J Physiol,* 245**:**F425-32, 1983.

11. Karet, FE, Finberg, K E, Nelson, R D, Nayir, A, Mocan, H, Sanjad, S A, Rodriguez-Soriano, J, Santos, F, Cremers, C W, Di Pietro, A, Hoffbrand, B I, Winiarski, J, Bakkaloglu, A, Ozen, S, Dusunsel, R, Goodyer, P, Hulton, S A, Wu, D K, Skvorak, A B, Morton, C C, Cunningham, M J, Jha, V, Lifton, R P: Mutations in the gene encoding B1 subunit of H^+-ATPase cause renal tubular acidosis with sensorineural deafness. *Nat Genet,* 21**:**84-90, 1999.

12. Kim, J, Kim, YH, Cha, JH, Tisher, CC & Madsen, KM: Intercalated cell subtypes in connecting tubule and cortical collecting duct of rat and mouse. *J Am Soc Nephrol,* 10**:**1-12, 1999.

13. Kim, J, Welch, W J, Cannon, J K, Tisher, C C, Madsen, K M: Immunocytochemical response of type A and type B intercalated cells to increased sodium chloride delivery. *Am J Physiol,* 262**:**F288-302, 1992.

14. Kovacikova, J, Winter, C, Loffing-Cueni, D, Loffing, J, Finberg, KE, Lifton, RP, Hummler, E, Rossier, B & Wagner, CA: The connecting tubule is the main site of the furosemide-induced urinary acidification by the vacuolar H(+)-ATPase. *Kidney Int,* 70**:**1706-16, 2006.

15. Madsen, KM, Verlander J W, Kim J, Tisher, C C: Morphological adaption of the collecting duct to acid-base disturbances. *Kidney Int,* Suppl 33**:**S57-63, 1991.

16. McLean, IW, Nakane, P K: Periodate-lysine-paraformaldehyde fixative. A new fixation for immunoelectron microscopy. *J Histochem Cytochem,* 22**:**1077-83, 1974.

17. Miller, RL, Zhang, P, Smith, M, Beaulieu, V, Paunescu, TG, Brown, D, Breton, S & Nelson, RD: V-ATPase B1-subunit promoter drives expression of EGFP in intercalated cells of kidney, clear cells of epididymis and airway cells of lung in transgenic mice. *Am J Physiol Cell Physiol,* 288**:**C1134-44, 2005.

18. Nelson, H, Nelson, N: Disruption of genes encoding subunits of yeast vacuolar H^+-ATPase causes conditional lethality. *Proc Natl Acad Sci U S A,* 87**:**3503-7, 1990.

19. Nelson, RD, Guo, X L, Masood, K, Brown, D, Kalkbrenner, M, Gluck, S: Selectively amplified expression of an isoform of the vacuolar H^+-ATPase 56-kilodalton subunit in renal intercalated cells. *Proc Natl Acad Sci U S A,* 89**:**3541-5, 1992.

20. Nishi, T, Forgac, M: The vacuolar (H+)-ATPases--nature's most versatile proton pumps. *Nat Rev Mol Cell Biol,* 3**:**94-103, 2002.

21. Paunescu, TG, Da Silva, N, Marshansky, V, McKee, M, Breton, S & Brown, D: Expression of the 56-kDa B2 subunit isoform of the vacuolar H^+-ATPase in proton-secreting cells of the kidney and epididymis. *Am J Physiol Cell Physiol,* 287**:**C149-C162, 2004.

22. Quentin, F, Chambrey, R, Trinh-Trang-Tan, MM, Fysekidis, M, Cambillau, M, Paillard, M, Aronson, PS & Eladari, D: The Cl^-/HCO_3^- exchanger pendrin in the rat kidney is regulated in response to chronic alterations in chloride balance. *Am J Physiol Renal Physiol,* 287**:**F1179-88, 2004.

23. Royaux, IE, Wall, S M, Karniski, L P, Everett, L A, Suzuki, K, Knepper, M A, Green, E D: Pendrin, encoded by the Pendred syndrome gene, resides in the apical region of renal intercalated cells and mediates bicarbonate secretion. *Proc Natl Acad Sci U S A,* 98**:**4221-6, 2001.

24. Sabolic, I, Wuarin, F, Shi, LB, Verkman, AS, Ausiello, DA, Gluck, S & Brown, D: Apical endosomes isolated from kidney collecting duct principal cells lack subunits of the proton pumping ATPase. *J Cell Biol,* 119**:**111-22, 1992.

25. Schuster, VL: Function and regulation of collecting duct intercalated cells. *Annu Rev Physiol,* 55**:**267-88, 1993.

26. Stehberger, P, Schulz, N, Finberg, KE, Karet, FE, Giebisch, G, Lifton, RP, Geibel, JP & Wagner, CA: Localization and regulation of the ATP6V0A4 (a4) vacuolar H+-ATPase subunit defective in an inherited form of distal renal tubular acidosis. *J Am Soc Nephrol,* 14**:**3027-3038, 2003.

27. Teng-umnuay, P, Verlander, J W, Yuan, W, Tisher, C C, Madsen, K M: Identification of distinct subpopulations of intercalated cells in the mouse collecting duct. *J Am Soc Nephrol,* 7**:**260-74, 1996.

28. Vallet, M, Picard, N, Loffing-Cueni, D, Fysekidis, M, Bloch-Faure, M, Deschenes, G, Breton, S, Meneton, P, Loffing, J, Aronson, PS, Chambrey, R & Eladari, D: Pendrin regulation in mouse kidney primarily is chloride-dependent. *J Am Soc Nephrol,* 17**:**2153-63, 2006.

29. Van Hille B, RH, Schmid P, Puettner I, Green JR, Bilbe G: Heterogenity of vacuolar H^+-ATPase: differential expression of two human subunit B isoforms. *Biochem J,* 303**:**191-198, 1994.

30. Verlander, JW, Hassell, K A, Royaux, I E, Glapion, D M, Wang, M E, Everett, L A, Green, E D, Wall, S M: Deoxycorticosterone upregulates PDS (Slc26a4) in mouse kidney: role of pendrin in mineralocorticoid-induced hypertension. *Hypertension,* 42**:**356-62, 2003.

31. Verlander, JW, Madsen, K M, Galla, J H, Luke, R G, Tisher, C C: Response of intercalated cells to chloride depletion metabolic alkalosis. *Am J Physiol,* 262**:**F309-19, 1992.

32. Wagner, CA, Finberg, K E, Breton, S, Marshansky, V, Brown, D, Geibel, J P: Renal vacuolar H^+-ATPase. *Physiol Rev,* 84**:**1263-314, 2004.

33. Wagner, CA, Finberg, K E, Stehberger, P A, Lifton, R P, Giebisch, G H, Aronson, P S, Geibel, J P: Regulation of the expression of the Cl^-/anion exchanger pendrin in mouse kidney by acid-base status. *Kidney Int,* 62**:**2109-17, 2002.

34. Wagner, CA, Geibel, J P: Acid-base transport in the collecting duct. *J Nephrol,* Suppl 5**:**S112-27, 2002.

35. Wagner, CA, Giebisch, G, Lang, F, Geibel, J P: Angiotensin II stimulates vesicular H^+-ATPase in rat proximal tubular cells. *Proc Natl Acad Sci U S A,* 95**:**9665-9668, 1998.

36. Wagner, CA, Lukewille, U, Valles, P, Breton, S, Brown, D, Giebisch, G H, Geibel, J P: A rapid enzymatic method for the isolation of defined kidney tubule fragments from mouse. *Pflugers Arch,* 446**:**623-32, 2003.

37. Wall, SM: Recent advances in our understanding of intercalated cells. *Curr Opin Nephrol Hypertens,* 14**:**480-484, 2005.

38. Wall, SM, Hassell, K A, Royaux, I E, Green, E D, Chang, J Y, Shipley, G L, Verlander J W: Localization of Pendrin in Mouse Kidney. *Am J Physiol Renal Physiol,* 284**:**F229-41, 2002.

39. Wall, SM, Kim, YH, Stanley, L, Glapion, DM, Everett, LA, Green, ED & Verlander, JW: NaCl restriction upregulates renal Slc26a4 through subcellular redistribution: role in Cl- conservation. *Hypertension,* 44**:**982-7, 2004.

40. Wang, YX, Shi, LB & Verkman, AS: Functional water channels and proton pumps are in separate populations of endocytic vesicles in toad bladder granular cells. *Biochemistry,* 30**:**2888-94, 1991.

41. Wax, MB, Saito, I, Tenkova, T, Krupin, T, Becker, B, Nelson, N, Brown, D, Gluck, S L: Vacuolar H^+-ATPase in ocular ciliary epithelium. *Proc Natl Acad Sci U S A,* 94**:**6752-7, 1997.

42. Yamashiro, CT, Kane, P M, Wolczyk, D F, Preston, R A, Stevens, T H: Role of vacuolar acidification in protein sorting and zymogen activation: a genetic analysis of the yeast vacuolar proton-translocating ATPase. *Mol Cell Biol,* 10**:**3737-49, 1990.

43. Yang, Q, Li, G, Singh, SK, Alexander, EA & Schwartz, JH: Vacuolar H+ -ATPase B1 subunit mutations that cause inherited distal renal tubular acidosis affect proton pump assembly and trafficking in inner medullary collecting duct cells. *J Am Soc Nephrol,* 17**:**1858-66, 2006.

Table 1

	Atp6v1b1 +/-	***Atp6v1b1 -/-***
pH	7.29 ± 0.02	7.40 ± 0.02 **
pCO_2 [mmHg]	48.2 ± 1.9	51.3 ± 3.1
pO_2 [mmHg]	42.6 ± 6.8	47.4 ± 10.9
HCO_3^- [mmol/l]	22.7 ± 0.6	31.2 ± 1.9 ***
K^+ [mmol/l]	3.6 ± 0.1	2.5 ± 0.1 ***
Na^+ [mmol/l]	145.6 ± 1.0	147.2 ± 0.8
Cl^- [mmol/l]	109.5 ± 1.0	101.2 ± 2.2 **
Crea [mmol/l]	0.11 ± 0.01	0.09 ± 0.11
Osmolarity [mOsm]	324.0 ± 8.5	341.6 ± 8.9

Table 2

	Atp6v1b1+/-		*Atp6v1b1-/-*	
	control	**DOCA/ $NaHCO_3$**	**control**	**DOCA/ $NaHCO_3$**
pH	6.29 ± 0.10	8.33 ± 0.05 ***	6.81 ± 0.05 ##	8.57 ± 0.01 *** &
V [ml/g BW/24hours]	0.07 ± 0.02	0.17 ± 0.02 *	0.09 ± 0.01	0.21 ± 0.04 *
CreaCl [µl/gBW/24hours]		58.9 ± 8.3		59.4 ± 11.4
Crea [mg/dl]	51.6 ± 2.12	33.8 ± 3.0	44.2 ± 1.9 #	23.1 ± 1.1 *** &
HCO_3^-/ Crea [mmol/l/mg/dl]	0.0 ± 0.0	4.5 ± 0.7 ***	0.2 ± 0.0 ###	10.0 ± 0.6 *** &&&
K^+/ Crea [mmol/l/mg/dl]	2.3 ± 0.3	2.0 ± 0.1	2.7 ± 0.1	2.2 ± 0.2
Na^+/Crea [mmol/l/mg/dl]	2.3 ± 0.3	10.2 ± 0.8 ***	2.2 ± 0.1	14.2 ± 0.4 *** &&
Cl^-/ Crea [mmol/l/mg/dl]	5.6 ± 0.7	3.7 ± 0.4 *	4.9 ± 0.4	3.2 ± 0.5 *
NH_4^+/ Crea [mmol/l/mg/dl]	0.89 ± 0.05	0.17 ± 0.04 ***	1.17 ± 0.05 ##	0.20 ± 0.05 ***
$H_2PO_4^-$/Crea [mmol/l/mg/dl]	0.004 ± 0.001	0.003 ± 0.001	0.003 ± 0.001	0.005 ± 0.001 * &
Citrate/ Crea	1.9 ± 0.6	13.8 ± 0.9 ***	0.2 ± 0.1	11.2 ± 1.8 **
FE (HCO_3^-) [%]		1.9 ± 0.3		2.5 ± 0.3
FE (K^+) [%]		5.3 ± 0.8		6.9 ± 0.6
FE (Na^+) [%]		0.68 ± 0.01		0.77 ± 0.03
FE (Cl^-) [%]		0.32 ±0.06		0.23 ± 0.04
Osmolarity [mOsm]	2256.8 ±188	1387.2 ± 133.9 **	1708.8 ± 84.6 #	1209.6 ± 76.4 **
Δ weight [%]		+ 3.6 ± 1.1		-0.3 ± 2.2

Table 3

Results from cell counting

	CNT		CCD	
	Atp6v1b1 +/-	***Atp6v1b1 -/-***	***Atp6v1b1 +/-***	***Atp6v1b1 -/-***
Pendrin negative AQP2/calbindin negative (%)	12.0 ± 2.3	3.7 ± 0.5 **	19.4 ± 2.2	4.5 ± 0.7 ***
Pendrin positive (%)	33.9 ± 1.5	30.6 ± 1.3	22.3 ± 1.4	30.8 ± 2.0***
AQP2/ calbindin positive (%)	54.1 ± 2.8	65.8 ± 1.5 ***	58.4 ± 2.5	64.7 ± 1.9

Atp6v1b1 +/-

Atp6v1b1 -/-

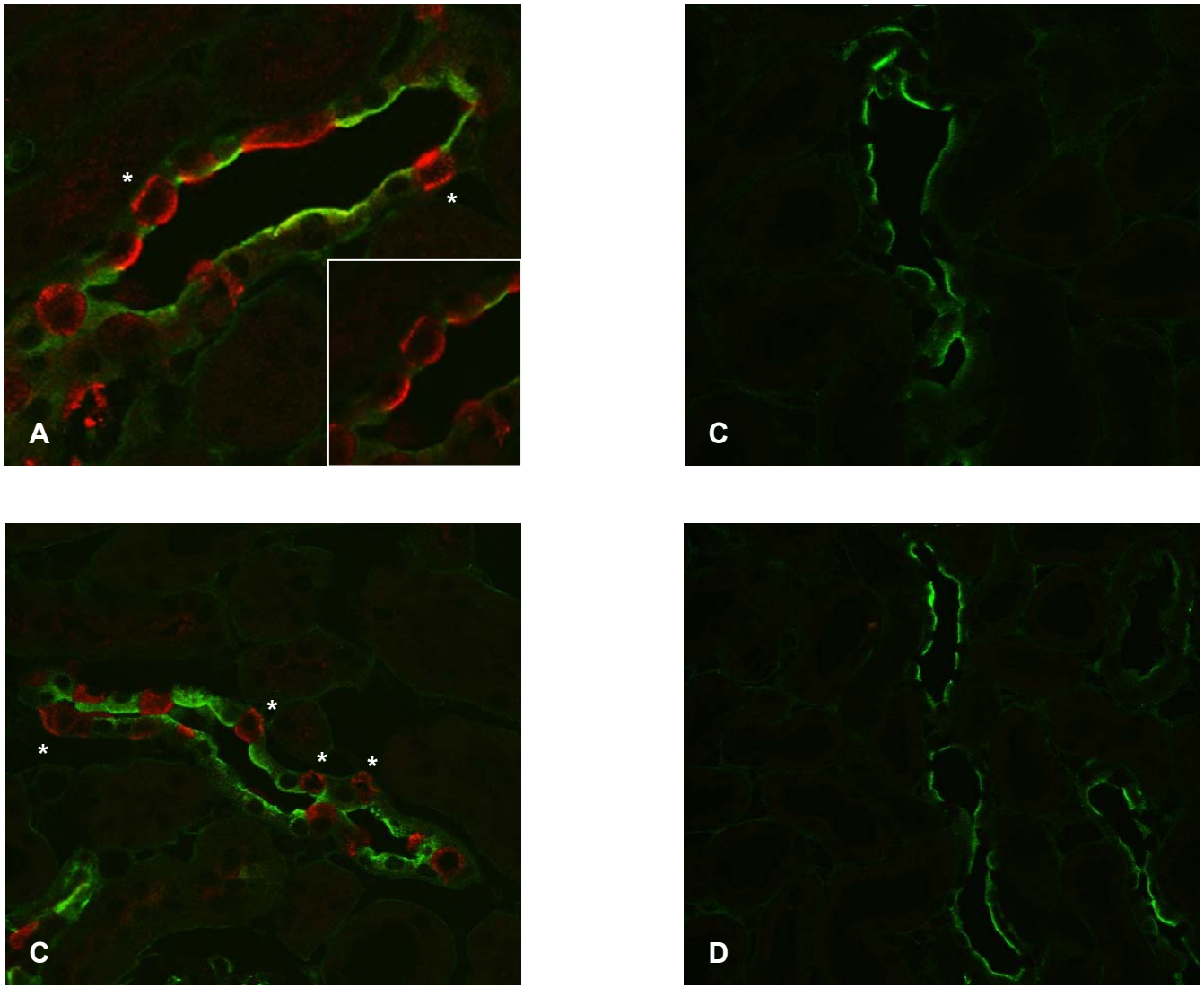

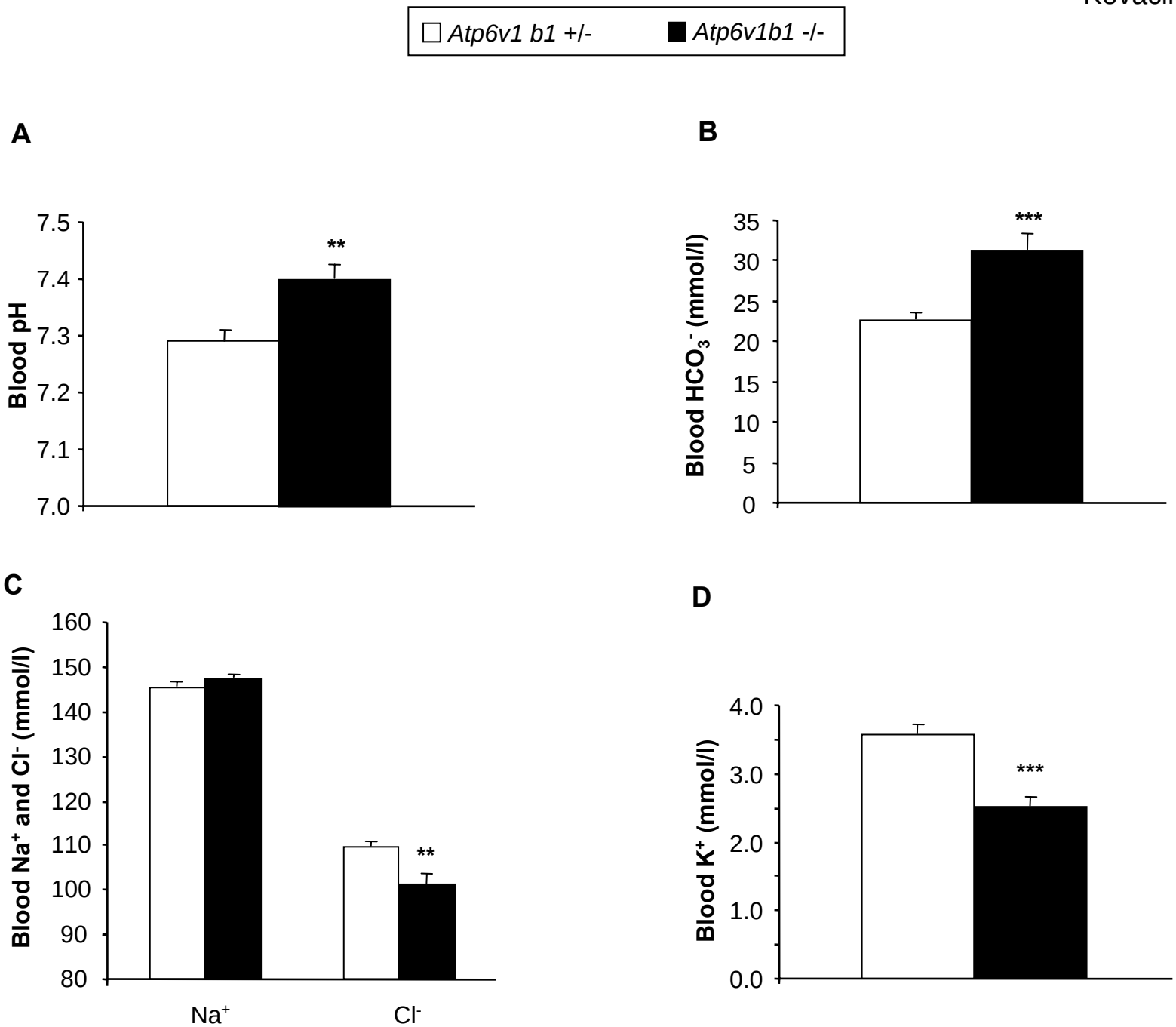
Atp6v1 b1 +/-
Atp6v1b1 -/-
A
Blood pH
7.5
7.4
7.3
7.2
7.1
7.0
**
B
Blood HCO3- (mmol/l)
35
30
25
20
15
10
5
0
***
C
Blood Na+ and Cl- (mmol/l)
160
150
140
130
120
110
100
90
80
**
Na+
Cl-
D
Blood K+ (mmol/l)
4.0
3.0
2.0
1.0
0.0
***

A

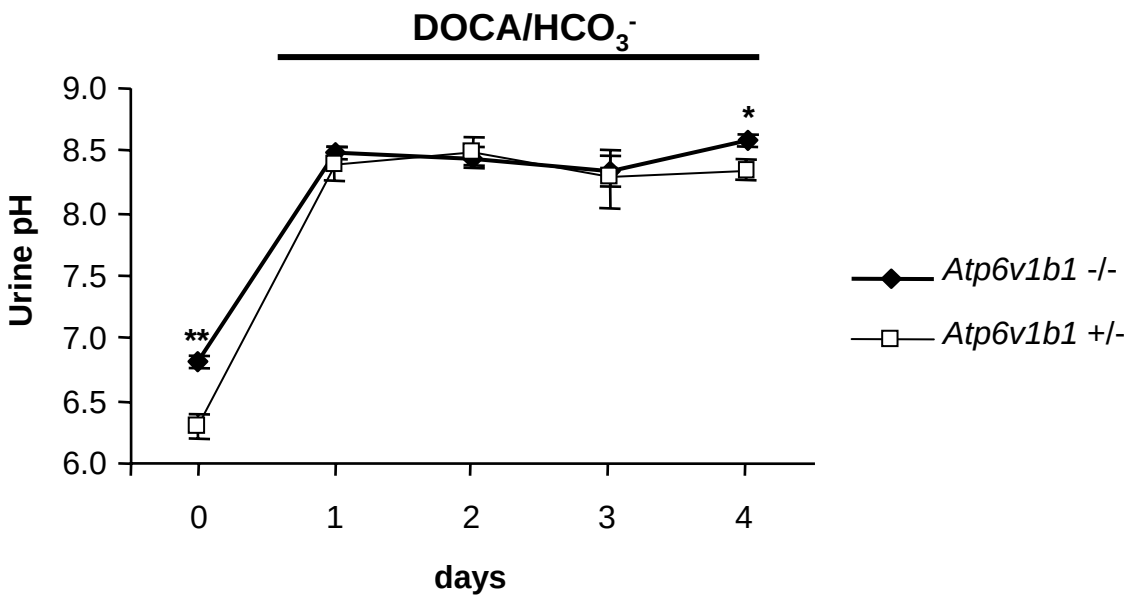
DOCA/HCO3-
Urine pH
9.0
8.5
8.0
7.5
7.0
6.5
6.0
**
*
0
1
2
3
4
days
Atp6v1b1 -/-
Atp6v1b1 +/-

B

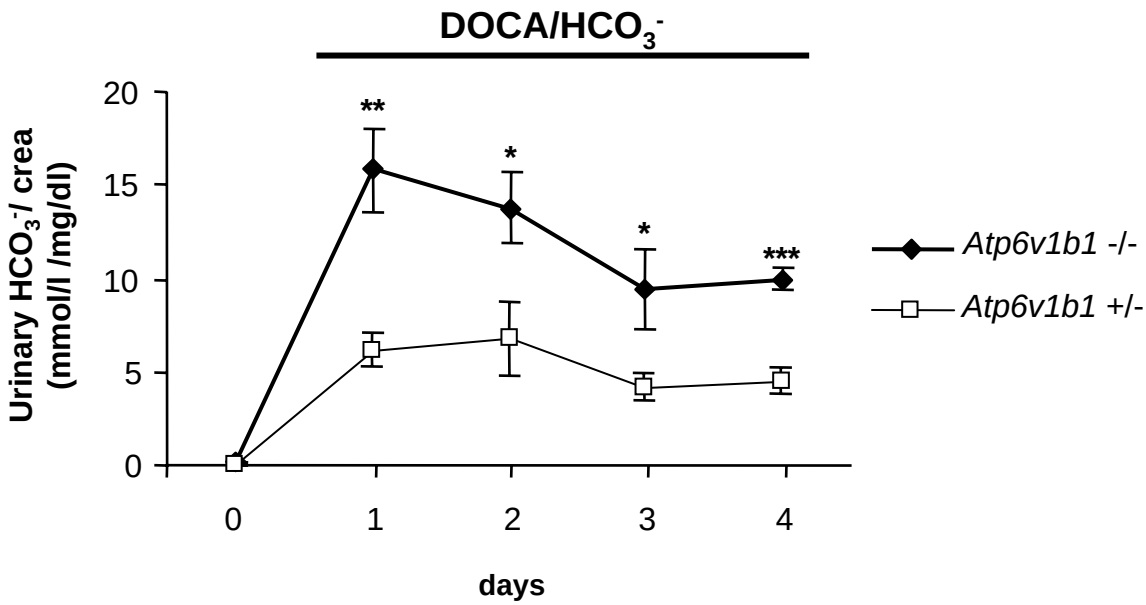
DOCA/HCO3-
Urinary HCO3-/ crea
(mmol/l /mg/dl)
20
15
10
5
0
**
*
*
***
0
1
2
3
4
days
Atp6v1b1 -/-
Atp6v1b1 +/-

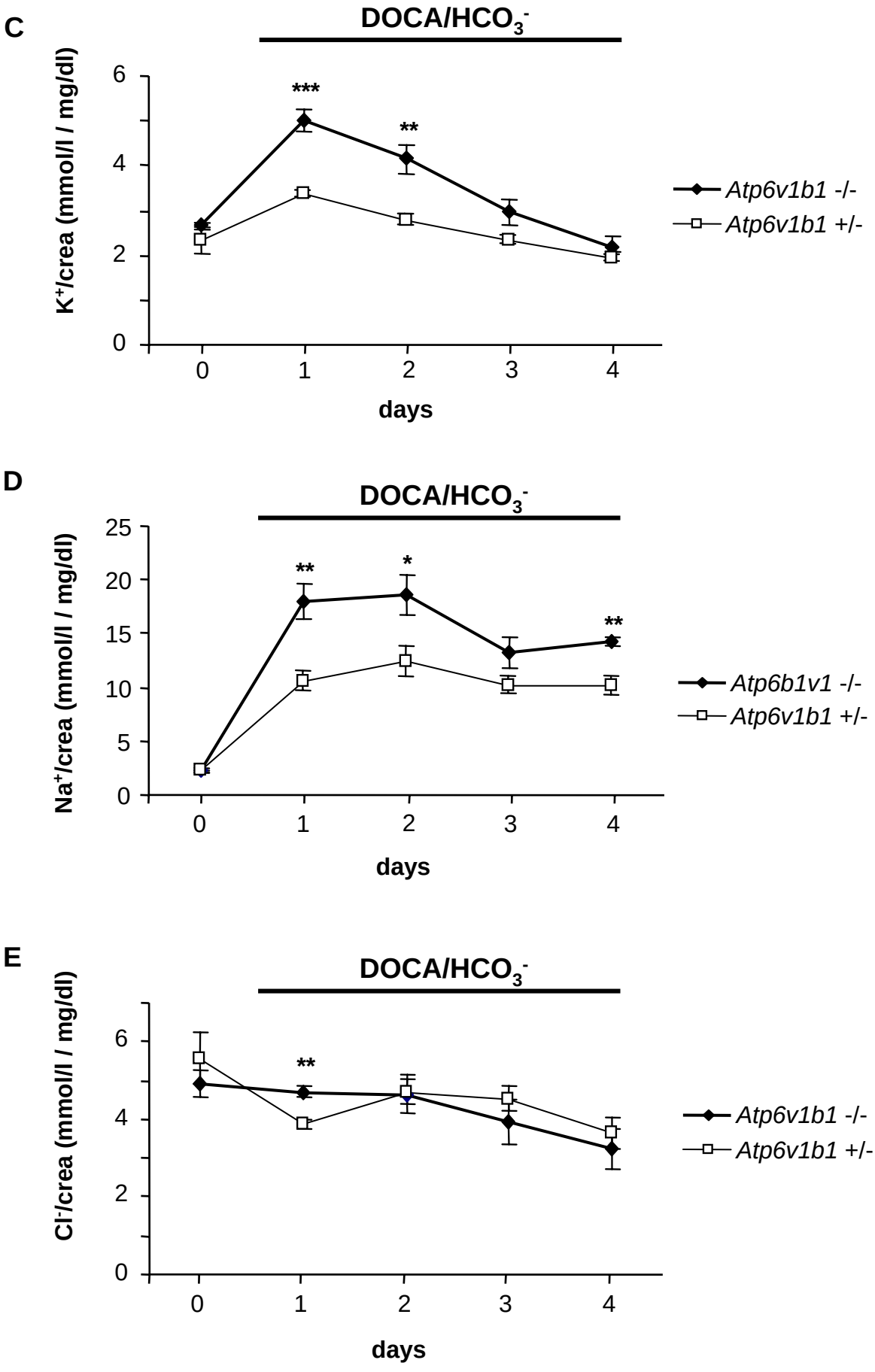
C
DOCA/HCO3-
K+/crea (mmol/l / mg/dl)
***
**
days
Atp6v1b1 -/-
Atp6v1b1 +/-
D
DOCA/HCO3-
Na+/crea (mmol/l / mg/dl)
**
*
**
days
Atp6b1v1 -/-
Atp6v1b1 +/-
E
DOCA/HCO3-
Cl-/crea (mmol/l / mg/dl)
**
days
Atp6v1b1 -/-
Atp6v1b1 +/-

Fig. 4

Kovacikova et al.

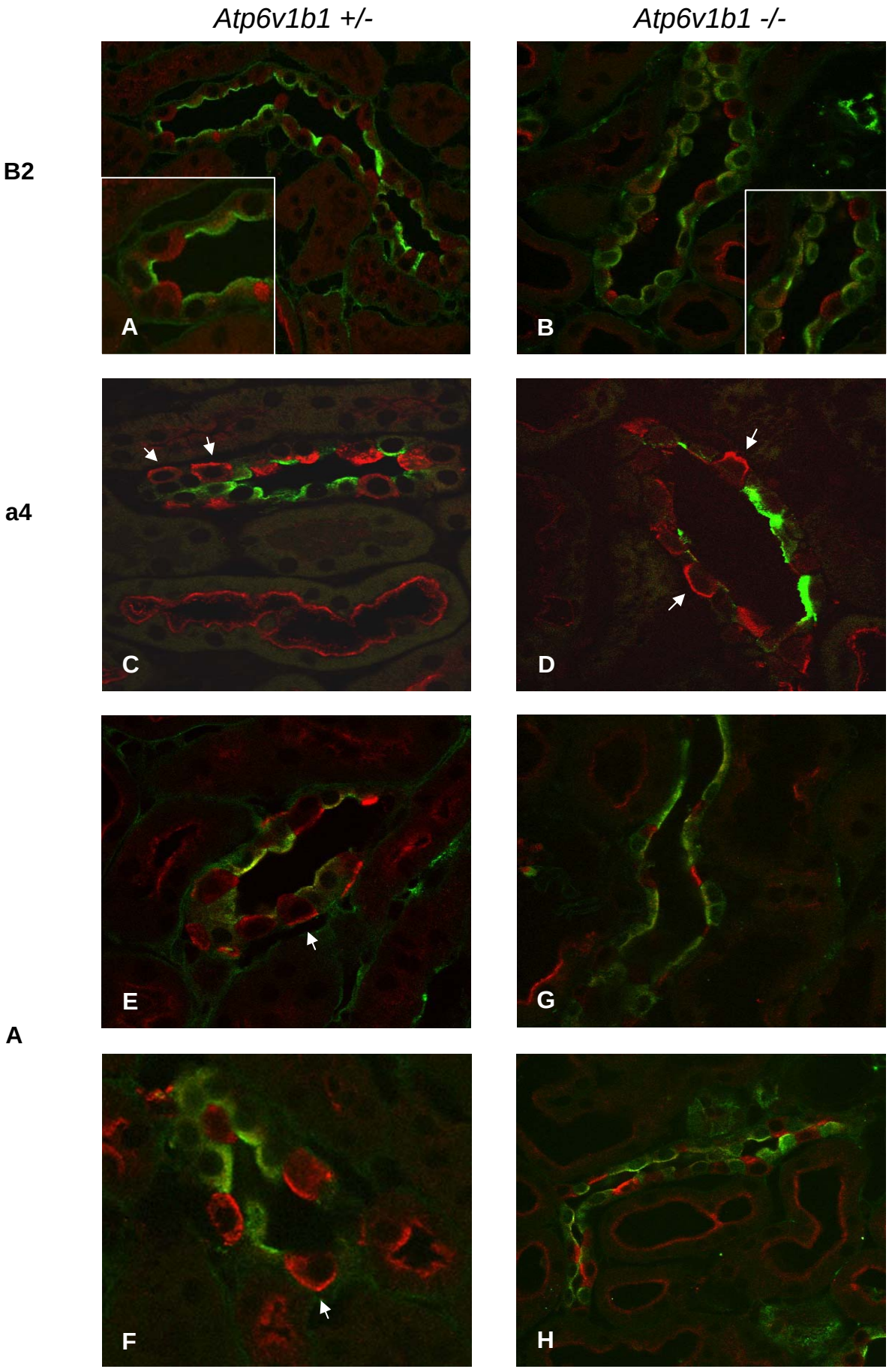

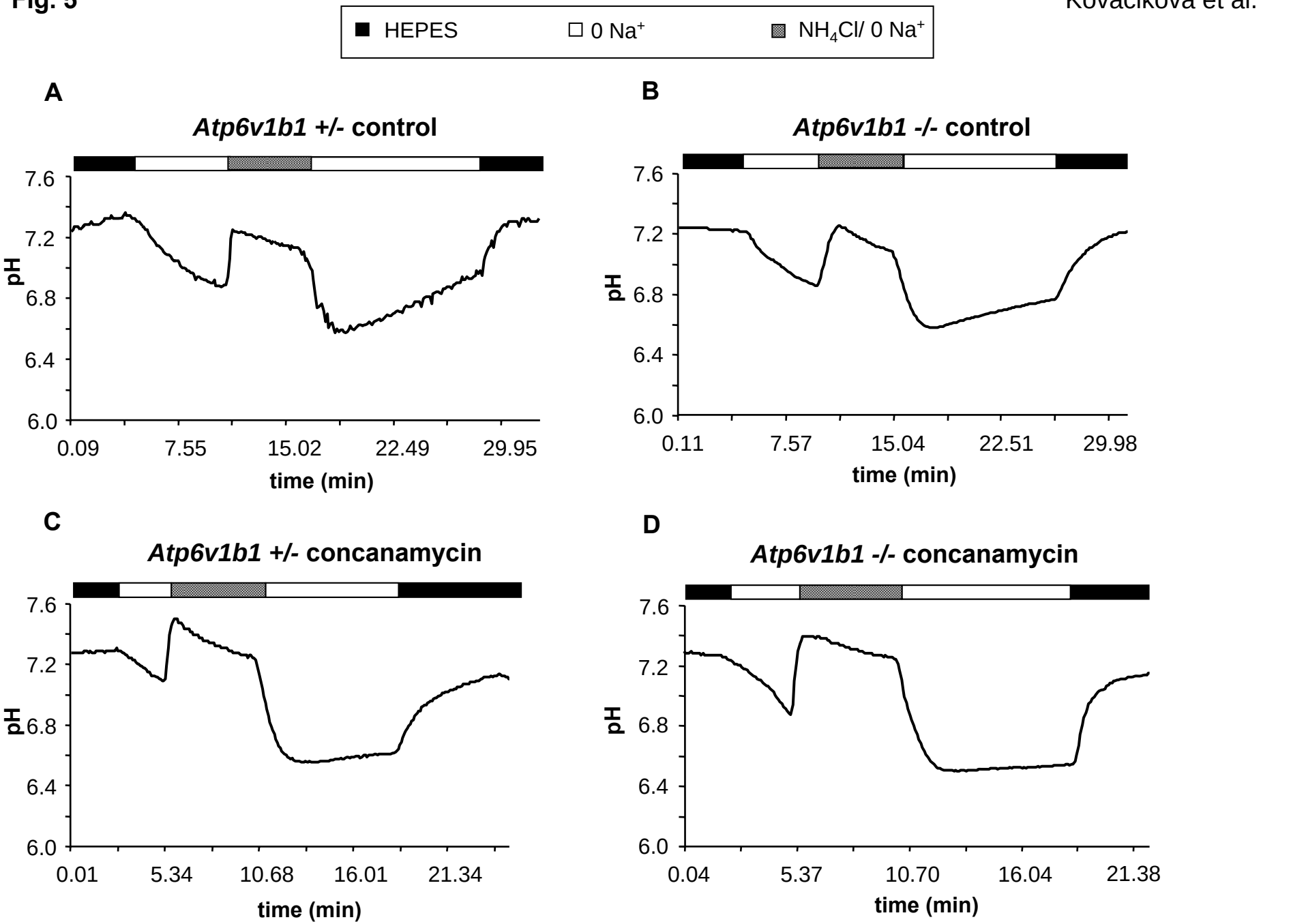
HEPES
0 Na+
NH4Cl/ 0 Na+
A
Atp6v1b1 +/- control
pH
7.6
7.2
6.8
6.4
6.0
0.09
7.55
15.02
22.49
29.95
time (min)
B
Atp6v1b1 -/- control
pH
7.6
7.2
6.8
6.4
6.0
0.11
7.57
15.04
22.51
29.98
time (min)
C
Atp6v1b1 +/- concanamycin
pH
7.6
7.2
6.8
6.4
6.0
0.01
5.34
10.68
16.01
21.34
time (min)
D
Atp6v1b1 -/- concanamycin
pH
7.6
7.2
6.8
6.4
6.0
0.04
5.37
10.70
16.04
21.38
time (min)

E

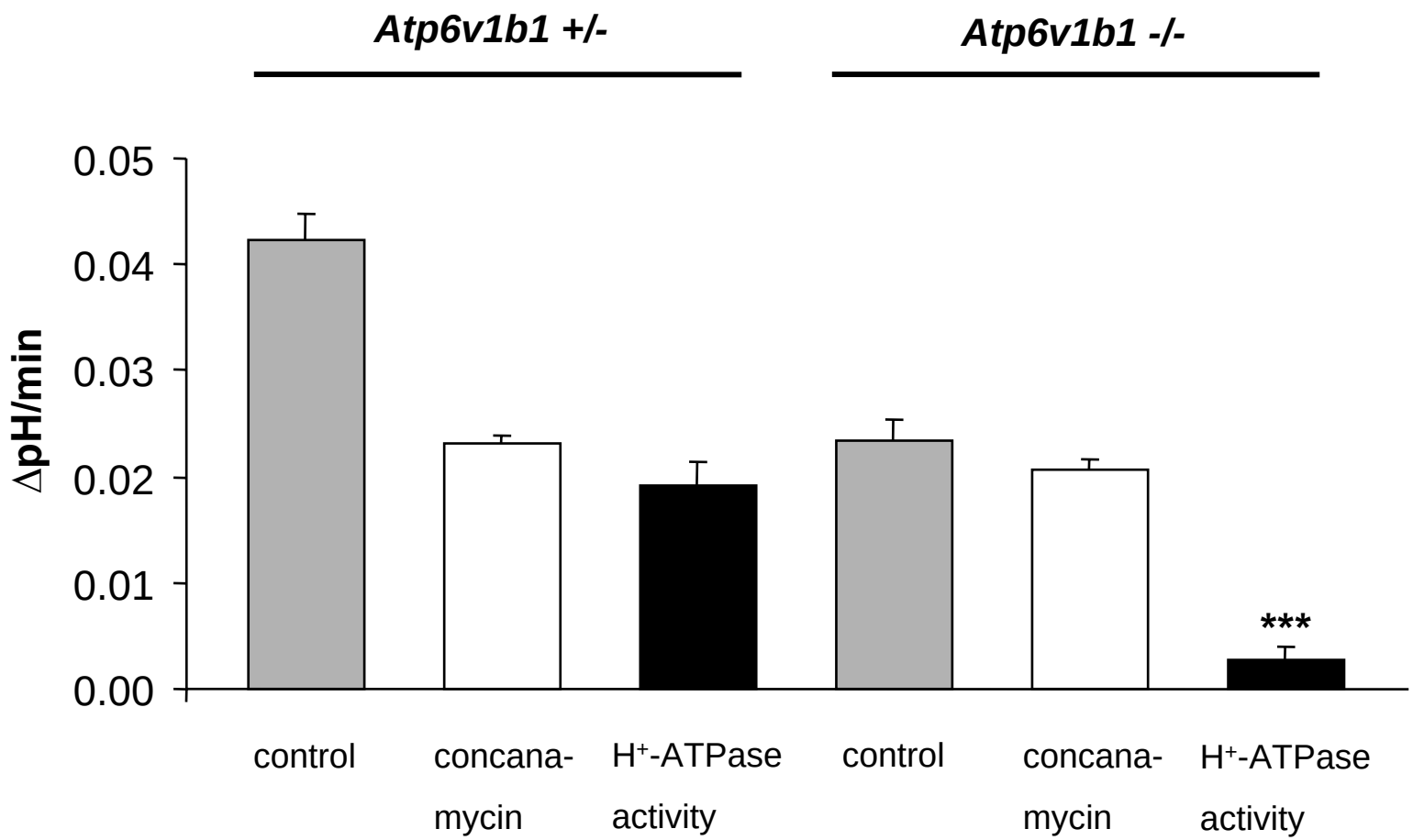
Atp6v1b1 +/-
Atp6v1b1 -/-
ΔpH/min
0.05
0.04
0.03
0.02
0.01
0.00
***
control
concana-mycin
H+-ATPase activity
control
concana-mycin
H+-ATPase activity

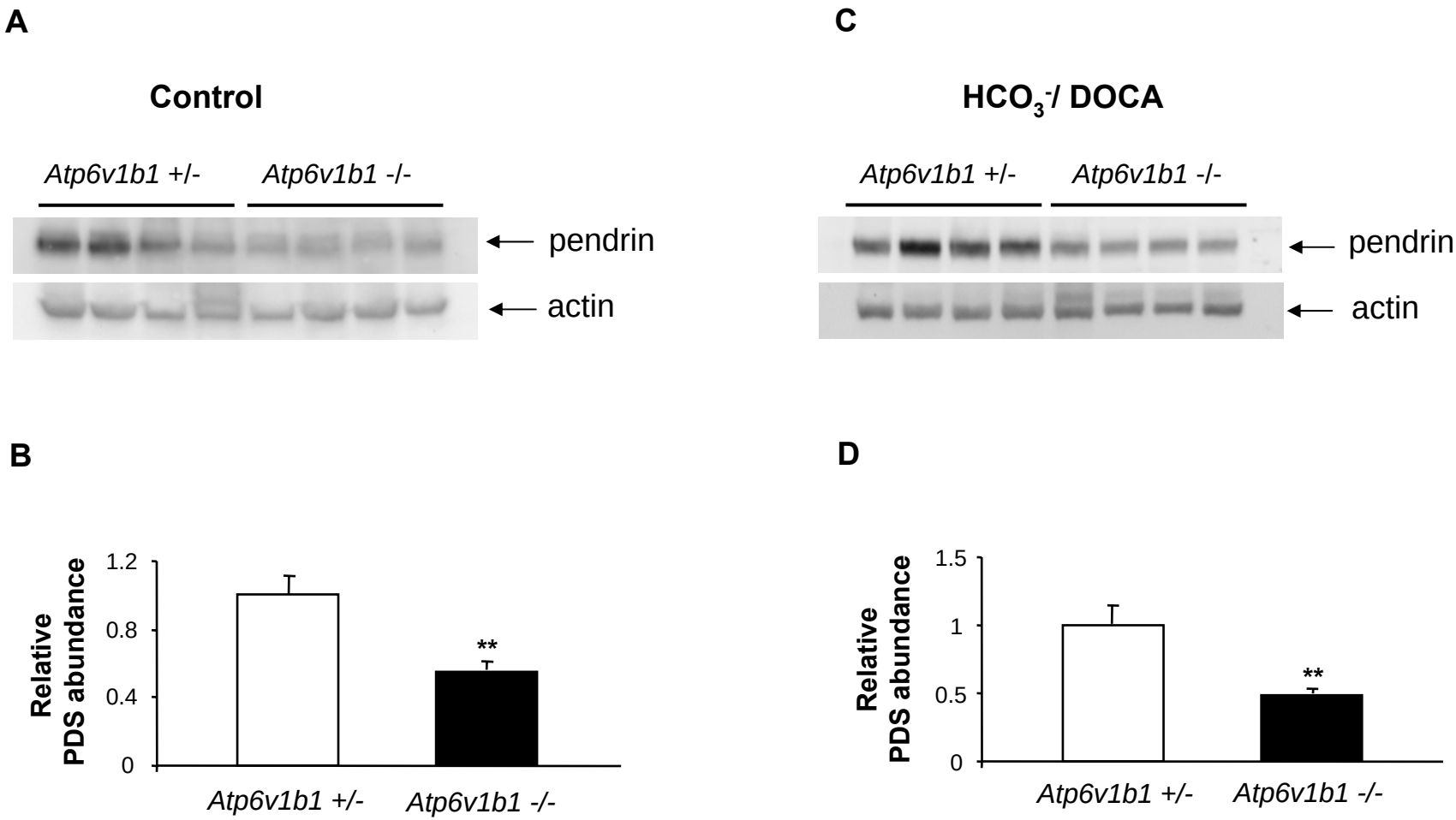
A
Control
Atp6v1b1 +/-
Atp6v1b1 -/-
pendrin
actin
C
HCO3-/ DOCA
Atp6v1b1 +/-
Atp6v1b1 -/-
pendrin
actin
B
Relative PDS abundance
1.2
0.8
0.4
0
**
Atp6v1b1 +/-
Atp6v1b1 -/-
D
Relative PDS abundance
1.5
1
0.5
0
**
Atp6v1b1 +/-
Atp6v1b1 -/-

Atp6v1b1 +/-

Atp6v1b1 -/-

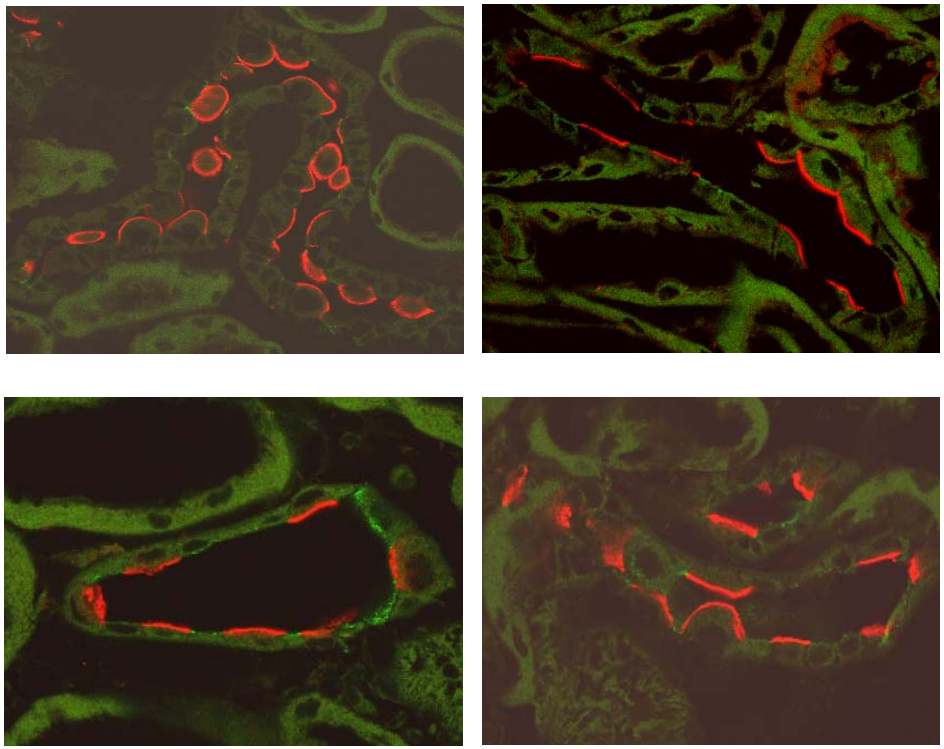

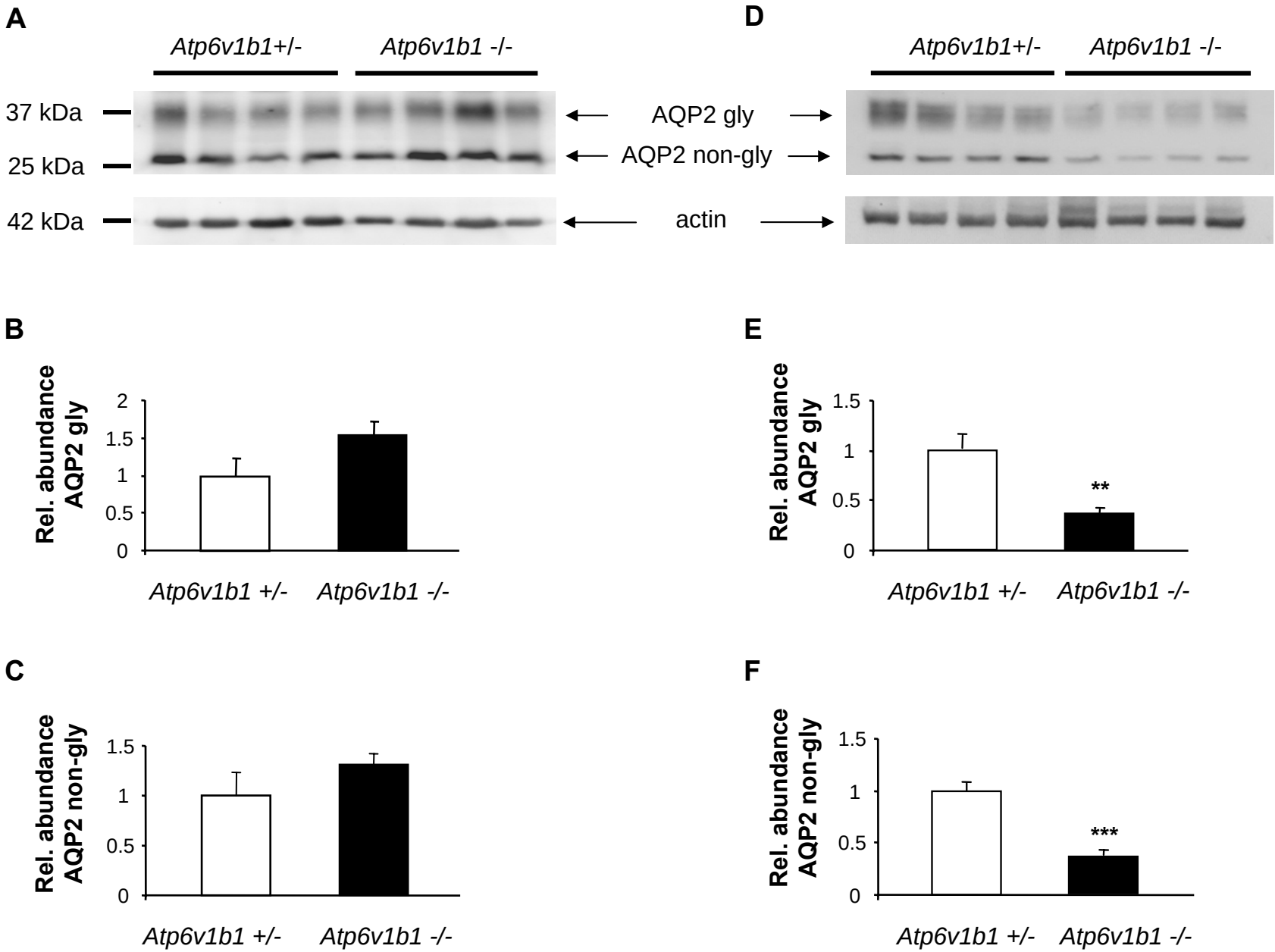
A
Atp6v1b1+/-
Atp6v1b1 -/-
37 kDa
25 kDa
42 kDa
AQP2 gly
AQP2 non-gly
actin
D
Atp6v1b1+/-
Atp6v1b1 -/-
B
Rel. abundance AQP2 gly
2
1.5
1
0.5
0
Atp6v1b1 +/-
Atp6v1b1 -/-
E
Rel. abundance AQP2 gly
1.5
1
0.5
0
**
Atp6v1b1 +/-
Atp6v1b1 -/-
C
Rel. abundance AQP2 non-gly
1.5
1
0.5
0
Atp6v1b1 +/-
Atp6v1b1 -/-
F
Rel. abundance AQP2 non-gly
1.5
1
0.5
0
***
Atp6v1b1 +/-
Atp6v1b1 -/-

9. SUMMARY OF THE RESULTS

9.1. Functional interaction between sodium reabsorption and urinary acidification by the vacuolar H^+-ATPase in the CNT and CD

Final urinary acidification is achieved by the action of vacuolar H^+-ATPases expressed in the IC of the CNT and CD. It has been hypothesised that this acidification is enhanced by sodium reabsorption through ENaC which is expressed on the apical membranes of neighbouring principal cells, thereby creating a more lumen-negative voltage.

Renal clearence experiments in a mouse model deficient for the B1 H^+-ATPase subunit and a mouse model with the specific inactivation of αENaC in the CD but not in the CNT enabled us to study the exact localization of this interaction. Furosemide was chosen as a tool for triggering urinary acidification by increasing sodium delivery to the CNT and CD. This effect of furosemide was abolished with amiloride and benzamil which block ENaC. In mice deficient for B1 H^+-ATPase subunit furosemide led to only a small urinary acidification. On the contrary, in mice with the specific inactivation of αENaC in the CD, furosemide alone and in combination with hydrochlorothiazide induced normal urinary acidification.

Taken together these findings suggest that the B1 vacuolar H^+-ATPase subunit is necessary for acute urinary acidification. Loss of αENaC in

the CD does not impair final urinary acidification. Hence, the expression of functional ENaC channels in the CNT is sufficient to cause furosemide-stimulated urinary acidification and identifies the CNT as a major segment in electrogenic urinary acidification.

9.2. The role of the B1 H^+-ATPase subunit in type B IC function

The role of the B1 H^+-ATPase subunit in the type A IC has been highlighted in humans and mice (30, 43). However B1 containing proton pumps are also present on the basolateral membrane of the type B IC where their function is to reabsorb protons. This process serves, together with bicarbonate secretion through the apical Cl^-/HCO_3^- exchanger pendrin, to dispose alkali equivalents. Thus, type B IC are crucial during metabolic alkalosis.

To date little was known about the role of the B1 H^+-ATPase subunit in the type B IC. To study this aspect, we induced metabolic alkalosis using deoxycorticosterone acetate (DOCA) and $NaHCO_3$ in B1 deficient mice. Following this treatment, B1 knock out mice developed systemic alkalosis accompanied by increased blood bicarbonate, hypokaliemia and hypochloremia. Furthermore, B1 deficient mice showed decreased total pendrin expression whereas the relative abundance of pendrin expressing cells was increased. H^+-ATPase activity in B-IC was strongly reduced,

demonstrating that B1 containing H^+-ATPases are essential for normal type B intercalated cell function. Furthermore, B1 deficient mice excreted larger quantities of urine which was associated with a lower AQP-2 water channel abundance and a higher relative frequency of principal cells in the connecting tubule.

Thus, the B1 H^+-ATPase subunit is essential for normal B-type IC function and its loss may also affect the function of the principal cells. The role of the B1 subunit function in bicarbonate secretion and water reabsorption have been previously not recognized and may also affect renal function in patients with ATP6V1B1 mutations.

9.3. The role of the B1 H^+-ATPase subunit in the type A and B IC: an integrative view

The vacuolar H^+-ATPase is a multisubunit protein with the B subunit forming a part of the cytosolic V_1 domain. This subunit exists in two isoforms - B1 and B2, with only the B1 subunit and not the B2 subunit possessing a PDZ binding motif. Whereas the B2 subunit is expressed in virtually all tissues, the B1 subunit expression is restricted to a limited number of tissues such as kidney, testis and inner ear.

The kidney specific B1 subunit is present in the vacuolar H^+-ATPase in the intercalated cells of the CNT and CD. Vacuolar H^+-ATPases are

expressed on the apical membrane of the acid-secretory type A IC and on the basolateral membrane of the base-secretory type B IC.

The role of the B1 subunit in the type A IC has been recognized in humans and mice. Human patients harbouring mutations in the B1 subunit suffer from dRTA, in which the distal nephron is unable to acidify the urine appropriately resulting in systemic acidosis. Mice deficient for the B1 subunit are not spontaneously acidotic despite the excretion of alkaline urine. However following NH_4Cl load or furosemide administration they acidify their urine to a lesser extent than wild type animals. Furthermore, activity of the H^+-ATPases lacking the B1 subunit is significantly reduced in the type A IC (unpublished observations), but is still preserved to a certain extent suggesting a possible compensation by the ubiquitous B2 subunit. This explanation is supported by the findings of other group (60).

In the type B IC loss of the B1 subunit is associated with a decreased pendrin expression. Pendrin is an apical Cl^-/HCO_3^- exchanger which functions in series with the basolateral proton pump. Furthermore, the activity of the H^+-ATPase lacking the B1 subunit is negligible in this type of cells. This finding provides evidence that the B2 subunit may not be able to compensate for the loss of the B1 subunit in type B IC. In addition, the B2 subunit was not observed in the basolateral membrane of the IC.

Taken together the data suggest that although the B2 subunit may be able to partially compensate for the absence of the B1 subunit in type A IC H^+-ATPases, no such compensation by B2 occurs for type B IC B1-deficient H^+-ATPases. This lack of compensation by the B2 subunit in

basolateral localized H^+-ATPase may be due to the lack of a PDZ binding domain restricting expression of B2 to apical membranes such as in type A IC.

10. PUBLICATIONS THAT DID NOT CONTRIBUTE TO THIS WORK

10.1. Impact of dietary protein intake on acid-base status in a mouse model for distal renal tubular acidosis

Kovacikova J, Wagner CA

Manuscript in preparation

Abstract:
Distal renal tubular acidosis (dRTA) is caused by impaired excretion of acid in the renal collecting duct and affects systemic mineral and electrolyte balance. A protein rich Western diet constitutes a physiological acid-load which requires increased urinary acidification. Patients with mutations in the intercalated cell specific B1 subunit of the vacuolar H^+-ATPase suffer from dRTA. Recently we described a mouse model lacking the B1 subunit with impaired urinary acidification. WT and B1 KO mice were fed over 10 weeks with a normal (NP, 20%) or high protein (HP, 50%) diet. Surprisingly B1 KO grew more on the HP and increased blood pH and bicarbonate levels. Urinary pH was more alkaline in the B1 KO. WT animals responded with an increased urinary excretion of Na, Cl, Pi, whereas B1 KO had low excretion rates. Thus, the physiological acid load with a HP diet does not lead to dRTA in mice lacking the B1 subunit and possibly triggers a complex compensatory mechanism.

10.2. Thyroid hormone modulates expression of acid-base transporters in rat kidney

Mohebbi N, **Kovacikova J**, Nowik M, Wagner CA

Am J Physiol Renal Physiol; manuscript submitted

Abstract:

Hypothyroidism in man is associated with incomplete distal renal tubular acidosis, presenting as the inability to respond appropriately to an acid challenge by excreting less acid. Here, we induced hypothyroidism in rats with methimozole (HYPO) and substituted one group with L-thyroxine (EU). After 4 weeks, acid base status was similar in both groups. However, after 24 hours acid loading with NH_4Cl HYPO rats displayed a more pronounced metabolic acidosis. The expression of the Na+/H+ exchanger NHE3, the na+/phosphate cotransporter Napi IIa and the B2 subunit of the vacuolar H+-ATPase was reduced in the brush border membrane of the proximal tubule of the HYPO group paralleled by a lower abundance of Na+/HCO3- cotransporter NBC_e1 and a higher expression of the acid-secretory type A intercallated cell specific Cl-/HCO3- exchanger AE1. In contrast to control conditions, the expression of NBCe1 was increased in the HYPO group during metabolic acidosis. In addition, net acid excretion was similar in both groups. The relative number of type A intercalated cells was increased in the connecting tubule and cortical collecting duct of the HYPO group during acidosis. Thus, thyroid hormones modulate the renal response to an acid challenge and alter the expression of several key acid-base transporters. Mild hypothyroidism is associated only with a very mild defect in renal acid handling which appears to be mainly located in the proximal tubule and is compensated by the distal nephron.

10.3. Distal renal tubular acidosis in mice lacking aldosterone synthase

Kovacikova J, Makhanova N, Kim HS, Smithies O, Wagner CA

Manuscript in preparation

Abstract:
The ability of the kidney to acidify urine is modulated by aldosterone. Acquired or inborn defects associated with aldosterone insufficiency result in a form of hyperkalemic distal renal tubular acidosis (type IV dRTA). However, previous animal models have been based on adrenalectomy which also affects a number of other hormones that may be involved in acid-base homeostasis. Here we examined a mouse model lacking aldosterone synthase (AS KO) catalyzing the final step in aldosterone synthesis. AS KO have lower blood pH, lower bicarbonate and chloride level as well as mild hyperkaliemia. These changes are accompanied by a higher urine output, a more alkaline urine, increased water and food inatake and diarrhoe. In the kidney, absence of aldosterone led to increased levels of AE1 mRNA and protein and increased AQP2 protein abundance. The expression of NHE3 both on mRNA as well as on protein level was not altered. Real time PCR did not reveal any changes in the abundance of SNAT3, PEPCK, pendrin, a4 and B1 H+-ATPase subunits in kidney. Despite metabolic acidosis the kidney did not adapt adequately by increasing net acid excretion enough suggesting a renal defect in ammoniagenesis and final urinary acidification. In addition, mild diarrhoe may lead to intestinal electrolyte and bicarbonate loss and could thereby contribute to the observed disturbances. Our results suggest that mice lacking aldosterone synthase have symptoms of dRTA type IV and therefore may serve as a model to further investigate aldosterone related regulation of renal (and extra-renal) acid-base transport.

10.4. Angiotensin II stimulates vacuolar H^+-ATPase activity in renal acid-secretory intercalated cells. The B1 vacuolar H^+-ATPase subunit (ATP6V1B1) is required for the stimulation

Rothenberger F, Velic A, Stehberger PA, **Kovacikova J**, Wagner CA

J Am Soc Nephrol; manuscript submitted

Abstract:
Final urinary acidification is mediated by the action of vacuolar H+-ATPases expressed in acid-secretory type A intercalated cells (A-IC) in the collecting duct. Angiotensin II (A II) has profound effects on renal acid-base transport in the proximal tubule, distal tubule, and collecting duct. Here we investigated its effects on vacuolar H+-ATPase activity in A-IC in freshly isolated mouse outer medullary collecting ducts. A II (10 nM) stimulated concanamycin-sensitive vacuolar H+-ATPase activity in A-ICin freshly isolated mouse outer medullary collecting ducts via AT1 receptors which were also detected mmunohistochemically in A-IC. A II increased intracellular Ca2+ levels transiently. Chelation of intracellular Ca2+ with BAPTA and depletion of ER Ca2+-stores prevented the stimulatory effect on H+-ATPase activity. The effect of A II on H+-ATPase activity was abolished by inhibitors of small G-proteins and phospholipase C, by blockers of Ca2+-dependent and independent isoforms of protein kinase C and ERK1/2 kinases. Disruption of the microtubular network and cleavage of cellubrevine attenuated the stimulation. Finally, A II failed to stimulate residual vacuolar H+-ATPase activity in A-IC from mice deficient for the B1 subunit of the vacuolar H+-ATPase. Thus, A II presents a potent stimulus for vacuolar H+-ATPase activity in OMCD intercalated cells and requires trafficking of stimulatory proteins or vacuolar H+-ATPases. The B1 subunit is indispensable for the stimulation by A II and its importance for stimulation of vacuolar H+-ATPase activity may

contribute to the inappropriate urinary acidification seen in distal renal tubular acidosis patients with mutations in this subunit.

10.5. Enhanced suicidal death of erythrocytes from gene-targeted mice lacking the Cl^-/HCO_3^- exchanger AE1

Akel A, Wagner CA, **Kovacikova J**, Kasinathan RS, Kiedaisch V, Koka S, Alper SL, Bernhardt I, Wieder T, Huber S, Lang F

Am J Physiol Cell Physiol; manuscript submitted

Abstract:

Genetic defects of the anion exchanger AE1 may lead to spherocytic erythrocyte morphology, severe hemolytic anemia and/or cation leak. In normal erythrocytes osmotic shock, Cl^- removal and energy depletion activate Ca^{2+}-permeable cation channels with Ca^{2+} induced suicidal erythrocyte death, i.e. surface exposure of phosphatidylserine, cell shrinkage and membrane blebbing, all features typical for apoptosis of nucleated cells. The present experiments explored whether AE1 deficiency favors suicidal erythrocyte death. Peripheral blood erythrocyte number was significantly smaller in gene-targeted mice lacking AE1 (*AE1*$^{-/-}$) than in their wild type littermates (*AE1*$^{+/+}$), despite an increased percentage of reticulocytes (*AE1*$^{-/-}$: 49%, *AE1*$^{+/+}$: 2%), an indicator of enhanced erythropoiesis. Annexin binding reflecting phosphatidylserine exposure was significantly larger in *AE1*$^{-/-}$erythrocytes/reticulocytes (~10 %) than in *AE1*$^{+/+}$erythrocytes (~1 %). Osmotic shock (addition of 400 mM sucrose), Cl^- removal (replacement with gluconate) or energy depletion (removal of glucose) led to significantly stronger annexin binding in *AE1*$^{-/-}$erythrocytes/reticulocytes than in *AE1*$^{+/+}$erythrocytes. The increase of annexin binding following exposure to the Ca^{2+} ionophore ionomycin (1 µM) was, however, similar in *AE1*$^{-/-}$ and in *AE1*$^{+/+}$erythrocytes. Fluo3 fluorescence revealed markedly increased cytosolic Ca^{2+} permeability in *AE1*$^{-/-}$ erythrocytes/reticulocytes. Clearance of CFSE-labelled erythrocytes/reticulocytes from circulating blood was more rapid in *AE1*$^{-/-}$ than in *AE1*$^{+/+}$mice and accelerated by ionomycin treatment in both genotypes. In

conclusion, lack of AE1 is associated with enhanced Ca^{2+} entry and subsequent scrambling of cell membrane phospholipids.

REFERENCES

1. **Agroyannis B, Koutsikos D, Tzanatos-Exarchou H, and Yatzidis H.** Erythrocytosis in type I renal tubular acidosis with nephrocalcinosis. *Nephrol Dial Transplant* 7: 365-366, 1992.

2. **Al-Awqati Q.** Plasticity in epithelial polarity of renal intercalated cells: targeting of the H(+)-ATPase and band 3. *Am J Physiol* 270: C1571-1580, 1996.

3. **Al-Awqati Q, Norby LH, Mueller A, and Steinmetz PR.** Characteristics of stimulation of H+ transport by aldosterone in turtle urinary bladder. *J Clin Invest* 58: 351-358, 1976.

4. **Allen AM, Zhuo J, and Mendelsohn FA.** Localization and function of angiotensin AT1 receptors. *Am J Hypertens* 13: 31S-38S, 2000.

5. **Ardaillou R.** Angiotensin II receptors. *J Am Soc Nephrol* 10 Suppl 11: S30-39, 1999.

6. **Bagnis C, Marshansky V, Breton S, and Brown D.** Remodeling the cellular profile of collecting ducts by chronic carbonic anhydrase inhibition. *Am J Physiol Renal Physiol* 280: F437-448, 2001.

7. **Barker PM, Nguyen MS, Gatzy JT, Grubb B, Norman H, Hummler E, Rossier B, Boucher RC, and Koller B.** Role of gammaENaC subunit in lung liquid clearance and electrolyte balance in newborn mice. Insights into perinatal adaptation and pseudohypoaldosteronism. *J Clin Invest* 102: 1634-1640, 1998.

8. **Bastani B, Purcell H, Hemken P, Trigg D, and Gluck S.** Expression and distribution of renal vacuolar proton-translocating adenosine triphosphatase in response to chronic acid and alkali loads in the rat. *J Clin Invest* 88: 126-136, 1991.

9. **Batlle DC.** Segmental characterization of defects in collecting tubule acidification. *Kidney Int* 30: 546-554, 1986.

10. **Bonny O, Chraibi A, Loffing J, Jaeger NF, Grunder S, Horisberger JD, and Rossier BC.** Functional expression of a pseudohypoaldosteronism type I mutated epithelial Na+ channel lacking the pore-forming region of its alpha subunit. *J Clin Invest* 104: 967-974, 1999.

11. **Breton S, Smith PJ, Lui B, and Brown D.** Acidification of the male reproductive tract by a proton pumping (H+)-ATPase. *Nat Med* 2: 470-472, 1996.

12. **Breton S, Wiederhold T, Marshansky V, Nsumu NN, Ramesh V, and Brown D.** The B1 subunit of the H^+ATPase is a PDZ-binding protein. *J Biol Chem* 275: 18219-18224, 2000.

13. **Brown D, Hirsch S, and Gluck S.** An H+-ATPase in opposite plasma membrane domains in kidney epithelial cell subpopulations. *Nature* 331: 622-624, 1988.

14. **Brown D, Hirsch S, and Gluck S.** Localization of a proton-pumping ATPase in rat kidney. *J Clin Invest* 82: 2114-2126, 1988.

15. **Brown D, Lui B, Gluck S, and Sabolic I.** A plasma membrane proton ATPase in specialized cells of rat epididymis. *Am J Physiol* 263: C913-C916, 1992.

16. **Brown MT, Cunningham MJ, Ingelfinger JR, and Becker AN.** Progressive sensorineural hearing loss in association with distal renal tubular acidosis. *Arch Otolaryngol Head Neck Surg* 119: 458-460, 1993.

17. **Canessa CM, Schild L, Buell G, Thorens B, Gautschi I, Horisberger JD, and Rossier BC.** Amiloride-sensitive epithelial Na+ channel is made of three homologous subunits. *Nature* 367: 463-467, 1994.

18. **Chan YL and Giebisch G.** Relationship between sodium and bicarbonate transport in the rat proximal convoluted tubule. *Am J Physiol* 240: F222-230, 1981.

19. **Chang H and Fujita T.** A numerical model of acid-base transport in rat distal tubule. *Am J Physiol Renal Physiol* 281: F222-F243, 2001.

20. **Choi JY, Shah M, Lee MG, Schultheis PJ, Shull GE, Muallem S, and Baum M.** Novel amiloride-sensitive sodium-dependent proton secretion in the mouse proximal convoluted tubule. *J Clin Invest* 105: 1141-1146, 2000.

21. **Couloigner V, Teixeira M, Hulin P, Sterkers O, Bichara M, Escoubet B, Planelles G, and Ferrary E.** Effect of locally applied drugs on the pH of luminal fluid in the endolymphatic sac of guinea pig. *Am J Physiol Regul Integr Comp Physiol* 279: R1695-1700, 2000.

22. **Dou H, Finberg K, Cardell EL, Lifton R, and Choo D.** Mice lacking the B1 subunit of H+ -ATPase have normal hearing. *Hear Res* 180: 76-84, 2003.

23. **DuBose TD and Alpern RJ.** Renal tubular acidosis. In: *The metabolic and molecular bases of inherited disease* (8th ed.), edited by Scriver CR, Beaudet AL, Sly WS and Valle D. New York: McGraw-Hill, 2001, p. 4983-5021.

24. **DuBose TD, Jr. and Caflisch CR.** Effect of selective aldosterone deficiency on acidification in nephron segments of the rat inner medulla. *J Clin Invest* 82: 1624-1632, 1988.

25. **DuBose TD, Jr., Gitomer J, and Codina J.** H+,K+-ATPase. *Curr Opin Nephrol Hypertens* 8: 597-602, 1999.

26. **Emmons C and Kurtz I.** Functional characterization of three intercalated cell subtypes in the rabbit outer cortical collecting duct. *J Clin Invest* 93: 417-423, 1994.

27. **Fejes-Toth G and Naray-Fejes-Toth A.** Differentiation of renal beta-intercalated cells to alpha-intercalated and principal cells in culture. *Proc Natl Acad Sci U S A* 89: 5487-5491, 1992.

28. **Fejes-Toth G and Naray-Fejes-Toth A.** Immunohistochemical localization of colonic H-K-ATPase to the apical membrane of connecting tubule cells. *Am J Physiol Renal Physiol* 281: F318-325, 2001.

29. **Ferrary E and Sterkers O.** Mechanisms of endolymph secretion. *Kidney Int Suppl* 65: S98-103, 1998.

30. **Finberg KE, Wagner CA, Bailey MA, Paunescu TG, Breton S, Brown D, Giebisch G, Geibel JP, and Lifton RP.** The B1-subunit of the H(+) ATPase is required for maximal urinary acidification. *Proc Natl Acad Sci U S A* 102: 13616-13621, 2005.

31. **Finberg KE, Wagner CA, Bailey MA, Wang T, Mentone SA, Kashgarian M, Giebisch G, Geibel JP, and Lifton RP.** Loss of plasma membrane H+-ATPase activity from cortical collecting duct intercalated cells of H+-ATPase B1-subunit deficient mice: a mouse model of distal renal tubular acidosis (Abstract). *J Am Soc Nephrol* 13: 4, 2002.

32. **Finberg KE, Wang T, C.A. W, Geibel JP, Dou H, and Lifton RP.** Generation and characterization of H^+-ATPase B1 subunit deficient mice (Abstract). *J Am Soc Nephrol* 12: 15, 2001.

33. **Frische S, Kwon TH, Frokiaer J, Madsen KM, and Nielsen S.** Regulated expression of pendrin in rat kidney in response to chronic NH4Cl or NaHCO3 loading. *Am J Physiol Renal Physiol* 284: F584-593, 2003.

34. **Geibel J, Giebisch G, and Boron WF.** Angiotensin II stimulates both Na(+)-H+ exchange and Na+/HCO3- cotransport in the rabbit proximal tubule. *Proc Natl Acad Sci U S A* 87: 7917-7920, 1990.

35. **Giebisch G.** Renal potassium transport: mechanisms and regulation. *Am J Physiol* 274: F817-833, 1998.

36. **Gruber G, Wieczorek H, Harvey WR, and Muller V.** Structure-function relationships of A-, F- and V-ATPases. *J Exp Biol* 204: 2597-2605, 2001.

37. **Hamm LL and Alpern RJ.** Cellular mechanisms of renal tubular acidification. In: *The Kidney: Physiology and Pathophysiology*, edited by Seldin DW and Giebisch G. Philadelphia: PA: Lippincott Williams & Wilkins, 2000, p. 1935-1979.

38. **Henger A, Tutt P, Riesen WF, Hulter HN, and Krapf R.** Acid-base and endocrine effects of aldosterone and angiotensin II inhibition in metabolic acidosis in human patients. *J Lab Clin Med* 136: 379-389, 2000.

39. **Herak-Kramberger CM, Breton S, Brown D, Kraus O, and Sabolic I.** Distribution of the vacuolar H+ atpase along the rat and human male reproductive tract. *Biol Reprod* 64: 1699-1707, 2001.

40. **Hummler E, Barker P, Gatzy J, Beermann F, Verdumo C, Schmidt A, Boucher R, and Rossier BC.** Early death due to defective neonatal lung liquid clearance in alpha-ENaC-deficient mice. *Nat Genet* 12: 325-328, 1996.

41. **Hummler E, Merillat AM, Rubera I, Rossier BC, and Beermann F.** Conditional gene targeting of the Scnn1a (alphaENaC) gene locus. *Genesis* 32: 169-172, 2002.

42. **Karet FE.** Inherited distal renal tubular acidosis. *J Am Soc Nephrol* 13: 2178-2184, 2002.

43. **Karet FE, Finberg KE, Nelson RD, Nayr A, Mocan H, Sanjad SA, Rodriguez-Soriano J, Santos F, Cremers CW, Di Pietro A, Hoffbrand BI, Winiarski J, Bakkaloglu A, Ozen S, Dusunsel R, Goodyer P, Hulton SA, Wu DK, Skvorak AB, Morton CC, Cunnigham MJ, Jha V, and Lifton RP.** Mutations in the gene encoding B1 subunit of H^+-ATPase cause renal tubular acidosis with sensorineural deafness. *Nat Genet* 21: 84-90, 1999.

44. **Kawasaki-Nishi S, Bowers K, Nishi T, Forgac M, and Stevens TH.** The amino-terminal domain of the vacuolar proton-translocating ATPase a subunit controls targeting and in vivo dissociation, and the carboxyl-terminal domain affects coupling of proton transport and ATP hydrolysis. *J Biol Chem* 276: 47411-47420, 2001.

45. **Kawasaki-Nishi S, Nishi T, and Forgac M.** Arg-735 of the 100-kDa subunit a of the yeast V-ATPase is essential for proton translocation. *Proc Natl Acad Sci U S A* 98: 12397-12402, 2001.

46. **Kim J, Kim YH, Cha JH, Tisher CC, and Madsen KM.** Intercalated cell subtypes in connecting tubule and cortical collecting duct of rat and mouse. *J Am Soc Nephrol* 10: 1-12, 1999.

47. **Kovacikova J, Winter C, Loffing-Cueni D, Loffing J, Finberg KE, Lifton RP, Hummler E, Rossier B, and Wagner CA.** The connecting tubule is the main site of the furosemide-induced urinary acidification by the vacuolar H^+-ATPase. *Kidney Int*: (in press), 2006.

48. **Leng XH, Manolson MF, Liu Q, and Forgac M.** Site-directed mutagenesis of the 100-kDa subunit (Vph1p) of the yeast vacuolar (H+)-ATPase. *J Biol Chem* 271: 22487-22493, 1996.

49. **Lombes M, Farman N, Oblin ME, Baulieu EE, Bonvalet JP, Erlanger BF, and Gasc JM.** Immunohistochemical localization of renal mineralocorticoid receptor by using an anti-idiotypic antibody that is an internal image of aldosterone. *Proc Natl Acad Sci U S A* 87: 1086-1088, 1990.

50. **Losel R and Wehling M.** Nongenomic actions of steroid hormones. *Nat Rev Mol Cell Biol* 4: 46-56, 2003.

51. **Madsen KM, Verlander JW, Kim J, and Tisher CC.** Morphological adaptation of the collecting duct to acid-base disturbances. *Kidney Int Suppl* 33: S57-63, 1991.

52. **McDonald FJ, Yang B, Hrstka RF, Drummond HA, Tarr DE, McCray PB, Jr., Stokes JB, Welsh MJ, and Williamson RA.** Disruption of the beta subunit of the epithelial Na+ channel in mice: hyperkalemia and neonatal death associated with a pseudohypoaldosteronism phenotype. *Proc Natl Acad Sci U S A* 96: 1727-1731, 1999.

53. **Merot J, Giebisch G, and Geibel J.** Intracellular acidification induces Cl/HCO3 exchange activity in the basolateral membrane of beta-intercalated cells of the rabbit cortical collecting duct. *J Membr Biol* 159: 253-262, 1997.

54. **Miller RL, Zhang P, Smith M, Beaulieu V, Paunescu TG, Brown D, Breton S, and Nelson RD.** V-ATPase B1-subunit promoter drives expression of EGFP in intercalated cells of kidney, clear cells of epididymis and airway cells of lung in transgenic mice. *Am J Physiol Cell Physiol* 288: C1134-1144, 2005.

55. **Mohebbi N, Kovacikova J, Nowik M, and Wagner C.** Thyroid hormone modulates expression of acid-base transporters in rat kidney. *Am J Physiol Real Physiol* manuscript submitted, 2007.

56. **Muller V and Gruber G.** ATP synthases: structure, function and evolution of unique energy converters. *Cell Mol Life Sci* 60: 474-494, 2003.

57. **Nelson H and Nelson N.** Disruption of genes encoding subunits of yeast vacuolar H^+-ATPase causes conditional lethality. *Proc Natl Acad Sci USA* 87: 3503-3507, 1990.

58. **Nelson N and Harvey WR.** Vacuolar and plasma membrane proton-adenosinetriphosphatases. *Physiol Rev* 79: 361-385, 1999.

59. **Nelson RD, Guo XL, Masood K, Brown D, Kalkbrenner M, and Gluck S.** Selectively amplified expression of an isoform of the vacuolar H+-ATPase 56-kilodalton in renal intercalated cells. *Proc Natl Acad Sci USA* 89: 3541-3545, 1992.

60. **Paunescu TG, Da Silva N, Marshansky V, McKee M, Breton S, and Brown D.** Expression of the 56-kDa B2 subunit isoform of the vacuolar H^+-ATPase in proton-secreting cells of the kidney and epididymis. *Am J Physiol Cell Physiol* 287: C149-C162, 2004.

61. **Powell B, Graham LA, and Stevens TH.** Molecular characterization of the yeast vacuolar H+-ATPase proton pore. *J Biol Chem* 275: 23654-23660, 2000.

62. **Puopolo K, Kumamoto C, Adachi I, Magner R, and Forgac M.** Differential expression of the "B" subunit of the vacuolar H(+)-ATPase in bovine tissues. *J Biol Chem* 267: 3696-3706, 1992.

63. **Rothenberger F, Velic A, Stehberger P, Kovacikova J, and Wagner CA.** Angiotensin II stimulates vacuolar H+-ATPase activity in renal acid-secretory intercalated cells. The B1 vacuolar H+-ATPase subunit (ATP6V1B1) is required for stimulation. *J Am Soc Nephrol*, 2007.

64. **Royaux IE, Wall SM, Karniski LP, Everett LA, Suzuki K, Knepper MA, and Green ED.** Pendrin, encoded by the Pendred's syndrome gene, resides in the apical region of renal intercalated cells and mediates bicarbonate secretion. *Proc Natl Acad Sci USA* 98: 4221-4226, 2001.

65. **Rubera I, Loffing J, Palmer LG, Frindt G, Fowler-Jaeger N, Sauter D, Carroll T, McMahon A, Hummler E, and Rossier BC.** Collecting duct-specific gene inactivation of alphaENaC in the mouse kidney does not impair sodium and potassium balance. *J Clin Invest* 112: 554-565, 2003.

66. **Schuster VL.** Function and regulation of collecting duct intercalated cells. *Annu Rev Physiol* 55: 267-288, 1993.

67. **Sebastian A, Sutton JM, Hulter HN, Schambelan M, and Poler SM.** Effect of mineralocorticoid replacement therapy on renal acid-base homeostasis in adrenalectomized patients. *Kidney Int* 18: 762-773, 1980.

68. **Smith AN, Skaug J, Choate KA, Nayir A, Bakkaloglu A, Ozen S, Hulton SA, Sanjad SA, Al-Sabban EA, Lifton RP, Scherer SW, and Karet FE.** Mutations in ATP6N1B, encoding a new kidney vacuolar proton pump 116-kD subunit, cause recessive distal renal tubular acidosis with preserved hearing. *Nat Genet* 26: 71-75, 2000.

69. **Stankovic KM, Brown D, Alper SL, and Adams JC.** Localization of pH regulating proteins H+ATPase and Cl-/HCO3- exchanger in guinea pig inner ear. *Hear Res* 144: 21-34, 1997.

70. **Stehberger P, Schulz N, Finberg KE, Karet FE, Giebisch G, Lifton RP, Geibel JP, and Wagner CA.** Localization and regulation of the ATP6V0A4 (a4) vacuolar H+-ATPase subunit defective in an inherited form of distal renal tubular acidosis. *J Am Soc Nephrol* 14: 3027-3038, 2003.

71. **Stevens TH and Forgac M.** Structure, function and regulation of the vacuolar (H+)-ATPase. *Ann Rev Cell Dev Biol* 13: 779-808, 1997.

72. **Stover EH, Borthwick KJ, Bavalia C, Eady N, Fritz DM, Rungroj N, Giersch AB, Morton CC, Axon PR, Akil I, Al-Sabban EA, Baguley DM, Bianca S, Bakkaloglu A, Bircan Z, Chauveau D, Clermont MJ, Guala A, Hulton SA, Kroes H, Li Volti G, Mir S, Mocan H, Nayir A, Ozen S, Rodriguez Soriano J, Sanjad SA, Tasic V, Taylor CM, Topaloglu R, Smith AN, and Karet FE.** Novel ATP6V1B1 and ATP6V0A4 mutations in autosomal recessive distal renal tubular acidosis with new evidence for hearing loss. *J Med Genet* 39: 796-803, 2002.

73. **Teng-umnuay P, Verlander JW, Yuan W, Tisher CC, and Madsen KM.** Identification of distinct subpopulations of intercalated cells in the mouse collecting duct. *J Am Soc Nephrol* 7: 260-274, 1996.

74. **Trombetta ES, Ebersold M, Garrett W, Pypaert M, and Mellman I.** Activation of lysosomal function during dendritic cell maturation. *Science* 299: 1400-1403, 2003.

75. **Van Hille B, Richener H, Schmid P, Puettner I, Green JR, and Bilbe G.** Heterogenity of vacuolar H^+-ATPase: differential expression of two human subunit B isoforms. *Biochem J* 303: 191-198, 1994.

76. **Verrey F, Hummler E, Schild L, and Rossier B.** Control of Na^+ transport by aldosterone. In: *The kidney* (3rd ed.), edited by Seldin DW and Giebisch G. Philadelphia: Lippincott, 2000, p. 1441-1471.

77. **Wagner CA, Finberg KE, Breton S, Marshansky V, Brown D, and Geibel JP.** Renal vacuolar H^+-ATPase. *Physiol Rev* 84: 1263-1314, 2004.

78. **Wagner CA, Finberg KE, Stehberger PA, Lifton RP, Giebish GH, Aronson PS, and Geibel JP.** Regulation of the expression of the Cl-/anion exchanger pendrin in mouse kidney by acid-base status. *Kidney Int* 62: 2109-2117, 2002.

79. **Wall SM.** Recent advances in our understanding of intercalated cells. *Curr Opin Nephrol Hypertens* 14: 480-484, 2005.

80. **Wall SM, Hassell KA, Royaux IE, Green ED, Chang JY, Shipley GL, and Verlander JW.** Localization of pendrin in mouse kidney. *Am J Physiol Renal Physiol* 284: F229-F241, 2003.

81. **Wang T, Yang CL, Abbiati T, Schultheis PJ, Shull GE, Giebisch G, and Aronson PS.** Mechanism of proximal tubule bicarbonate absorption in NHE3 null mice. *Am J Physiol* 277: F298-302, 1999.

82. **Wax MB, Saito I, Tenkova T, Krupin T, Becker B, Nelson N, Brown D, and Gluck SL.** Vacuolar H+-ATPase in ocular ciliary epithelium. *Proc Natl Acad Sci USA* 94: 6752-6757, 1997.

83. **Weinstein AM.** A mathematical model of rat cortical collecting duct: determinants of the transtubular potassium gradient. *Am J Physiol Real Physiol* 280: F1072-F1092, 2001.

84. **Weinstein AM.** A mathematical model of the inner medullary collecting duct of the rat: acid/base transport. *Am J Physiol* 274: F856-F867, 1998.

85. **Weinstein AM.** A mathematical model of the outer medullary collecting duct of the rat. *Am J Physiol Reanal Physiol* 279: F24-F45, 2000.

86. **Wingo CS.** Active proton secretion and potassium absorption in the rabbit outer medullary collecting duct. Functional evidence for proton-potassium-activated adenosine triphosphatase. *J Clin Invest* 84: 361-365, 1989.

87. **Wingo CS, Madsen KM, Smolka A, and Tisher CC.** H-K-ATPase immunoreactivity in cortical and outer medullary collecting duct. *Kidney Int* 38: 985-990, 1990.

88. **Winter C, Schulz N, Giebisch G, Geibel JP, and Wagner CA.** Nongenomic stimulation of vacuolar H+-ATPases in intercalated renal tubule cells by aldosterone. *Proc Natl Acad Sci U S A* 101: 2636-2641, 2004.

89. **Yamashiro CT, Kane PM, Wolczyk DF, Preston RA, and Stevens TH.** Role of vacuolar acidification in protein sorting and zymogen activation: a genetic analysis of the yeast vacuolar proton-translocating ATPase. *Mol Cell Biol* 10: 3737-3749, 1990.